

**STRESS RESPONSES AND THE
PHYSIOLOGICAL CELL FATE OF
HUMAN OCULAR CELLS**

Simon Sidney Robert Ball

A thesis presented for the degree of

Doctor of Philosophy

University of East Anglia

School of Biological Sciences

May 2021

This copy of the thesis has been supplied on condition that anyone who consults it is understood to recognise that its copyright rests with the author and that use of any information derived therefrom must be in accordance with current UK Copyright Law. In addition, any quotation or extract must include full attribution.

Abstract

The eye is under constant attack from external sources, such as UV light and internal sources, such as reactive oxygen species which can give rise to oxidative stress. This insult to the ocular cells can lead to multiple forms of damage that can ultimately result in cell death. In the present study, the primary area of interest was DNA damage and the DNA repair systems that are in place to minimise the impact of this trauma, control cell fate and how they can potentially be involved in normal physiological processes.

With this central theme in mind, the first area investigated was to establish a distribution profile of DNA repair related proteins within the lens. Non-cultured whole human donor lenses obtained from the East Anglian Eye Bank were fixed in 4% v/v formaldehyde, paraffin embedded and sectioned at 6 μm . Samples were subjected to antigen retrieval before fluorescent immunohistochemistry using Alexa-488 secondary antibody and nuclear counterstaining with DAPI. Sections were visualised using a Zeiss Axioplan fluorescence microscope and digital camera. DNA repair proteins, PARP-1, DNA-PK and Ku80 were present in the cell nucleus of the lens epithelial layer. Within fibre cells, newly laid cells also presented a predominantly nuclear expression before levels rapidly declined. This reduced expression appeared to precede changes in chromatin appearance that could be attributed to lens fibre cell de-nucleation.

Developing tools to assess DNA damage is important. To respond to this need, a second area of focus was to adapt a qPCR method to detect DNA damage to produce a Real Time Long Amplicon PCR (LA QPCR) assay version that can be used to detect nuclear and mitochondrial DNA lesions. The assay was evaluated using DNA extracted from the lens cell line FHL124 treated with the DNA strand break inducing agents Neocarzinostatin and Bleomycin. Following optimisation and validation, the Real Time LA QPCR method successfully detected DNA lesions in nuclear and mitochondrial DNA against a range of DNA damaging agents.

The next phase of the experimental study was to assess the putative applications of sulforaphane (SFN), an isothiocyanate abundant in brassicas, to provide benefit for ocular applications. It is important to note that SFN has concentration dependent actions. At low concentrations it is reported to be cytoprotective and at high concentrations cytotoxic. In the present study the aim was to exploit these traits for different needs.

Preservation of the corneal endothelium is vital for successful corneal grafts, therefore the ability of SFN to counter oxidants was tested. Application of 100 μM hydrogen peroxide (to give an oxidative stress) to the corneal endothelial cell line HCEC12 resulted in enhanced cell death. 2 μM SFN pre-treatment significantly protected cells. DNA damage was also observed with hydrogen peroxide addition. While the degree of damage observed using the comet assay was not significantly lower with sulforaphane treatment, a significant reduction in nuclear DNA and mitochondrial lesions was detected with LA QPCR.

Higher concentrations of SFN were applied to lens cells, which could provide benefit for the treatment of PCO, that results from a wound healing response induced by cataract surgery. Exposure to 100 μ M SFN resulted in cell death, increased ROS levels and greater DNA damage. To determine if ROS were responsible for DNA damage and cell death, the ROS scavenger N-acetyl cysteine (NAC) was used. Pre-treatment with 1mM NAC prevented SFN induced DNA damage and cell death suggesting ROS play a key role in mediating SFN responses.

Overall, the work presented has advanced our knowledge of DNA damage and repair. In the lens DNA repair proteins are expressed in the nuclei of cells within the epithelium and cortical fibre cells. A loss of these proteins precedes nuclear condensation and fragmentation in fibre cells, suggesting a potential role in this process. In developing the LA QPCR, this provides an additional method to assess DNA damage in nuclear and mitochondrial DNA and appears more sensitive the commonly used comet assay. SFN could serve as an additive to corneal storage medium to increase endothelial cell viability and probability of graft success. SFN when applied at higher concentrations could also provide better PCO management through induction of DNA damage and cell death with ROS playing a critical role in mediating these actions.

Access Condition and Agreement

Each deposit in UEA Digital Repository is protected by copyright and other intellectual property rights, and duplication or sale of all or part of any of the Data Collections is not permitted, except that material may be duplicated by you for your research use or for educational purposes in electronic or print form. You must obtain permission from the copyright holder, usually the author, for any other use. Exceptions only apply where a deposit may be explicitly provided under a stated licence, such as a Creative Commons licence or Open Government licence.

Electronic or print copies may not be offered, whether for sale or otherwise to anyone, unless explicitly stated under a Creative Commons or Open Government license. Unauthorised reproduction, editing or reformatting for resale purposes is explicitly prohibited (except where approved by the copyright holder themselves) and UEA reserves the right to take immediate 'take down' action on behalf of the copyright and/or rights holder if this Access condition of the UEA Digital Repository is breached. Any material in this database has been supplied on the understanding that it is copyright material and that no quotation from the material may be published without proper acknowledgement.

Acknowledgements

I would like to take the opportunity to thank all who had helped me throughout my PhD studies. I would like to thank my primary supervisor Professor Michael Wormstone for his unrelenting support and guidance, and my secondary supervisor Professor Richard Bowater for his advice.

I would also like to thank former and present members of the Norwich Eye Research Group, Dr Andrew Smith, Dr Julie Eldred, Dr Sarah Russell, Yvette Wormstone, for their support and assistance and Richard Evans-Gowing for his histological technical instruction.

A special thank you to the East Anglian Eye Bank for providing donor tissue used in this study and lastly, a big thank you to The Humane Research Trust for funding my PhD..

Table of contents

Abstract	II
Acknowledgements	IV
Table of Contents	V
List of Figures	IX
List of Tables	XII
Abbreviations	XIII
Chapter 1	1
General Introduction	1
1.1 The Eye	1
1.2 Cornea	2
1.21 Cornea Endothelium	3
1.3 The Lens	4
1.31 Cataract	7
1.32 Cataract Surgery	9
1.33 Posterior Capsule Opacification	10
1.4 Oxidative Stress	11
1.41 Antioxidant Systems in the Lens	12
1.5 DNA Damage and Repair	13
1.51 Poly (ADP-ribose) Polymerase.....	16
1.6 Isothiocyanates (ITCs)	18
1.61 Sulforaphane	18
1.7 Aims	21
Chapter 2	
Materials and Methods	23
2.1 Cell Culture	23

2.2 MTS assay	24
2.3 CytoTox-Fluor	24
2.4 Caspase-Glo 3/7	25
2.5 DCFDA assay	25
2.6 svβgal assay	25
2.7 Alkaline Comet assay	26
2.8 Real Time Long Amplicon QPCR	27
2.9 Immunohistochemistry	31

Chapter 3

DNA repair proteins in the anatomical organisation in the human lens

3.1 Introduction	33
3.2 Aims	36
3.3 Results	37
3.31 NHEJ proteins Ku80 and DNA-PK are expressed in human lens epithelium	37
3.32 PARP-1 and PAR are expressed in human lens epithelium	39
3.33 AIF and mitochondria are expressed in human lens epithelium	41
3.34 NHEJ proteins Ku80 and DNA-PK are expressed in the bow region of the human lens	43
3.35 PARP-1 and PAR are expressed in the bow region of the human lens ..	45
3.36 AIF and mitochondria are expressed in the bow region of the human lens	47
3.4 Discussion	49

Chapter 4

Real Time Long Amplicon PCR assay for the detection of DNA damage

4.1 Introduction	52
------------------------	----

4.2 Aims	54
4.3 Results	55
4.31 Demonstration of DNA standards	55
4.32 Melting curve analysis	57
4.33 Optimisation of SYBR Green I dye in master mix	58
4.34 Concentration response curves for DNA damaging	59
4.35 NCS and bleomycin increase DNA strand breaks in FHL124 cells as measured by the comet assay	61
4.36 NCS and bleomycin increase nuclear and mitochondrial DNA lesions in FHL124 cells	62
4.4 Discussion	65

Chapter 5

Protective effects of SFN against an oxidative stress model on corneal

endothelial cells: Implication for cornea tissue storage	69
5.1 Introduction	69
5.2 Aims	72
5.3 Results	73
5.31 H ₂ O ₂ effect on viability in HCEC-12 cells	73
5.32 H ₂ O ₂ effect on cell fate markers in HCEC-12 cells	74
5.33 H ₂ O ₂ effect on ROS and DNA strand breaks in HCEC-12 cells	76
5.34 Determining optimal SFN concentration in HCEC-12 cells	78
5.35 SFN protects cell viability against H ₂ O ₂ induced oxidative stress	79
5.36 SFN reduces H ₂ O ₂ induced cell death and apoptosis	80
5.37 SFN has no effect on cellular ROS induced by H ₂ O ₂ but potentially decreases DNA strand breaks	81

5.38 SFN does protect against H ₂ O ₂ induced nuclear and mitochondrial DNA lesions but does not affect mitochondrial copy number	83
5.4 Discussion	86

Chapter 6

ROS plays a critical role in SFN in induced DNA damage and cell death	91
6.1 Introduction	91
6.2 Aims	92
6.3 Results	94
6.31 SFN reduces FHL124 cell viability	94
6.32 SFN increases ROS in FHL124 cells	95
6.33 SFN increases DNA strand breaks in FHL124 cells	95
6.34 Optimisation of NAC concentration in FHL124 cells	96
6.35 NAC protects FHL124 cell viability from SFN	97
6.36 NAC quenches SFN induced ROS	98
6.37 NAC prevents SFN induced DNA damage	99
6.4 Discussion	102

Chapter 7

General Discussion	105
References	110
Publications	130

List of Figures

Figure 1.1: Cross section of the human eye	2
Figure 1.2: A cross-section of the human cornea	3
Figure 1.3: A diagrammatic cross-section of the human lens	6
Figure 1.4: A diagrammatic cross-section of the human lens	7
Figure 1.5: Types of cataracts based on the position of the opacity in the human lens	8
Figure 1.6: Diagram illustrating PCO	11
Figure 1.7: Non-homologous end joining	15
Figure 1.8: PARP-1 and PAR	17
Figure 1.9: Chemical structure of sulforaphane	18
Figure 1.10: Mechanism of Nrf2 activation by SFN	20
Figure 3.1: Expression of Ku80 and DNA-PK in the central epithelium of the human lens	38
Figure 3.2: Expression of PARP-1 and PAR in the central epithelium of the human lens	40
Figure 3.3: Expression of AIF and mitochondria in the central epithelium of the human lens	42
Figure 3.4: Expression of Ku80 and DNA-PK in the bow region of the human lens	44
Figure 3.5: Expression of PARP-1 and PAR in the bow region of the human lens	46
Figure 3.6: Expression of AIF and mitochondria in the bow region of the human lens	48
Figure 4.1: Amplification of DNA standards	56

Figure 4.2: Melting curves for nuclear and mitochondrial fragments	57
Figure 4.3: Amplification plot of β -Polymerase fragment	58
Figure 4.4: Dose response of NCS and bleomycin treatments on cell viability in FHL124 cells	60
Figure 4.5: DNA strand breaks from treatment of NCS and bleomycin in FHL124 cells	61
Figure 4.6: Lesions/10kb in nuclear and mitochondrial DNA in FHL124 cells treated with NCS	63
Figure 4.7: Lesions/10kb in nuclear and mitochondrial DNA in FHL124 cells treated with bleomycin	64
Figure 5.1: The effect of increasing concentrations of H ₂ O ₂ treatment on cell viability in HCEC-12 cells over 24 h	73
Figure 5.2: Measure of cell death and apoptosis of HCEC-12 cells in response to H ₂ O ₂ treatment after 24 h	75
Figure 5.3: sv β gal activity as a measure of cellular senescence in HCEC-12 cells in response to H ₂ O ₂ treatment after 24 h	76
Figure 5.4: ROS levels in HCEC-12 cells resulting from treatment of H ₂ O ₂ after 2 h	77
Figure 5.5: DNA strand breaks in HCEC-12 cells from treatment with 100 μ M H ₂ O ₂ over 4 h	77
Figure 5.6: The effects of SFN concentration on HCEC-12 cell viability over 24 h and 72 h	78
Figure 5.7: Cell viability of FHL124 cells, pre-treated with 1 μ M and 2 μ M SFN 24 h prior to H ₂ O ₂ treatments after 24 h	79
Figure 5.8: Measure of cell death and apoptosis in HCEC-12 cells pre-treated with 2 μ M SFN 24 h prior to H ₂ O ₂ treatment after 24 h	80

Figure 5.9: svβgal activity as a measure of cellular senescence in HCEC-12 cells pre-treated with 2 μM SFN 24 h prior to H ₂ O ₂ treatments after 24 h	81
Figure 5.10: ROS levels in HCEC-12 cells pre-treated with 2 μM SFN 24 h prior to H ₂ O ₂ treatments after 2 h	82
Figure 5.11: DNA strand breaks in HCEC-12 cells pre-treated with 2 μM SFN 24 h prior to treatment of 100 μM H ₂ O ₂ over 4 h	82
Figure 5.12: Lesions/10kb in nuclear and mitochondrial DNA in HCEC-12 cells pre-treated with 2 μM SFN 24 h prior to treatment of 100μM H ₂ O ₂ over 4 h	84
Figure 5.13: Mitochondrial DNA copy number in HCEC-12 cells pre-treated with 2 μM SFN 24 h prior to treatment of 100μM H ₂ O ₂ over 4 h	85
Figure 6.1: Concentration response of SFN treatment on cell viability in FHL124 cells over 24 h	94
Figure 6.2: ROS levels from treatment of 100 μM SFN in FHL124 cells after 2 h	95
Figure 6.3: DNA strand breaks from treatment of 100 μM SFN in FHL124 cells over 4 h	96
Figure 6.4: The effect of increasing concentrations of NAC treatment on cell viability in FHL124 cells over 24 h	97
Figure 6.5: Cell viability of FHL124 cells after pre-treatment of different NAC concentrations 1 h prior to SFN treatment after 24 h	98
Figure 6.6: ROS levels in FHL124 cells pre-treated with NAC 1 h prior to treatment of SFN after 2 h	99
Figure 6.7: DNA strand breaks in FHL124 cells pre-treated with NAC 1 h prior to treatment of 100μM SFN after 2 h	100
Figure 6.8: Lesions/10kb in nuclear and mitochondrial DNA in FHL124 cells pre-treated with NAC 1 h prior to treatment of 100 μM SFN after 2 h	101

List of Tables

Table 1.1: Reagent reaction mix for 50 μ L total volume	29
Table 1.2: List primers used in Real Time LA QPCR	30
Table 1.3 Summary of antibodies used for immunohistochemistry	32

Abbreviations

•OH	Hydroxyl radical
AIF	Apoptosis-inducing factor
ATP	Adenosine 5'-triphosphate
BER	Base excision repair
DMEK	Descemet's membrane and endothelial keratoplasty
DNA-PK	DNA protein kinase
DSB	Double-strand break
ECD	Endothelial cell density
EMEM	Eagle's Minimum Essential Medium
FHL124	Fetal human lens cell 124
GSH	Reduced glutathione
H ₂ O ₂	Hydrogen peroxide
HCEC-12	Human corneal endothelial cell-12
IOL	Intraocular lens
ITC	Isothiocyanate
Keap1	Kelch-like ECH-associated protein 1
LA QPCR	Long amplicon quantitative polymerase chain reaction
LEC	Lens epithelial cell
NAC	N-acetylcysteine
NER	Nucleotide excision repair
NHEJ	Non-homologous end joining
Nrf2	Nuclear factor erythroid 2-related factor 2
O ₂ –	Superoxide anion
PAR	Poly (ADP-ribose)

PARP	Poly(ADP-ribose) polymerase
PCO	Posterior capsule opacification
PK	Penetrating keratoplasty
ROS	Reactive oxygen species
SFN	Sulforaphane
SSB	Single-strand break

Chapter 1

General Introduction

1.1 The Eye

The human eye is a sense organ that facilitates vision and contains many components to achieve this. The globe of the eye consists of a white outer layer of connective tissue known as the sclera which is covered by the conjunctiva, a mucous membrane that maintains moisture. The anterior of the eye houses the cornea; a transparent lamellar structure that permits light to enter the eye. The iris contracts to control the amount of light entering the eye via the pupil. This contraction and dilation are performed by the pupillae muscles of the iris, which regulates the amount of light let in. Behind the iris sits the lens; a transparent crystalline structure that focuses light onto the retina, a tissue which consists of photoreceptors that convert light into neural impulses (Fig 1.1). Anterior to the lens is the clear aqueous humour, (whose fluid is continually secreted by the ciliary body) which provides nutrient to both cornea and lens (Forrester et al., 2016). Behind the lens is the vitreous humour, a gelatinous mass that fills the space between the lens and the retina. It is essential because it provides nutrition to several avascular ocular tissues including the lens and the corneal endothelium. The aqueous and vitreous humours are separated by the lens and suspensory ligaments (Forrester et al., 2016). The lens is attached to the ciliary body by suspensory ligaments known as the zonules of Zinn. The vitreous provides support and as a store for metabolites of the lens and retina. The retina is responsible for converting light signals from the lens into neuronal impulses that are then transmitted to the brain, where vision is processed. These nerve impulses are produced from light sensitive pigment rhodopsin known as rods and cones via the optical nerve (Forrester et al., 2016).

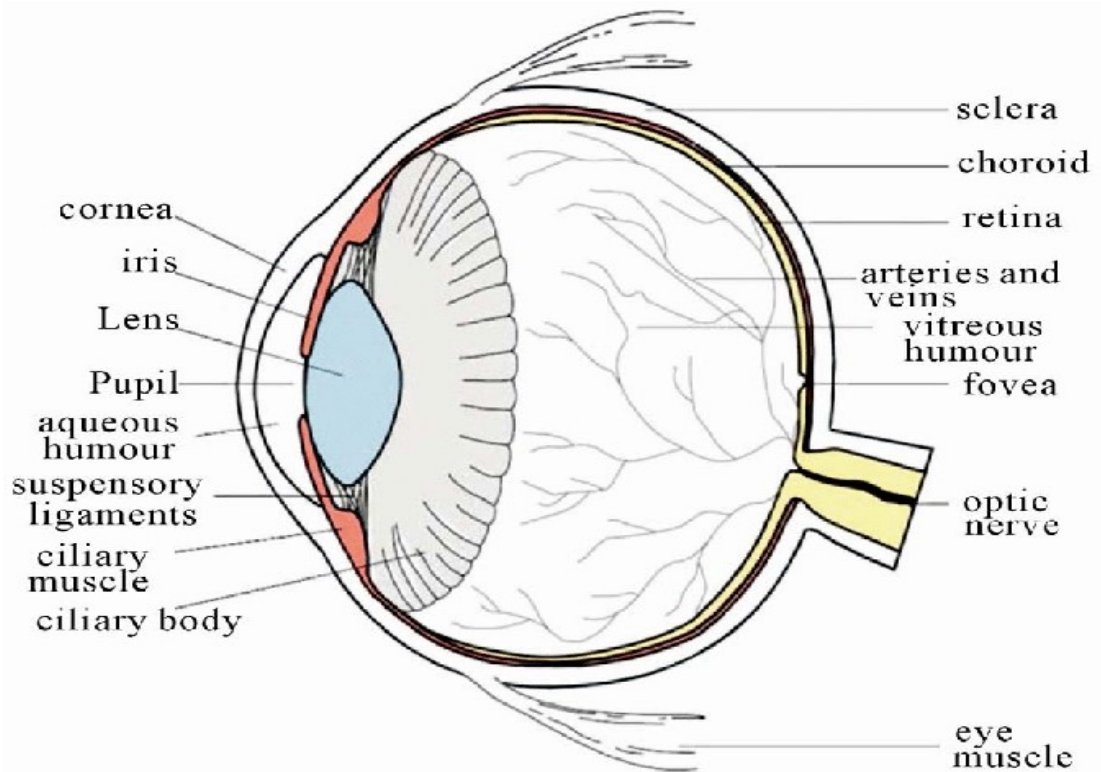


Figure 1.1 Cross section of the human eye (Mansour et al., 2013)

1.2 Cornea

The cornea is a convex transparent, innervated avascular organ that provides most of the refractive power of the eye. It also functions as a protective barrier to the anterior surface of the eye (Sridhar, 2018). It derives nutrients from tear fluid and posteriorly from the aqueous humour and its structure consists of multiple layers. The outermost layer is the epithelium, comprised of nonkeratinized stratified squamous cells, 5-7 cells thick. These cells have a high turnover rate and have a lifespan of 7-10 days (Sridhar, 2018). The next layer is the Bowman's membrane which consists mainly of Type I and V collagen and proteoglycans. Below this is the corneal stroma that provides structural integrity comprising up to 85% of the corneal thickness, primarily being made up by type 1 collagen

fibrils. The next layer is Descemet's membrane which consists of type IV collagen and laminin and is continuously secreted by the last layer, the endothelium (Fig 1.2).

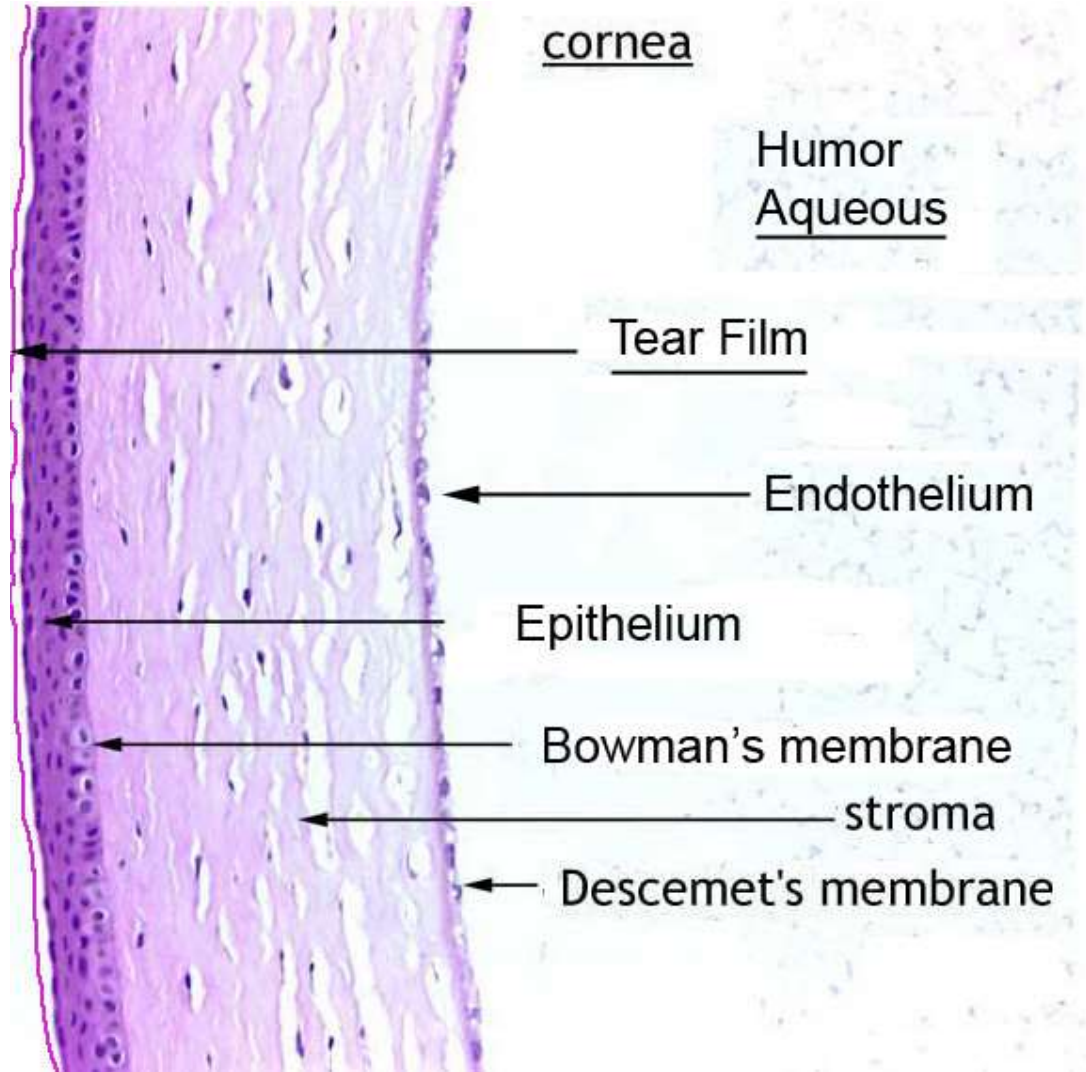


Figure 1.2 A cross-section of the human cornea (Díaz, 2009).

1.21 Corneal Endothelium

The corneal endothelium is made up of a single monolayer of hexagonal cells which are 5 μM in depth and with a diameter of 20 μM . These cells maintain stromal deuterence by

using Na⁺ K⁺ ATPase pumps to regulate cornea water content, maintaining transparency in the cornea. Corneal endothelial cells form a barrier but permits water and substrates from the aqueous humour and are in arrested G1 phase of the cell cycle and seldom divide (Bourne, 2003). Because of this, endothelial cell number decline with age and contributes to loss of function to the cornea.

Corneal opacities account for 4-5% of blindness worldwide (Resnikoff et al., 2004), the major causes of which include corneal edema, keratoconus and corneal hereditary diseases such as Fuchs' dystrophy. In the majority of cases the only viable treatment is a cornea transplant; the replacement of the affected corneal tissue with that of a healthy donor.

The two most common types of corneal transplant are penetrating keratoplasty (PK), replacement of the full corneal thickness including Descemet's membrane and endothelial keratoplasty (DMEK), the replacement of the endothelial layer which accounts for one third of all corneal transplants (Gain et al., 2016).

1.3 The Lens

The lens is an avascular and non-innervated organ whose primary function is to focus light onto the retina. The lens is surrounded by a collagen capsule which acts as a barrier to diffusion and assists in shaping the lens during accommodation. This capsule varies in thickness from 2-28 μ M, with it being thickest at the equator. The lens capsule is continually produced throughout life anteriorly by the epithelium and posteriorly by the fibre cells (Forrester, 2016).

The lens epithelial and fibre cells are the two distinct cell types that comprises the lens. The anterior is covered by a single monolayer of cuboidal epithelial cells which are bathed by the aqueous humour from which it derives its nutrients. The lens epithelium maintains

lens transparency via Na⁺/K⁺-ATPase pumps and regulates most of the homeostatic functions of the lens. Central lens epithelial cells are non-dividing and only proliferate and divide at the equator before migrating down and inwards from the equator and differentiate into lens fibre cells that form the bulk of the lens (Fig 1.3). Newly formed fibre cells progressively push towards the centre of the lens forming tightly packed concentric layers. Fibroblast growth factors (FGF) form an anterior-posterior gradient that influences this epithelial cell differentiation (Fig 1.4) (Duncan et al., 1997; Tholozan and Quinlan, 2007). The lens fibre cells are denucleated, elongated cells primarily comprised of transparent, water-soluble proteins called crystallins (Andley, 2007; Tholozan and Quinlan, 2007). During differentiation, fibre cells lose organelles leading to an organelle free zone in the lens. The crystallins form approximately 90% of the water-soluble proteins in the lens and create the refractive index necessary to focus light onto the retina.

The lens fibre cells contain high concentration of crystallin proteins α , β and γ that contribute to lens transparency, maintaining the lens' refractive index (Hejtmancik and Shiels, 2015). α crystallins act as molecular chaperones that prevent aberrant protein interactions functioning as protective proteins against stress (Andley, 2007). The lens fibre cells are reliant on the epithelium. Disruption in the epithelium render proteins of the lens susceptible to damage and lens as a whole susceptible to a loss of transparency, termed cataract.

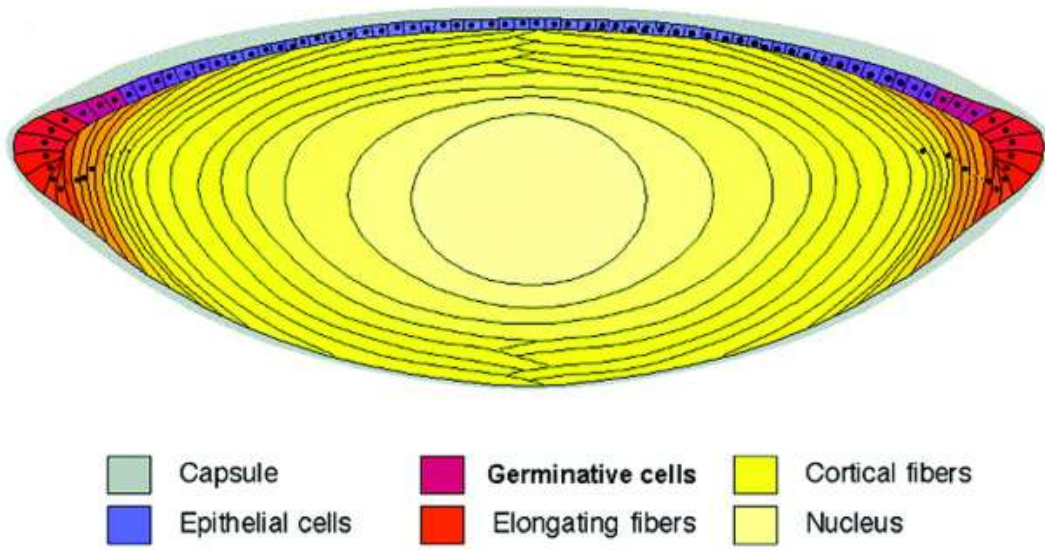


Figure 1.3 A diagrammatic cross-section of the human lens (Maidment et al., 2004).

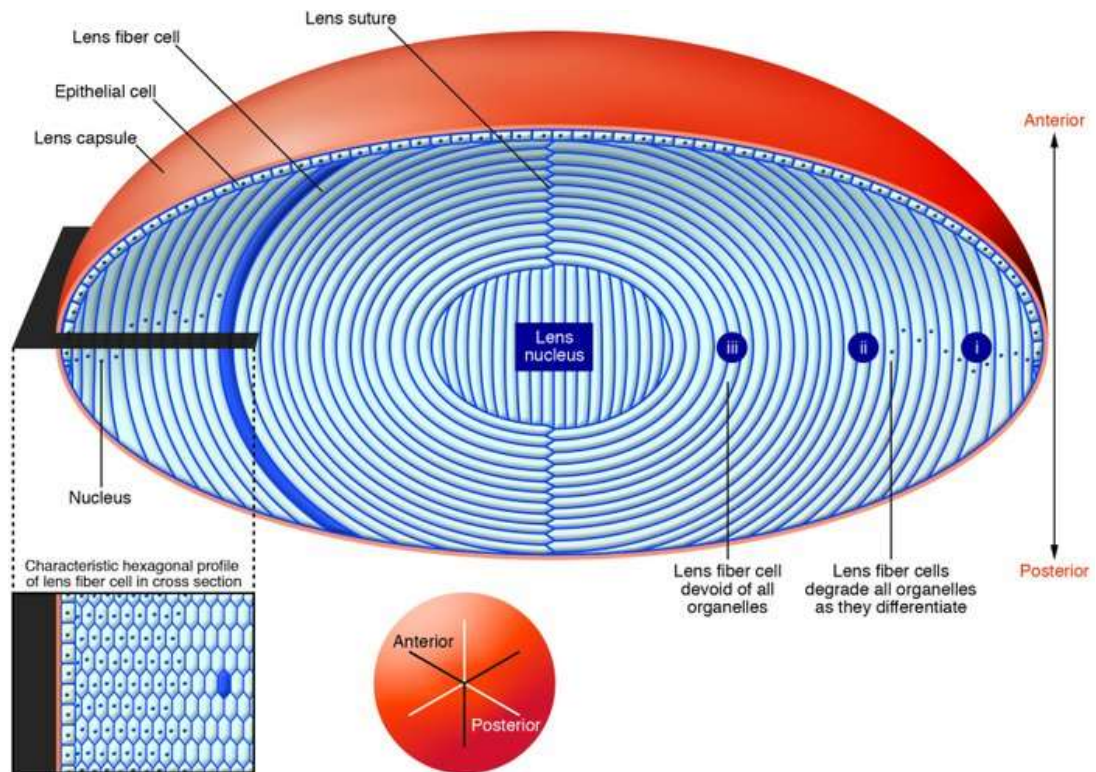


Figure 1.4 A diagrammatic cross-section of the human lens (Song et al., 2009).

1.31 Cataract

Cataract is the leading cause of blindness globally and is defined as an opacity in the lens (Michael and Bron, 2011). Predominantly it is an age-related disease, whilst progression of cataracts is slow, if left untreated, eventually blinding may occur. Some other factors also contribute to cataract, such as UV-B exposure, and ionizing radiation (Allen and Vasavada, 2006). The World Health Organisation states that cataract accounts for 39.1% of all blindness worldwide (Resnikoff et al., 2008). In the United States, the prevalence of cataract is approximately 5% at age 65. This increases to around 50% for people older than 75 years (Klein, 1993) with cataract rates doubling after each decade.

Cataract is defined as any opacity or clouding of the lens which impacts vision when situated along the visual axis. There are several forms of age-related cataract and classification is based on their location within the lens (Figure 1.5). The most common forms of cataract are nuclear sclerosis cataract, cortical cataract, anterior sub-capsular cataract and posterior sub-capsular cataract.

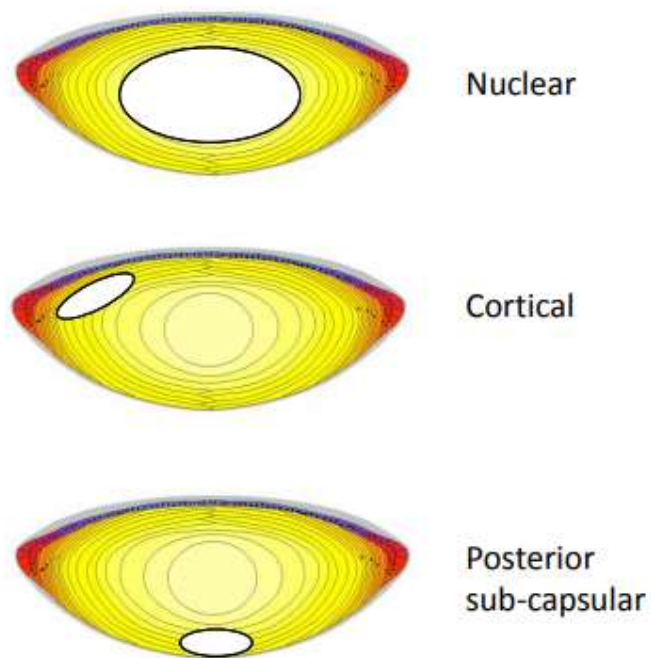


Figure 1.5 Types of cataracts based on the position of the opacity in the human lens (Wormstone et al., 2006).

These cataracts may be caused by a disruption in the lens epithelium which helps maintains lens transparency leading to modification to the crystalline proteins in the lens fibre cells (Michael and Bron, 2011). It is also associated with aging with a marked increase of cataract formation from the age of 50 (Duncan et al., 1997). Older fibres of the lens are not replaced and so structural changes to the fibres occur which cannot be reversed by the production of newer fibres, accumulation occurs and transparency is reduced.

Nuclear cataract occurs in the nucleus of the lens normally caused by post-translational modification to the lens crystallins. It is also associated with deposition of brown or yellow pigment within the lens over time. Cortical cataract forms in the lens cortex, which is where newly formed lens fibre cells are situated. With age, changes in membrane permeability causes osmotic imbalances and protein aggregation resulting in white spokes that interrupt the visual axis (Bollinger and Langston, 2008). Posterior subcapsular cataract occurs as an opacity at the back of the lens, under the capsule often in the visual axis.

1.32 Cataract surgery

Surgical intervention is currently the only procedure to treat cataract and is the most commonly performed surgical procedure in the world (Keeffe and Taylor, 1996).

Modern cataract surgery involves phacoemulsification to break up and remove the cataractous fibre cell mass. A small incision of approximately 2 mm is made at the edge of the cornea to allow access to the lens capsule, in which a capsulorhexis (a small circular tear approximately 5 mm in diameter) is made allowing access to the lens fibres. An ultrasonic probe is inserted, which breaks up and removes the cataractous lens to create a capsular bag consisting of the posterior capsule and the remaining anterior capsule minus the capsulorhexis into which an artificial intraocular lens (IOL) is inserted. This restores

refraction and free passage of light to the retina (Asbell et al., 2005; Wormstone et al., 2009). Current treatment is the replacement of the opacified lens with an artificial intraocular lens (IOL).

1.33 Posterior capsule opacification

Posterior capsule opacification (PCO) is a common complication of cataract surgery. Residual epithelial cells left over from surgery have an induced inflammatory response from the trauma and cells grow and encroach onto the visual axis on the posterior lens capsule causing light scatter producing a “secondary cataract”. These are presented as hypertrophic cells known as Elschnig rings and capsular bag wrinkling (Fig 1.6).

Presently, the only treatment for cataract is the surgical removal of the affected lens and its replacement with an artificial intraocular lens (IOL). During this process, an incision is made in the anterior lens capsule and the lens fibres removed via emulsification, leaving behind a capsular bag that the IOL can be housed in, restoring visual clarity (Wormstone, 2009).

PCO can cause decreased visual acuity in 20-40 % of patients, 5 years post-surgery (Awasthi et al., 2009). Currently, the only treatment is a corrective procedure using a Nd:YAG laser to restore visual function (Meacock et al., 2003). This is an expensive procedure and not without medical risk, imposing a significant economic impact (Aaronson et al., 2019). Thus, therapies for the prevention of PCO is an important area of research.

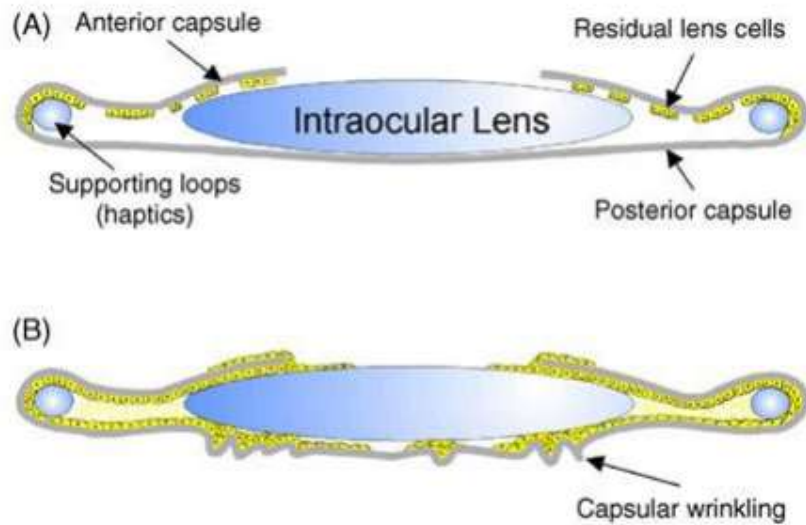


Figure 1.6 Diagram illustrating PCO. (A) During cataract surgery the cataractous lens is removed creating a capsular bag into which an IOL is inserted, restoring free passage of light. (B) Not all epithelial cells are removed and the remaining epithelial cells grow and invade the normally cell free posterior capsule causing contraction or wrinkling, producing light scatter and secondary loss of vision (Wormstone et al., 2002).

1.4 Oxidative stress

Cataract may be a consequence of oxidative stress, an imbalance of reactive oxygen species (ROS) and antioxidants in a cell leading to an excess of free radicals that puts the cell under stress, damaging cellular components and potentially leading to cell fate changes such as senescence or death. ROS molecules include the superoxide anion (O_2^-), hydroxyl radical ($\bullet OH$) and hydrogen peroxide (H_2O_2). Contrary to O_2^- and $\bullet OH$, which are extremely unstable and react at or near their site of formation, H_2O_2 is less reactive, freely diffusible and relatively long-lived (Linetsky and Ortwerth, 1995). ROS are the mediators of oxidative stress; they are continuously generated and can arise through endogenous processes such as cellular metabolism or exogenously via processes such as UV-induced photochemical reactions or exposure to ionizing radiation (Cooke et al.,

2003). The damage can consist of protein modifications, lipid peroxidation and DNA fragmentation, all of which have been proposed to contribute to cataractogenesis. The lens is able to defend itself against oxidation using antioxidants from either enzymatic or non-enzymatic systems (Kise et al., 1994).

1.41 Antioxidant systems in the lens

High levels of ROS, either due to their increased production, or due to a decrease in the cell's ability to eliminate them, leads to the state of oxidative stress and subsequent cellular damage. The lens possesses an array of antioxidant defences to protect it from oxidative damage. Primary antioxidants include non-enzymatic (e.g., glutathione, vitamin C, vitamin E and carotenoids) and enzymatic (e.g., superoxide dismutase, glutathione peroxidase and catalase) systems (Michael and Bron, 2011).

Reduced glutathione (GSH) is the main antioxidant in the lens; however, its concentration declines with age, reducing the effectiveness of lens antioxidant defences (Michael and Bron, 2011). As GSH is oxidised it rapidly becomes recycled by glutathione reductase using NADPH as a reducing agent. With age, however, production of GSH and its reduction by glutathione reductase declines, potentially rendering proteins of the lens susceptible to oxidative stress.

With increasing oxidative stress, proteins in the lens become thiolated, leading to oxidation of proteins and the formation of protein aggregates, disrupting the transparency of the lens causing opacification.

In the cornea, oxidative stress is implicated in the pathology of numerous disorders, including endotheliopathies such as Fuchs' dystrophy (Shoham et al., 2008).

1.5 DNA damage and Repair

Excess ROS from oxidative stress causes damage to cellular components including DNA. Oxidative stress is an imbalance between pro and antioxidants. Sources of stress can be from endogenous or exogenous sites. Endogenous stress may arise from metabolism whereas exogenous may be UV light or ionising radiation.

DNA is constantly bombarded with ROS generating DNA lesions such as strand breaks or abasic sites. Approximately, there are 10,000 DNA lesions per cell per day and without repair of this damage DNA mutations may occur following replication or cell death may occur. However, DNA repair pathways have evolved to counter this problem and maintain a stable genome, thus ensuring the proper functioning of the cell. Types of DNA repair mechanisms can be defined by either single strand or double strand repair.

The base excision repair (BER) pathway is responsible for single base repair in DNA, this includes oxidised bases, single strand breaks (SSB) or abasic sites. BER undergoes either long patch or short patch repair. Initially BER is initiated by a DNA glycosylate that recognises and removes the damaged base. This process involves the endonuclease APE1, DNA polymerase β and DNA ligase. Long patch repair involves the repair of 2-10 nucleotides but uses different proteins to repair DNA, these include DNA polymerase δ/ϵ , flap endonuclease FEN1 and ligase I (Krokan and Bjørås, 2013).

Nucleotide excision repair (NER) excised bulky DNA adducts primarily caused by UV light. When the damage is recognised, removal of a short single stranded segment of DNA is removed. This is recognised by complexes XPC and XPE. Once excised, DNA polymerase replaces the excised segment (Jackson and Bartek, 2009). DNA helicases XPB and XPD unwind the DNA either side of the lesion with RPA binding to the single stranded DNA to stabilise it. Endonucleases XPG and XPF remove the lesion by producing

a single strand break to each side. The gap is then filled and sealed by a DNA polymerase and a DNA ligase (Lombard et al., 2005).

Cells have numerous DNA repair enzymes to repair specific type of DNA damage. DNA double strand breaks (DSB) can be generated from exogenous sources of DNA damage such as ionizing radiation and endogenous sources such as ROS produced during cellular metabolism. The predominant pathway for the repair of DNA double strand breaks is non-homologous end joining (NHEJ) and occurs primarily during the G1 phase of the cell cycle. Another pathway, Homologous recombination (HR) is active in the repairs of DSBs in the S and G2 phases of the cell cycle.

NHEJ does not require a template strand and involves the re-ligation of DNA double strand breaks without need for a comparative DNA sequence. The key proteins involved are Ku70, Ku80, ligase IV, XRCC4, DNA-PKcs and Artemis. Ku70 and Ku80 bind as a heterodimer to the DNA either side of the break allowing recruitment of DNA-PKcs (DNA dependent kinase catalytic subunit) which together with the Ku70/Ku80 heterodimer forms DNA-PK (DNA protein kinase). DNA-PK phosphorylates and activates itself and other proteins of NHEJ such as Artemis, a nuclease which processes DNA ends unable to be directly re-joined. Activated DNA-PK is also auto-phosphorylated, inducing disassembly of the NHEJ complex allowing for the ligation of the broken DNA ends by the ligase IV-Xrcc4 complex (Fig. 1.7) (Costantini et al., 2007; Lombard et al., 2005).

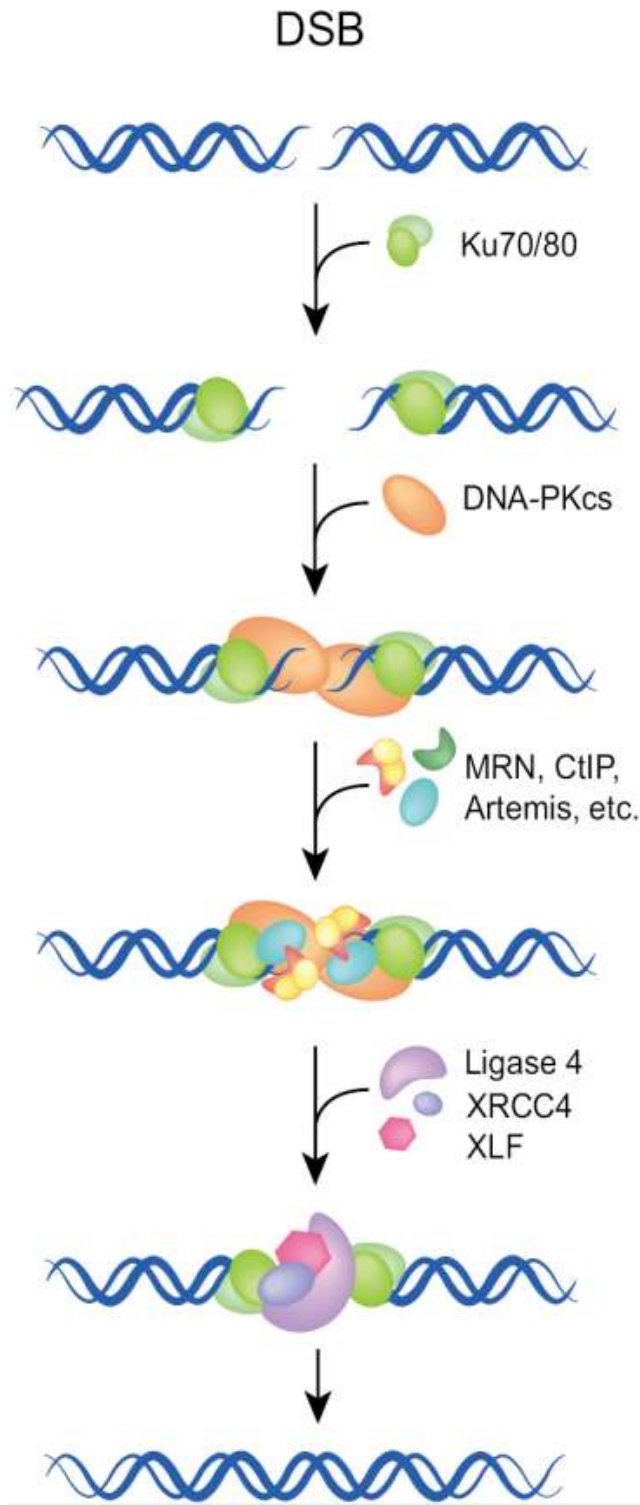


Figure 1.7 Non-homologous end joining (Dueva and Iliakis, 2013).

1.51 Poly(ADP-ribose) polymerase

Poly(ADP-ribose) polymerases (PARPs) are involved in single strand DNA repair. They catalyse the post translational modification of their target or acceptor proteins by the addition of ADP-ribose polymers which are synthesised using nicotinamide adenine dinucleotide (NAD⁺) (Fig1.8). The poly(ADP-ribose) (PAR) polymer (which can reach up to hundreds of units in length) possesses a negative charge and therefore when bound to target proteins they alter their structure and function. The process of poly(ADP-ribosylation) is a reversible process; PAR polymers are rapidly degraded by poly(ADP-ribose) glycohydrolase (PARG) (Sousa et al., 2012).

Activation of PARP and hence PAR production is caused by DNA damage. PARP-1 is the most abundant of the PARP enzymes and is the primary PARP protein in response to DNA damage. PARP-1 is approximately 113 kDa and contains three functional domains: DNA binding, auto modification and catalytic. Upon DNA damage, including both single and double DNA strand breaks, production of PAR is increased up to 500 times (Heeres and Hergenrother, 2007). Once bound to the strand break PARP-1 auto PARylises allowing recruitment of other DNA repair proteins. Interestingly they interact with the NHEJ proteins Ku70, Ku80, DNA ligase IV and DNA-PK (Sousa et al., 2012).

Inhibition of PARP in the human lens leads to opacification from H₂O₂ induced oxidative stress (Smith et al., 2016). Non-homologous end-joining (NHEJ) is a DNA repair system that repairs double stranded DNA breaks (DSB). Inhibition of one of its protein complexes Ku80, thus disrupting the ability to repair DSBs, also leads to lens opacification from H₂O₂ induced oxidative stress in the human lens (Smith et al., 2015).

Therefore, DNA damage whether from exogenous sources or oxidative stress may play role in changing cell physiological fate in the eye.

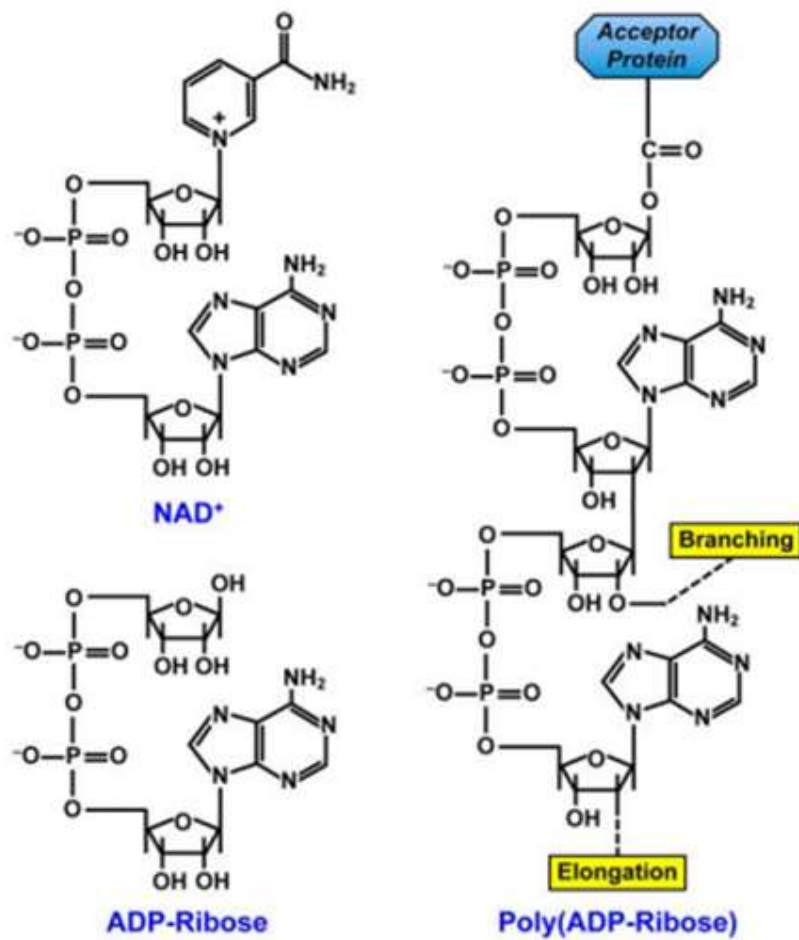


Figure 1.8 PARP-1 and PAR (Luo and Kraus, 2012).

1.6 Isothiocyanates (ITCs)

Isothiocyanates are characterized by the presence of an N=C=S functional group which is found in a variety of cruciferous vegetables. One of these, Sulforaphane (SFN), naturally present in cruciferous vegetables, has been well studied for its protective and damaging properties. Formed from the conversion of glucosinolates, it has been linked to protection against cancer, toxicity and certain diseases (Vanduchova et al., 2018). All glucosinolates contain a common glycone moiety and a variable aglycone side chain derived from amino acids. They are hydrolysed to an aglycone R-C (-SH) =N-O-SO₃ – by the enzyme myrosinase.

1.61 Sulforaphane

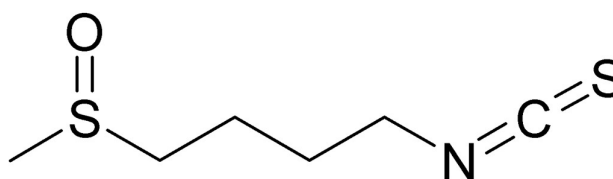


Figure 1.9 Chemical structure of sulforaphane (SFN) (Joozdani et al., 2015).

Sulforaphane (SFN, R-1-isothiocyanato-4-methylsulfinylbutane) is a dietary phytochemical with low toxicity commonly and widely consumed with cruciferous vegetables and many dietary nutraceuticals, and its administration to humans is usually well tolerated (Fig. 1.9).

Upon entry into a cell SFN is conjugated with glutathione, a process that is catalysed by glutathione-s-transferases. A series of additional steps then follow: γ -glutamyl

transpeptidase cleaves glutamine and glycine is cleaved by cysteinylglycinase giving rise to a N-acetylcysteine conjugate of SFN known as mercapturic acid (Bricker et al., 2014)

SFN has demonstrated chemoprotective effects through multiple mechanisms such as phase I enzyme inhibition, induction of apoptosis and cell cycle arrest. SFNs cytoprotective mechanisms have been shown by the inducement of the phase II detoxification enzymes.

Phase I and phase II enzymes are involved in drug metabolism. Phase I enzymes are responsible for oxidation, reduction and hydrolysis of xenobiotics, which is the first step in their detoxification. However, pro-carcinogens can result from this process which can form damaging adducts with DNA, RNA, and proteins. SFN has been shown to inhibit phase I enzymes such as CYP3A4 in human hepatocytes, thereby reducing the frequency of carcinogen production (Myzak and Dashwood, 2006).

Phase II enzymes detoxify the xenobiotic metabolites from phase I enzyme reactions by conjugation, reducing their reactivity and allow their excretion. SFN is the most potent naturally occurring phase II detoxification enzyme inducer in both animals and humans (Fahey et al., 2002; Talalay, 2000). SFN has been found to induce the activity of phase II enzymes QR, GST- α and γ - glutamylcysteine synthetase and increase intracellular glutathione synthesis in human prostate cancer lines (Brooks et al., 2001) and significantly induce both UGT1A1 and GSTA1 mRNA and protein levels in human hepatoma cells and colorectal adenocarcinoma cells (Basten et al., 2002).

Kelch-like ECH-associated protein 1 (Keap1) and nuclear factor erythroid 2-related factor 2 (Nrf2) regulate gene expression of phase II detoxification enzymes. Nrf2 is sequestered in the cytoplasm by Keap1. Upon cell injury, Nrf2 is released from Keap1 and translocates to the nucleus and binds to the antioxidant response element activating phase II enzyme

transcription. SFN has been shown to induce Nrf2 translocation by reacting with the thiol group of the Keap1 in the cytoplasm, dissociating it with Nrf2 (Fig 1.10) (Dinkova-Kostova et al., 2017).

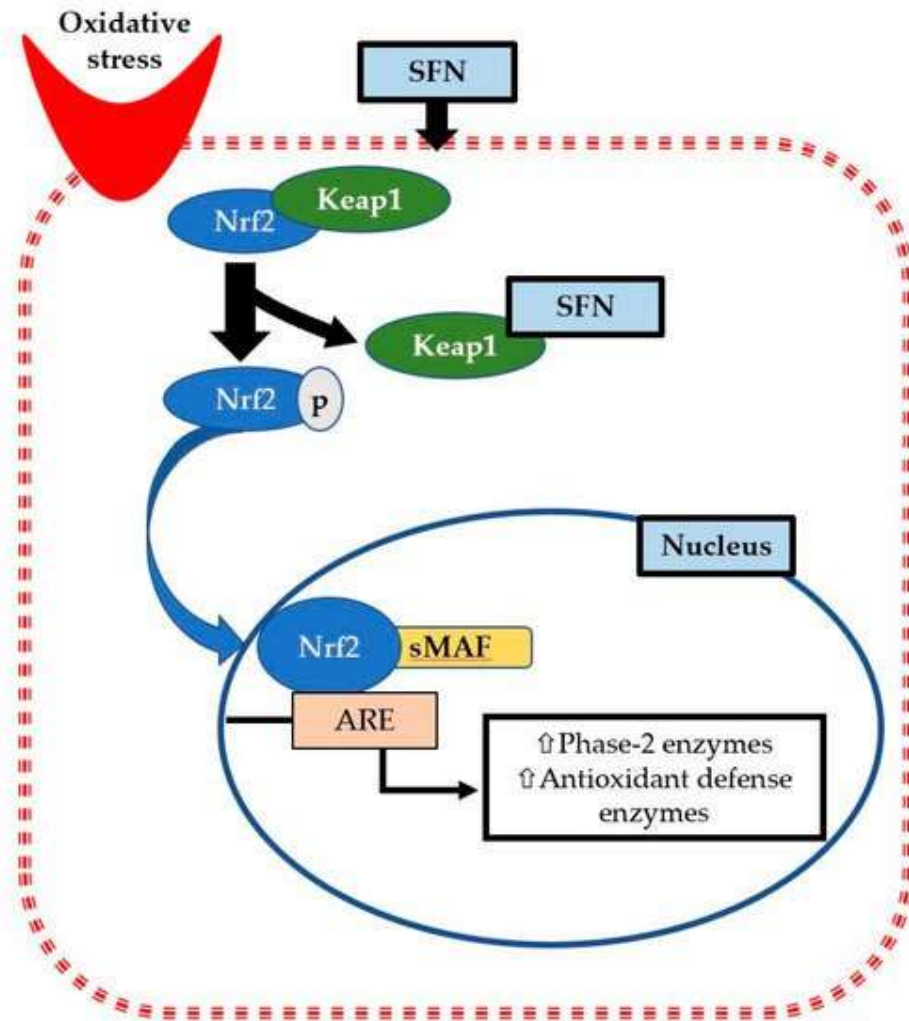


Figure 1.10 Mechanism of Nrf2 activation by SFN (Ruhee and Suzuki, 2020).

1.7 Aims

The human lens epithelium is subjected to an array of genotoxic stressors that may impact its ability to maintain its function and preserve lens clarity. As a result, damaged lens epithelial cell DNA are repaired by specific DNA repair systems depending on the type of lesion that has occurred. PARP-1 is involved in SSB repair, whereas DSBs are primarily repaired by NHEJ which involves Ku80 and DNA-PK. Research in this area in the human lens is limited, therefore studies may be beneficial.

In the bow region of the lens, in a process that is not fully understood, epithelial to lens fibre transition results in the breakdown and loss of nuclei. Therefore, expression of DNA repair enzymes may be perturbed prior to denucleation, preventing the repair of chromatin, thus permitting the lens epithelium to lens fibre cell transition to occur. The PARP-1 associated caspase independent cell death pathway, parthanatos involving AIF may also present a role in this 'attenuated apoptosis'.

DNA damage is of a vital research importance as it negatively impacts cell function and is implicated in many diseases. Current assays to measure DNA damage are usually limited to only specific DNA lesions in nuclear DNA. A quantitative PCR based assay was developed to detect both nuclear and mitochondrial DNA damage in tissues and cells. However, there are drawbacks to this assay and developing it to a Real Time quantitative PCR assay will significantly reduce assay time and increase throughput and accuracy.

SFN has differing effects on lens epithelial cells that are concentration dependant. It exhibits cytotoxic effects at high concentrations ($\geq 10 \mu\text{M}$) and shown to induce ER stress and increase cell death in lens epithelial cells and may have potential therapeutic use for PCO. Generation of ROS may be a mechanism by which SFN mediates its cytotoxic effects.

At lower concentrations ($\leq 2 \mu\text{M}$), SFN has been shown to be cytoprotective against H_2O_2 induced oxidative stress, which can lead to DNA damage and cell death in lens cells. Cornea donor tissue are reliant upon endothelial cells to maintain tissue function and clarity but are subjected to stressors such as oxidative stress whilst in storage media. Treatment with SFN may protect against H_2O_2 induced DNA damage and cell death in cornea endothelial cells. This may demonstrate a potential therapeutic use of SFN as an additive in cornea storage media to help mitigate the negative effects of oxidative stress and help preserve cornea storage tissue.

The aims of this thesis are:

- 1) To identify the expression of DNA repair proteins Ku80, DNA-PK, PARP-1 and its associated PAR polymer and AIF in the central epithelium and bow regions of the human lens and elucidate their involvement in lens epithelial to fibre cell transition.
- 2) To develop a Real Time long amplicon QPCR assay to detect DNA damage that improves the scope and throughput of an established qPCR based DNA damage assay.
- 3) To determine if ROS plays a role in the cytotoxic effects of SFN to lens epithelial cells in relation to PCO management.
- 4) To determine if SFN can protect against DNA damage and negative cell fate outcomes against oxidative stress in HCEC-12 cells and explore its potential use as an additive to reduce endothelial cell loss in human donor corneas.

Chapter 2

Materials and Methods

2.1 Cell Culture

Fetal human lens 124 cell line (FHL124) is a non-virally transformed lens epithelial cell line from human capsule epithelial explants (Reddan et al., 1999). They present 99.5% homology with native lens epithelium (Wormstone et al., 2004). FHL124 cells were cultured in Eagle's Minimum Essential Medium (EMEM) (Gibco, UK) with 5% v/v fetal calf serum (FCS) (Gibco, UK) and 50 µg/mL gentamicin (Sigma, UK) at 35 °C in 5% CO₂ and 95% air.

FHL124 cells were seeded onto 96 well plates at 5000 cells per well for the MTS assay, 50,000 cells per 35 mm tissue culture plates for the alkaline comet assay and Real Time long amplicon assay. Medium was replaced with EMEM only, 24 h prior to experimental conditions.

Human corneal endothelial cells-12 (HCEC-12) is a corneal endothelial cell line virally transformed using a plasmid encoding large and small SV40 T-antigen from corneal human donor tissue (Valtink et al., 2008). HCEC-12 cells were cultured in F99 medium (Sigma, UK) and medium 199 (Sigma, UK) at a 1:1 ratio with 5% v/v FCS and 50 µg/mL gentamicin.

HCEC-12 cells were seeded onto 96 well plates at 7500 per well for MTS, CytoTox-Fluor, Caspase-Glo, svβgal and DCFDA assays and 100,000 cells per dish on 35 mm tissue culture plates for the alkaline comet assay and Real Time long amplicon assay. Medium

was replaced with F99 and medium 199 only, at a 1:1 ratio, 24 h prior to experimental conditions.

2.2 MTS assay

MTS (CellTiter 96 Aqueous; Promega, UK) is a cell proliferation assay. It is a colorimetric based method used to determine viable cells based on the conversion of a tetrazolium salt into a formazan product. Absorbance readings are proportionate to the number of living cells. The assay was used in accordance with the manufacturer's guidelines.

Cells seeded onto 96 wells plates had medium replaced with EMEM only, 24 h prior to experimental conditions. At experimental endpoint, EMEM in wells were aspirated and replaced with 100 μ L fresh EMEM mixed with the MTS reagent at a 10:1 ratio and incubated for 1 h. Absorbance was read with a FLUOstar Omega plate reader (BMG LabTech, UK) at 490nm and the reagent mix in empty wells served as blank for all subsequent measurements. Cell viability was expressed as a percentage of untreated controls.

2.3 CytoTox-Fluor

CytoTox-Fluor (Promega, UK) is a fluorescent assay that measures a relative number of dead cells. It uses a fluorogenic peptide substrate (bis-alanyl-alanyl-phenylalanyl-rhodamine 110; bis-AAF-R110) to measure dead cell protease activity and cannot cross into cells with intact membranes and therefore gives no signal for live cells.

Cells seeded onto 96 wells plates had medium replaced with EMEM only, 24 h prior to experimental conditions. At experimental endpoint, EMEM in wells were aspirated and replaced with 100 μ L fresh EMEM mixed with the CytoTox-Fluor reagent at a 10:1 ratio

and incubated for 1 h. Fluorescence was read on FLUOstar Omega plate reader at 485nm_{ex}/520nm_{em} and readings expressed as a percentage of untreated controls.

2.3 Caspase-Glo 3/7

Caspase-Glo 3/7 (Promega, UK) is a luminescent assay that measures caspase 3 and 7 activity in cells using a proprietary luciferase. The assay was used in accordance with the manufacturer's guidelines. Briefly, Cells seeded onto 96 well plates had medium replaced with EMEM only, 24 h prior to experimental conditions. At experimental endpoint, EMEM in wells were aspirated and 100 µL Caspase-Glo reagent was added to each well, incubated at room temperature for 30 mins and luminescence read on FLUOstar Omega plate reader.

2.4 DCFDA assay

DCFDA (Abcam, UK) is an assay for the detection of ROS. It uses the fluorogenic dye 2',7' -dichlorofluorescein diacetate which is deacetylated in the cell and oxidised by ROS, emitting fluorescence. The assay was used in accordance with the manufacturer's guidelines and plates were read on FLUOstar Omega plate reader at 485nm_{ex}/520nm_{em} and readings expressed as percentage of untreated controls.

2.5 svβgal assay

Cellular Senescence Activity Assay (Enzo Life Sciences, UK) measures svβgal activity using a fluorometric assay. The assay was used in accordance with the manufacturer's

guidelines on 96 well plates and read on FLUOstar Omega plate reader at 360nm_{ex}/465nm_{em}. Readings expressed as relative to untreated controls.

2.6 Alkaline comet assay

The alkaline comet assay, also known as single cell gel electrophoresis (SCGE), is a technique for the detection of DNA strand breaks in cells. At the end of experimental conditions, cells on 35 mm dishes were washed with ice cold phosphate buffered saline (PBS), harvested and counted, then re-suspended in PBS with 10% DMSO and stored at -80 °C before the start of the assay.

20,000 cells per sample was centrifuged at 4 °C at 3000 rpm for five minutes. Cells were then re-suspended in 0.6% low melting point agarose (Sigma, UK), then 80 µL was placed in duplicate onto slides pre-coated with 1% agarose and covered with a coverslip and allowed to set on ice for 10 minutes. Coverslips were removed and slides were placed in ice cold lysis buffer (100mM disodium EDTA (Fisher Scientific, UK), 2.5 M NaCl (Fisher Scientific, UK), 10 mM Tris-HCl (Fisher Scientific, UK)) at a pH of 10 with 1% triton-x-100 for one hour. Slides were then washed with ice cold distilled H₂O twice for 10 minutes each, before being placed into a flatbed electrophoresis tank immersed in electrophoresis buffer (300 mM NaOH, 1 mM disodium EDTA, pH 13) for 30 mins prior to electrophoresis at 21V (1V/cm) for 30 minutes. Slides were then placed in neutralisation buffer (0.4 M Tris-HCl, pH 7.5) for 30 mins and then washed twice with ice cold distilled H₂O and left to dry overnight.

Slides were then stained with SYBR Green I (Sigma, UK) diluted to a 1x concentration from a 10,000x stock into TE buffer for 5 mins and dried at room temperature. Slides were then visualised by a Zeiss Axiovert fluorescence microscope (Zeiss, UK) and 100 comets

per gel per slide were imaged and then quantified using Comet Assay IV Lite analysis software (Perceptive Instruments, UK) as tail intensity vs untreated controls.

2.7 Real Time Long Amplicon QPCR

The Real Time Long Amplicon QPCR (Real Time LA QPCR) measures DNA lesions in DNA extracted from cells or tissues in gene specific nuclear and mitochondrial DNA. Cells from 35 mm dishes at experimental end point were extracted using the same method for the alkaline comet assay and stored at -80 °C until the assay was performed. DNA was extracted using Qiagen Genomic tip 20/G for each sample and the tissue extraction protocol was followed in accordance with the manufacturer's guidelines. Extracted DNA pellets were dissolved in 50 µL water and quantified using Picogreen dye in 96 well plates (Thermo Fisher Scientific) against a standard curve of known concentration of Lambda DNA (Thermo Fisher Scientific) and read on FLUOstar Omega plate reader at 485nm_{ex}/520nm_{em}. Samples were then diluted to 10 ng/mL and added to a reagent master mix (Table 1.1) into 96 well PCR plates.

Primers were used for the amplification for small and large fragments for nuclear and mitochondrial DNA (Table 1.2). Primers are taken from the LA QPCR protocol (Furda et al., 2014) which have been thoroughly tested and verified to amplify a single specific PCR product and have been successful in detecting DNA damage. To detect nuclear DNA damage, primers were used to amplify a 12.2 kb fragment of the β-Polymerase gene (accession number L11607). The fragment size is large enough to meet the sensitivity requirements of the assay whilst small enough to reduce cycle threshold and assay time. Primers to amplify small 202 bp fragment of the 12.2 kb fragment were designed to act as an internal control and enable mitochondrial copy number comparison between samples.

To detect mitochondrial DNA damage, primers were used to amplify a 8.9 kb fragment of the 16.5 kb mitochondrion genome (accession number J01415). This fragment size is more than 50% of the mitochondrial genome, providing sufficient sensitivity for the assay whilst reducing PCR cycle threshold and therefore assay time.

Real Time PCR was performed using the DNA Engine Opticon 2 Real Time PCR system (Biorad, UK) and data assessed by Opticon Monitor software. The protocol first heats the sample for 3 mins at 93 °C, then repeats the following cycle 30 times, 93 °C for 15 sec, 62 °C for 30 sec, then 68 °C for 1 min per 1 kb expected product size. Samples are then subjected to melting curve analysis. Calculations were performed using the $2^{-\Delta\Delta CT}$ using the small fragments as a reference to their corresponding large fragment.

Table 1.1. Reagent reaction mix for 50 μL total volume

Volume	Reagent	Final concentration
5 μL	Accutaq LA 10x Buffer	1x
2.5 μL	dNTP Mix (10 mM each)	500 μM
10 μL	Template DNA (10 ng/ μL)	1 ng/ μL
1 μL	DMSO	2%
1 μL	Forward primer (20 pmole/ μL)	400 nM
1 μL	Reverse primer (20 pmole/ μL)	400 nM
29 μL	Water PCR reagent	
0.5 μL	Accutaq LA DNA Polymerase	0.05 units/ μL
50 μL Total volume		

Table 1.2 List of primers used in Real Time LA QPCR

Primer	Size	Sequence	
β-Polymerase			
Accession number L11607			
Large fragment	12.2 kb	TTT CAT CAT GCG GAG	Sense
		ATG TTG GAT GG	
Small fragment	202 bp	TCT AAG CCT CCT TAT	Antisense
		TCG AGC CGA	
Small fragment	202 bp	ACA CCT GAA TAG TTG	Sense
		GAC AGA A	
Small fragment	202 bp	CAT GTC ACC ACT GGA	Antisense
		CTC TGC AC	
Mitochondrion, complete genome			
Accession number J01415			
Large fragment	8.9 kb	TTT CAT CAT GCG GAG	Sense
		ATG TTG GAT GG	
Small fragment	211 bp	TCT AAG CCT CCT TAT	Antisense
		TCG AGC CGA	
Small fragment	211 bp	CCT CCC ATT CAT TAT	Sense
		CGC CGC CCT TGC	
Small fragment	211 bp	GTC TGG GTC TCC TAG	Antisense
		TAG GTC TGG GAA	

2.8 Immunohistochemistry

To establish cross-sections of the human lens, non-cultured whole human lenses were fixed in 4% v/v formaldehyde (Sigma-Aldrich) in PBS, dehydrated in a graded alcohol series, cleared in xylene and embedded in paraffin. Sections of lens (6 μm) were cut and mounted on glass slides. Sections were deparaffinised in xylene and rehydrated in descending ethanol concentrations and then subjected to antigen retrieval in sodium citrate buffer (10 mM sodium citrate, 0.05% Tween 20, pH 6.0) for 20 min. After three washes in PBS for 5 min, sections were blocked in 10% normal donkey serum in PBS for 1 hr and then incubated with primary antibody (Table 1.3) diluted 1:200 in PBS overnight at 4 °C. Following three further washes in PBS, sections were incubated with alexa488-conjugated donkey anti-rabbit (Invitrogen) diluted 1:400 in PBS for 1 hr protected from light. Sections were counterstained with DAPI, washed once in PBS and mounted with a coverslip. Samples were viewed with fluorescence microscopy (widefield microscope Zeiss AxioPlan 2ie, Zeiss, Gottingen, Germany) and images captured with a digital camera and AxioVision software (Zeiss, Cambridge, UK).

Table 1.3 Summary of antibodies used for immunohistochemistry

Antibody	Type	Dilution	Manufacturer
Primary antibody			
Anti-Ku80	Rabbit monoclonal	1:200	Cell Signaling Technology
Anti-DNA-PK	Rabbit monoclonal	1:200	Cell Signaling Technology
Anti-PARP-1	Rabbit monoclonal	1:200	Cell Signaling Technology
Anti-PAR	Rabbit monoclonal	1:200	Cell Signaling Technology
Anti-AIF	Rabbit monoclonal	1:200	Cell Signaling Technology
Anti-Mitochondria	Rabbit monoclonal	1:200	AbCam
Secondary antibody			
Anti-Rabbit Alexa488-conjugate	Donkey Secondary	1:400	Invitrogen

Chapter 3

DNA repair proteins in the anatomical organisation in the human lens

3.1 Introduction

It is remarkable that the human lens remains clear for so many years and in doing so allows the gift of sight considering that every day of life the lens is bombarded with both exogenous (e.g. UV light, radiation) and endogenous (oxidative stress) insult (Wormstone and Wride, 2011). The lens epithelium is the first line of defence and a loss of epithelial cell function can have catastrophic effects on the lens as a whole, ultimately resulting in cataract, which typically present within the lens fibre compartment. Interestingly, lens epithelial cells from human cataractous lenses have been shown to have increased DNA damage, implying an association with cataract pathogenesis (Kleiman and Spector, 1993; Zhang et al., 2010). Therefore, maintaining genomic stability may be vital in preserving lens clarity.

Like most human cells, the lens epithelium possesses DNA repair systems that help maintain genomic stability. DSBs are the most severe DNA lesion and failure to effectively repair them may eventually lead to cell death. The importance of DSB DNA repair systems in the lens have been investigated. Ku80 and DNA-PK are both components of the non-homologous end joining pathway (NHEJ) and have an important role in maintaining DNA integrity. Ku80 has been shown to help maintain lens clarity against oxidative stress (Smith et al., 2015). Ku80 siRNA knockdown in human lenses subjected to H₂O₂ induced oxidative stress demonstrated accelerated opacification when compared to scrambled control lenses subjected to the same stress. PARP-1, involved in both SSB and DSBs has also been implicated in protecting human lens from oxidative stress (Smith et al., 2016).

PARP-1 inhibition led to increased DNA strand breaks from H₂O₂ induced oxidative stress. However, inhibition also protected from cell death and reduced lens opacity in response to H₂O₂ induced oxidative stress (Smith et al., 2016). This may be due to inactivation of AIF induced cell death known as parthanatos that is activated by excess free PAR production by PARP-1 as a result of increasing genotoxic stress (Smith et al., 2016).

Lens fibre cells make up the bulk of the lens. These cells are rich in crystallin proteins and provide refractive power. The cortical fibres possess organelles and nuclei. The cortical lens fibre cells elongate to add distinct layers to the inner lens. The central nuclear fibre cells do not possess organelles, but these can be seen to be absent as the fibre cell layers get closer to the central lens. As a result, the central nuclear lens fibre cells do not possess nuclei or organelles, which allows light entering the eye to pass through the lens undisturbed. Due to the absence of nuclei and organelles in the nuclear region, these cells are largely reliant upon the lens epithelial cells for their maintenance and protection against ROS induced damage which if unregulated may lead to damaged proteins and opacification.

Lens fibre cells are generated from epithelial cells in the lens equator. This epithelium to lens fibre cell transition is still not a completely resolved process and little research in the human lens has been performed owing to scarcity of human donor tissue. A key step is denucleation in fibre cells, which precedes loss of other organelles. During this denucleation process it has been shown that the nuclear lamins are phosphorylated by cyclin-dependent kinase 1 (CDK1) facilitating the breakdown of the nuclear envelope (Chafee et al., 2014). This allows the lysosomal nuclease DNase II β to gain access to the nucleus and break down chromatin, initiating nuclear breakdown of the cell (De Maria and Bassnett, 2007). In mice, it has been shown to be DNA DSBs as identified from γ H2AX staining in the initial stages of cell fibre differentiation (Wang et al., 2005). As generation

of DSBs occur, and their repair is readily performed by the NHEJ system, this may potentially interrupt the breakdown of nuclear DNA that facilitates the lens differentiation process. It is currently unknown what role DSB DNA repair systems play and whether their expression is attenuated before DNase II β enters the nucleus and breaks down DNA.

Lens fibre cells undergo an 'attenuated apoptosis' whereby loss of nuclei and organelles occur but the cell cytoskeleton remains intact (Dahm, 1999). Enzymes associated with apoptosis may have a role in this process. Caspases are thought to play a role, however in caspase 3 and 6 knockout mice there were no significant differences in the OFZ compared to controls (Zandy et al., 2005). Conversely, caspase independent mechanisms associated with apoptosis may have an involvement. Interestingly, in human lens tissue, inhibition of PARP-1 prevents H₂O₂ induced cell death, possibly by inhibiting the build-up of free PAR thereby preventing the release of mitochondrial bound AIF which activates a caspase independent cell death mechanism known as parthanatos (Smith et al., 2016). Therefore, determining the expression and distribution of PARP-1 in differentiating lens fibre cell may elucidate a role in this process.

DNA repair systems in the lens are vital to protect lens epithelial cells (LECs) and help maintain its function of supporting lens fibre cells and in turn lens clarity (Smith et al., 2015; Smith et al., 2016). Although there has been much work in other animals, different species may have different mechanisms or expression levels compared to humans.

Research into the expression of DNA repair enzymes in human lens tissue is limited and may provide insight into their role in the human lens. LECs in the central epithelium are the most important in maintaining lens clarity owing to their exposure to stress factors such as UV light. Conversely, elucidating the expression of NHEJ and PARP-1 related

enzymes in the bow region of the lens may provide insight into the mechanism of lens fibre cell differentiation and maturation.

3.2 Aims

Research into DNA repair systems in the human lens is limited; therefore, studies in this area may be beneficial. Lens epithelial to fibre cell transition in the lens results in loss of nuclei and organelles and loss of expression of DNA repair proteins may facilitate this process. The present study will test the hypothesis that during lens epithelial to fibre cell transition, DNA repair protein expression is perturbed to allow chromatin breakdown. The transition of AIF from a mitochondrial bound to nuclear expression, will indicate that parthanatos may have a role in this process.

The aim in the present study is to visualise the expression of the DNA repair enzymes Ku80, DNA-PK, PARP-1 and its associated PAR polymer, plus mitochondria and AIF in the central epithelium and bow region of the human lens using immunohistochemistry on human lenses from donor tissue and elucidate their role in lens epithelial to fibre cell transition

3.3 Results

3.31 NHEJ proteins Ku80 and DNA-PK are expressed in human lens epithelium

NHEJ DNA repair proteins Ku80 and DNA-PK are present in the lens epithelium in human lens tissue (Fig 3.1). Both present strong nuclear staining but also considerably weaker cytoplasmic staining. Although Ku80 and DNA-PK are known to be predominantly expressed in the nucleus, they are not exclusive to it but it is where expression is most concentrated.

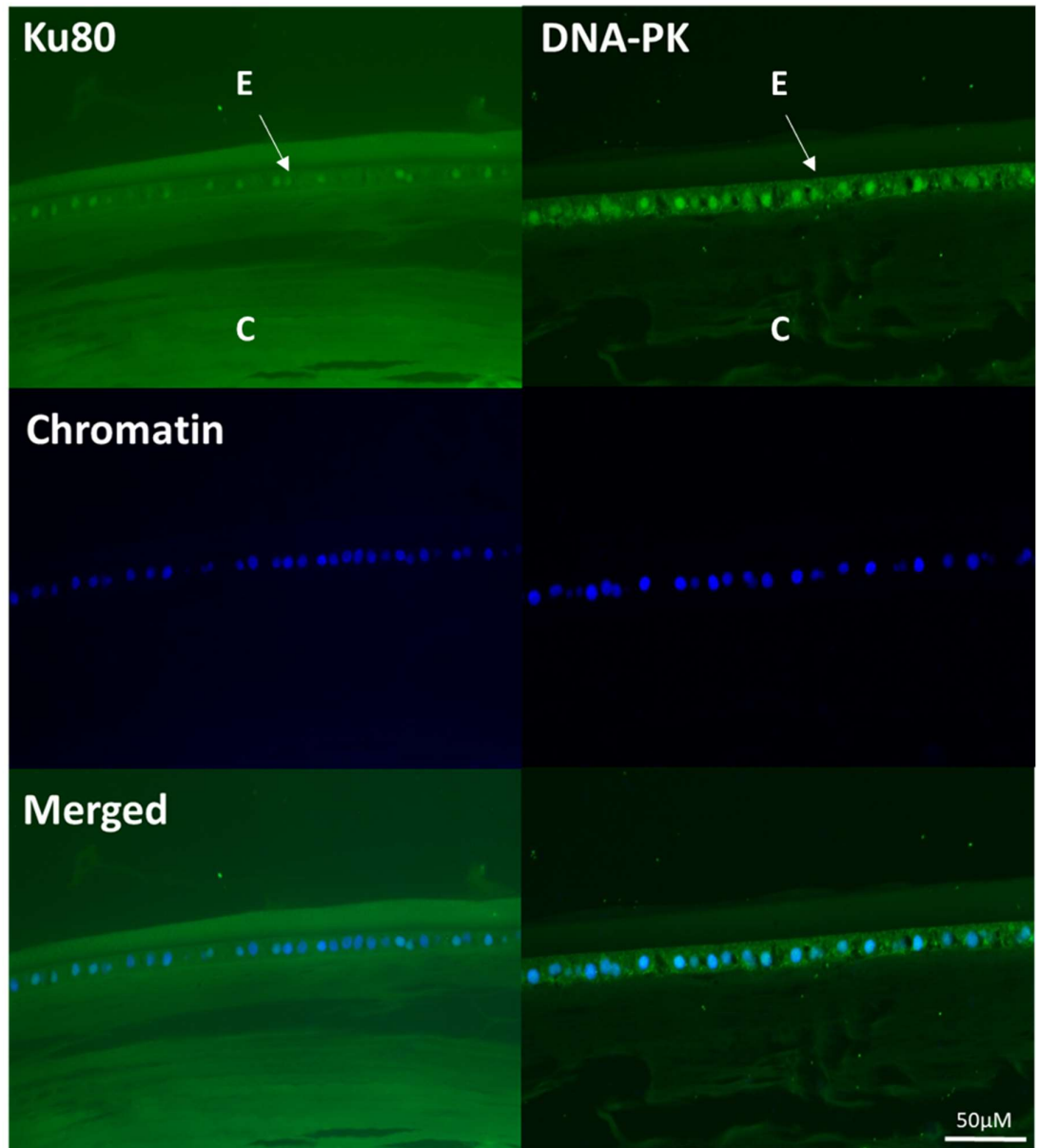


Figure 3.1 Expression of Ku80 and DNA-PK in the central epithelium of the human lens. Target protein stained with alexa488-conjugated secondary antibody (green) and chromatin with DAPI (blue). Immunohistochemistry performed on lens donor tissue (average age 76 ± 3.3 years, $n=3$). The distribution pattern presented was consistent amongst all donor tissue. E-epithelium, C-cortex.

3.32 PARP-1 and PAR are expressed in human lens epithelium

PARP-1 and PAR was present in the lens epithelium in human lens tissue (Fig 3.2). PARP-1 presented strong nuclear staining in lens epithelial cells. PAR staining was largely confined to the nucleus but strong staining was intermittent. PAR also presented minimal cytoplasmic expression in lens epithelial cells.

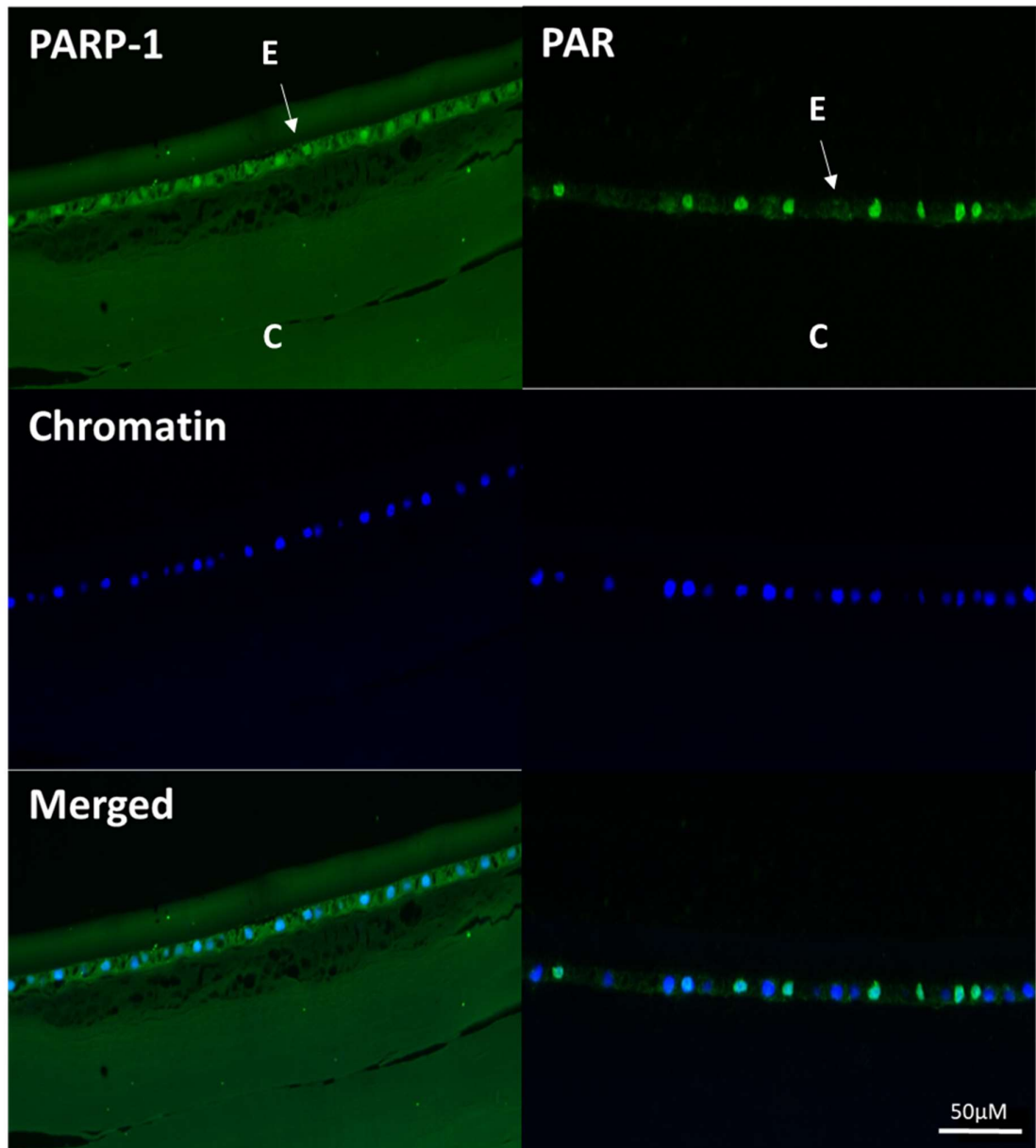


Figure 3.2 Expression of PARP-1 and PAR in the central epithelium of the human lens. Target protein stained with alexa488-conjugated secondary antibody (green) and chromatin with DAPI (blue). Immunohistochemistry performed on lens donor tissue (average age 76 ± 3.3 years, $n=3$). Data consistent amongst all donor tissue. E-epithelium, C-cortex.

3.33 AIF and mitochondria are expressed in human lens epithelium

AIF and mitochondria were present in the lens epithelium in human lens tissue (Fig 3.3).

Both AIF and mitochondria presented only cytoplasmic staining and similar staining pattern in lens epithelial cells.

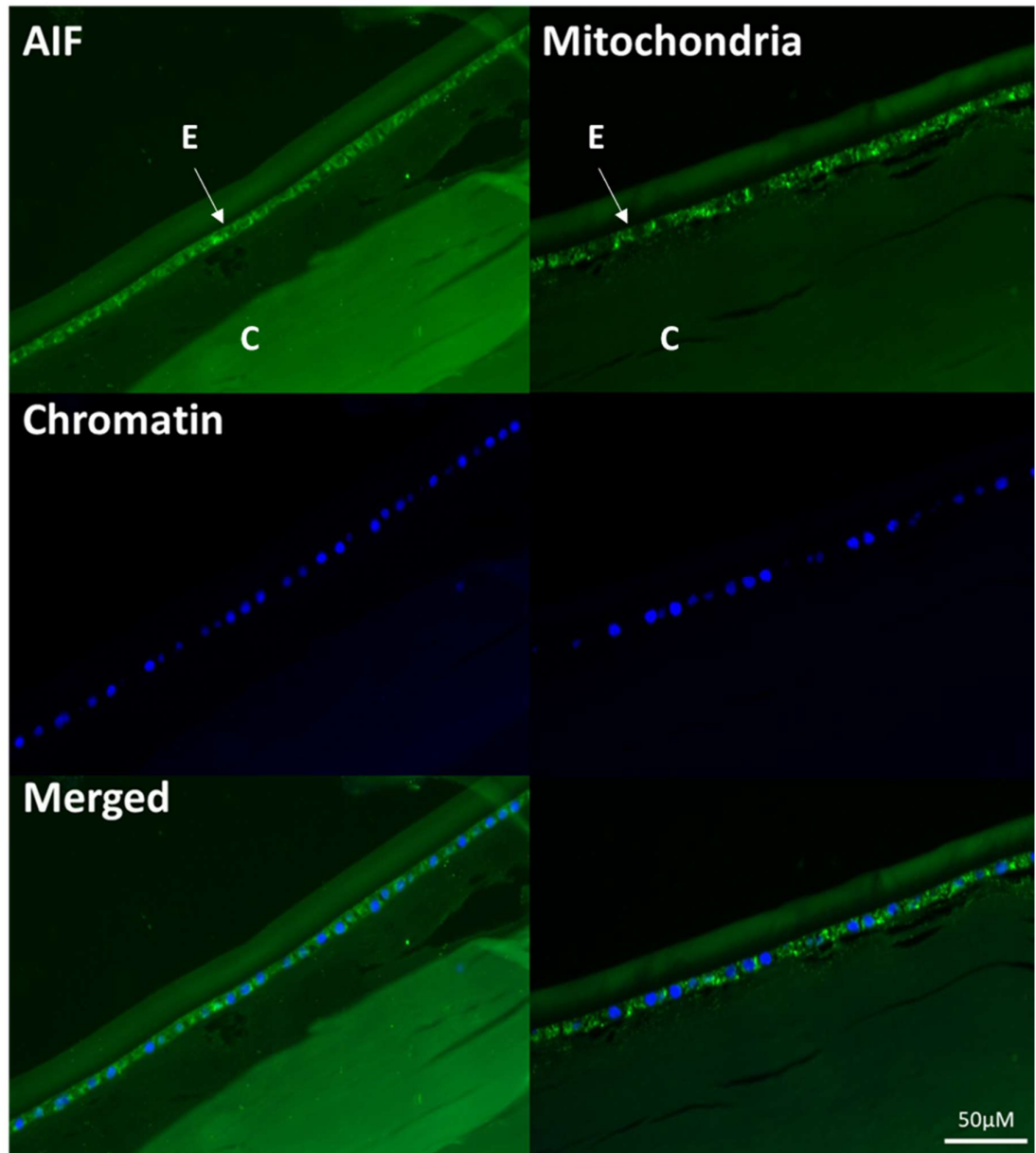


Figure 3.3 Expression of AIF and mitochondria in the central epithelium of the human lens. Target protein stained with alexa488-conjugated secondary antibody (green) and chromatin with DAPI (blue). Immunohistochemistry performed on lens donor tissue (average age 76 ± 3.3 years, $n=3$). Data consistent amongst all donor tissue. E-epithelium, C-cortex.

3.34 NHEJ proteins Ku80 and DNA-PK are expressed in the bow region of the human lens

Ku80 and DNA-PK were present in the bow region of the lens (Fig 3.4). Within newly laid lens fibre cells, both proteins presented strong nuclear staining before levels rapidly declined as the fibre cells got closer to the centre. This reduced expression appeared to precede changes in chromatin appearance that could be attributed to lens fibre cell denucleation. Fragmented nuclei showed no staining for either Ku80 or DNA-PK. The staining presented deep in the lens cortex is background staining owing to the exposure time required to accurately capture staining in the single cell layered epithelium.

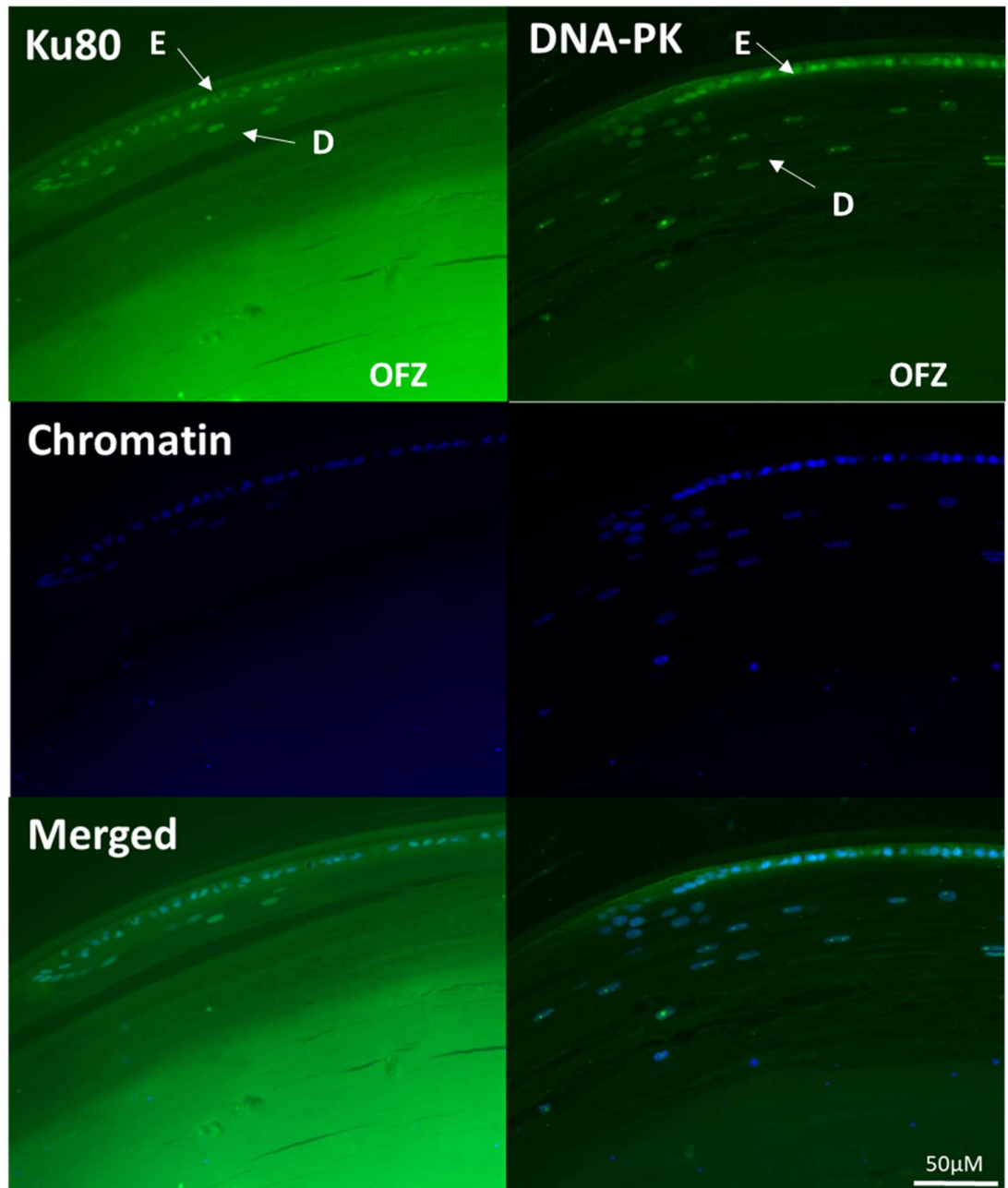


Figure 3.4 Expression of Ku80 and DNA-PK in the bow region of the human lens. Target protein stained with alexa488-conjugated secondary antibody (green) and chromatin with DAPI (blue). Immunohistochemistry performed on lens donor tissue (average age 76 ± 3.3 years, $n=3$). Data consistent amongst all donor tissue. E-epithelium, D-differentiating fibre cells, OFZ-organelle free zone.

3.35 PARP-1 and PAR are expressed in the bow region of the human lens

PARP-1 and PAR were present in the bow region of the lens (Fig 3.5). PARP-1 displayed a similar expression pattern to that of the NHEJ related proteins. PARP-1 displayed strong nuclear staining within newly laid lens fibre cells but expression seemed to halt as nuclei appeared to condense. Similar to Ku80 and DNA-PK, staining in the deep cortex was the result of the exposure time required to accurately capture staining in the single cell layered epithelium. PAR also showed strong nuclear staining in newly laid lens fibre cells but continued to be expressed in condensed nuclei, halting when nuclei fragmented.

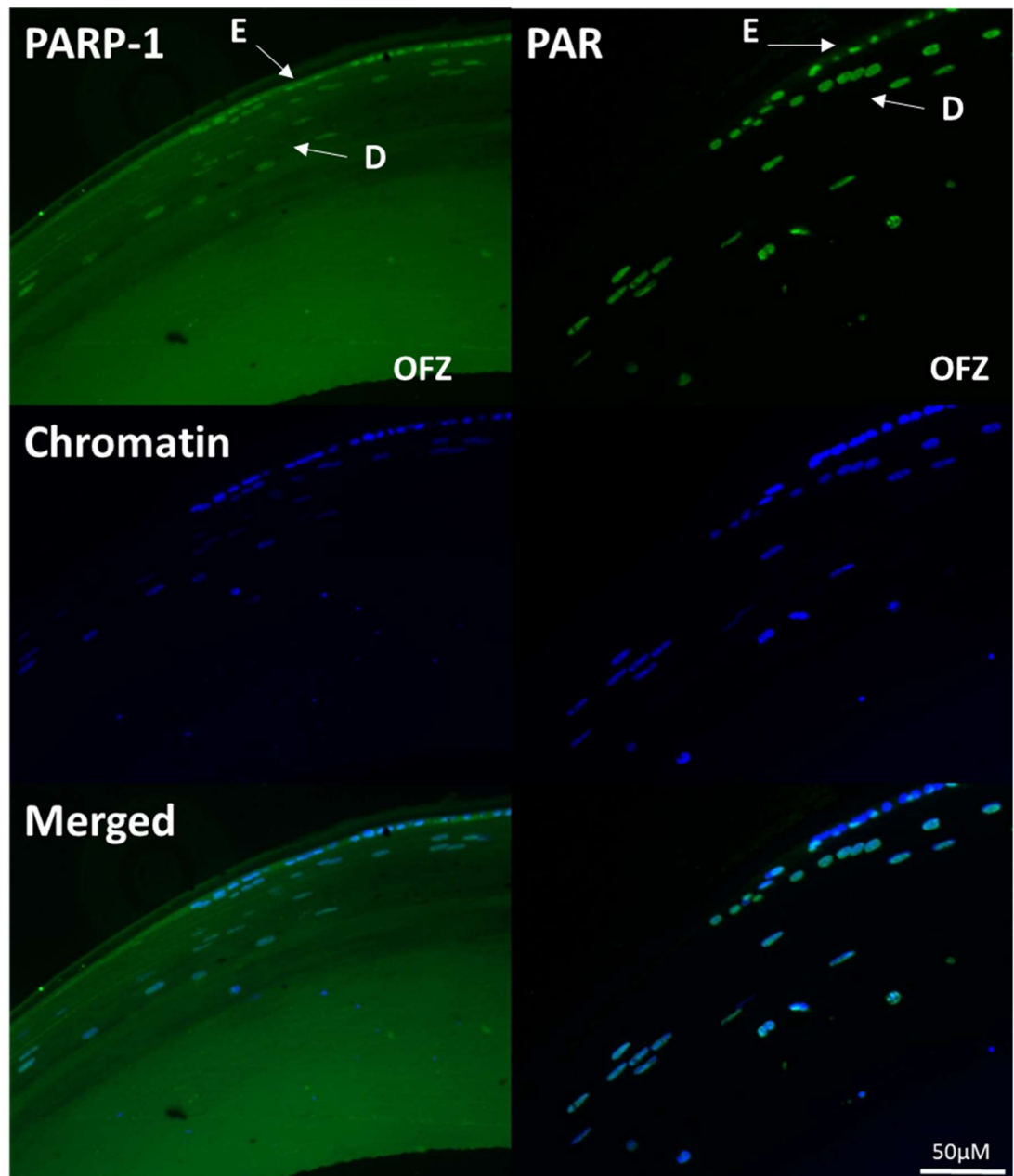


Figure 3.5 Expression of PARP-1 and PAR in the bow region of the human lens. Target protein stained with alexa488-conjugated secondary antibody (green) and chromatin with DAPI (blue). Immunohistochemistry performed on lens donor tissue (average age 76 ± 3.3 years, $n=3$). Data consistent amongst all donor tissue. E-epithelium, D-differentiating fibre cells, OFZ-organelle free zone.

3.36 AIF and mitochondria are expressed in the bow region of the human lens

AIF and mitochondria were present in the bow region of the lens (Fig 3.6). Within newly laid lens fibre cells, AIF presented strong cytoplasmic staining before levels rapidly declined. This reduced expression appeared to precede changes in chromatin appearance that could be attributed to lens fibre cell de-nucleation. At no time did AIF seem to appear in the nuclei of epithelial or fibre cells. AIF appeared to have the same staining profile as mitochondria.

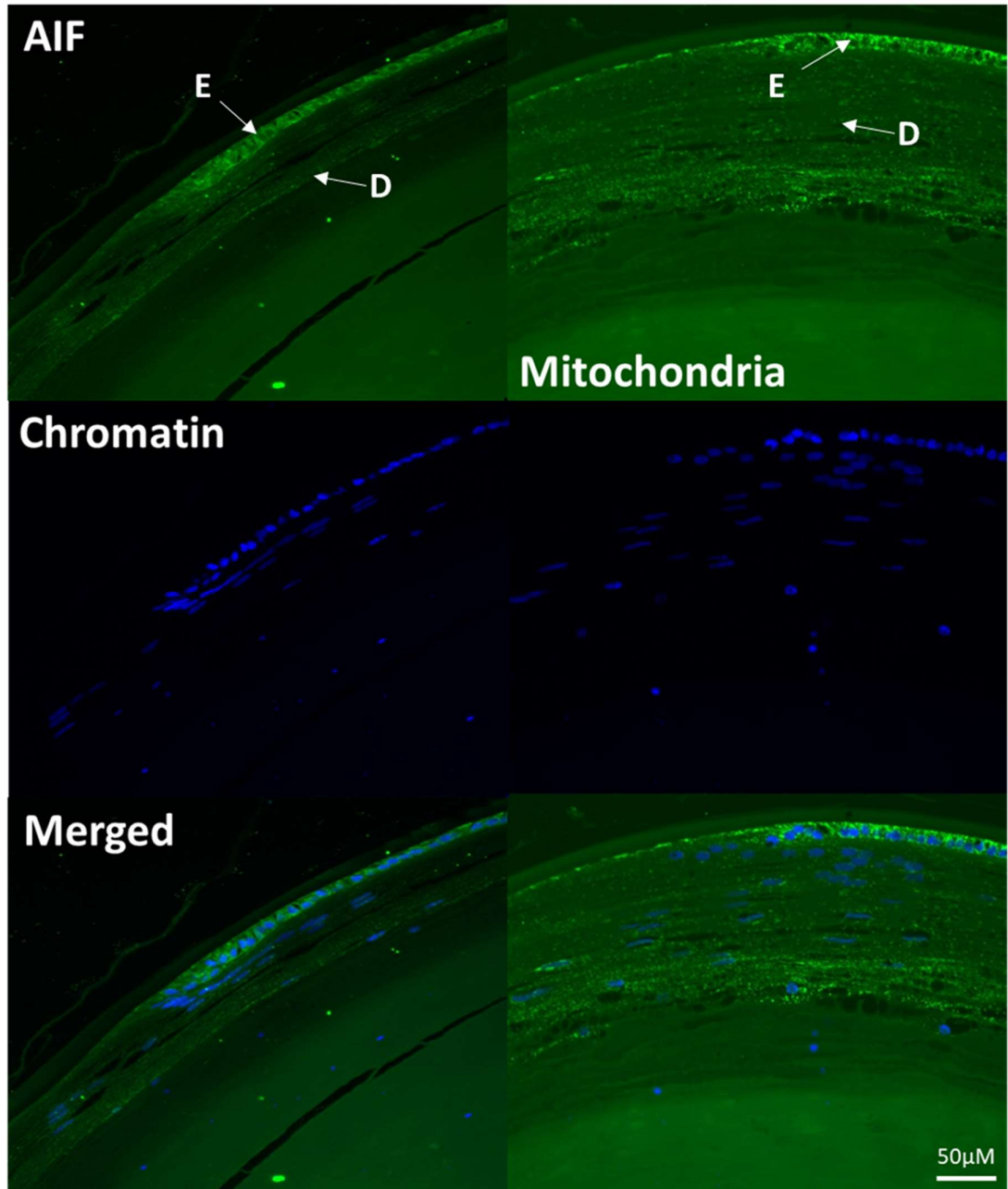


Figure 3.6 Expression of AIF and mitochondria in the bow region of the human lens. Target protein stained with alexa488-conjugated secondary antibody (green) and chromatin with DAPI (blue). Immunohistochemistry performed on lens donor tissue (average age 76 ± 3.3 years, $n=3$). Data consistent amongst all donor tissue. E-epithelium, D-differentiating fibre cells, OFZ-organelle free zone.

3.4 Discussion

The lens is subject to numerous endogenous and exogenous insults that damage DNA and therefore impinge on the lens epithelium's ability to maintain lens clarity. Therefore expression of DNA repair proteins are vital to maintain lens integrity.

Utilising immunohistochemistry on human lens donor tissue, expression of the NHEJ proteins Ku80 and DNA-PK were shown to be expressed greatest in the nucleus in the central epithelium of lens epithelial cells. This is consistent with expressions patterns in the epithelial lens cell line FHL124 (Smith et al., 2015). Expression of these components of the NHEJ repair pathway are important in maintaining genomic stability and preserving the function of the cell which in turn maintains lens clarity. Components of the NHEJ repair pathway are essential in protecting against oxidative stress induced damage. The functional importance of this has been shown with siRNA knockdown of Ku80, which increased the rate of opacification in cultured human lenses exposed to oxidative stress (Smith et al., 2015)

Similarly, PARP-1 expression was also present in the nuclei of epithelial cells in the central epithelium. Again, this coincides with immunocytochemistry data of PARP-1 expression in FHL124 cells (Smith et al., 2016). Inhibition of PARP-1 in human lens tissue has been shown to increase lens opacification when exposed to H₂O₂ induced oxidative stress (Smith et al., 2016). PAR, a product that PARP-1 catalyses the synthesis of, and an indicator of PARP-1 activity, is also predominantly expressed in the nuclei of LECs in the central epithelium. The level of staining varied from cell to cell, with some nuclei showing little expression. As PAR is an indicator of PARP-1 activity, this could suggest differences in the relative amount of DNA stand breaks between cells.

Loss of DNA expression as well as organelle loss is a feature of the lens epithelial cell to lens fibre cell transition. This is a gradual process that proceeds towards the central lens body (De Maria and Bassnett, 2007). This study shows that reduced expression does occur and coincides with fragmentation loss of nuclei and this effect shows a gradual loss as lens fibre cells move centrally. Organelle loss abruptly occurs, with mitochondrial expression showing a clear band of expression to degradation in the lens fibre cells. This pattern ties in well with the distinct fibre segments within the human lens described by Taylor et al (1996).

In the bow region, Ku80 and DNA-PK were expressed in the epithelial cell nuclei and newly formed lens fibre cells with elongated nuclei. As fibre cells moved closer to the lens centre, expression is abruptly halted at the point nuclei appeared to condense. Therefore, the reduced expression of these repair proteins may aid the breakdown of chromatin in differentiating fibre cells. PARP-1 also shows similar nuclear expression in elongated nuclei with expression abruptly halting after condensation. Interestingly PAR, a product of PARP-1 continued to be expressed in condensed nuclei, only halting after the epithelial nuclei completely fragmented.

It is recognised that caspases and suicidal proteases can cleave PARP to generate signature PARP-1 fragments that are associated with particular forms of pathological cell death. During apoptosis, PARP-1 has been shown to be cleaved by caspases 3 and 7 into 80 kD and 20 kD fragments (Chaitanya et al., 2010). In the lens, previous studies have also suggested that PARP-1 is cleaved by additional caspases including caspase 2,3,4 and 6; PARP-1 fragments have been detected in the outer layers of lens fibre cells in rat and chicken lens (Wride et al., 1999; Ishizaki et al., 1998). Although there is no direct evidence of caspase mediated cleavage of PARP in differentiating lens fibre cells, caspase inhibitors have been shown to also inhibit PARP cleavage (Ishizaki et al., 1998). Therefore caspases

may play role in degrading PARP in lens fibre cells. Loss of PARP-1 expression in this study appears to occur in lens fibre cells at the point of nuclei breakdown. It is therefore possible that this may coincide with activation of caspases that could cleave PARP-1 and prevent repair to DNA that is being cleaved by DNases such as DNase II β (De Maria and Bassnett, 2007).

The involvement of caspase independent cell death parthanatos (Luo and Kraus, 2012) was considered and investigated in the bow region of the lens. Expression of AIF, which is bound to mitochondria but released to the cell nucleus during parthanatos (Luo and Kraus, 2012), was expressed exclusively in the cytosol of lens fibre cells and not in the nuclei. Upon condensation of the lens fibre cell nuclei, cytosolic expression of AIF abruptly ends and no expression is present thereafter. The data seems to suggest there is no AIF present in the nuclei of the lens fibre cells during differentiation, indicating that parthanatos is not activated and suggests that this caspase independent form of cell death is unlikely to play a role in lens cell denucleation. This is further evidenced by the staining of mitochondria in the bow region which presents the same staining pattern of AIF, indicating that AIF was bound to the mitochondria throughout the differentiation process.

In summary, the work presented demonstrates that important DNA repair proteins are present within the adult human lens. Moreover, it was found that loss of expression of PARP-1, Ku80 and DNA-PK preceded lens fibre cell denucleation and this process may facilitate this important physiological event. The fact that AIF was not expressed within the nuclei at any stage of fibre cell maturation and denucleation, may indicate that parthanatos does not contribute to this process.

Chapter 4

Real Time Long Amplicon QPCR assay for detection of DNA damage

4.1 Introduction

DNA damage can have significant consequences on cell fate. DNA mutations as a result of DNA lesions can compromise cell function, where an increased severity of damage may lead to cell death. DNA damage is implicated in diseases of the eye such as cataract (Ates et al., 2010) and alter physiological lens cell function and promote lens opacity (Smith et al., 2015; Smith et al., 2016). It has also been implicated in diseases such as Fuchs dystrophy which affect corneal endothelial cells. Therefore it is important to develop assays that detect DNA damage.

The alkaline comet assay is the most commonly used method for measuring DNA damage (Neri et al., 2015). However, it is limited to detection of nuclear DNA strand breaks in cells and primarily quantified as tail movement or intensity compared to control (Collins, 2004). Other assays such as γ H2AX immunostaining indirectly detect DSBs only. As DNA strand breaks make up only part of all types of DNA damage, assays have been developed to be more sensitive and detect a wider range of DNA lesions.

A protocol first published by Santos et al (2006) utilised a PCR based method to achieve this. The long amplicon quantitative PCR (LA QPCR) relies on the principle that DNA lesions slow or block DNA polymerase during a PCR reaction, therefore damaged DNA will amplify to a lesser extent than undamaged DNA (Santos et al., 2006) and thus, the difference between cycle thresholds can be measured. Large fragments 8 kb-25 kb in size are amplified in order to obtain enough sensitivity for lesions to be detected as smaller

fragments would not contain enough strand breaks to detect an accurate representation. LA QPCR is more versatile when compared to the comet assay, able to detect nuclear and mitochondrial DNA damage from DNA extracted from tissues and cells (Furda et al., 2014). A key strength of the assay is to detect gene specific DNA lesions in DNA strands of known length allowing DNA damage to be quantified as lesions per kb. Additionally, the assay allows DNA damage to be measured along the whole length of the mitochondrial genome (excluding the D-loop region) (Furda et al., 2014), which is of great importance as mitochondrial DNA damage is associated with a range of disorders, especially in the eye (Jarrett et al., 2010). As there are multiple copies of mitochondrial DNA per cell, a short fragment is amplified to use as a reference marker to normalise mitochondrial copy number. This works on the principal that short fragments (less than 300 bp) have a low probability of containing DNA lesions and can be considered to represent undamaged DNA (Furda et al., 2014).

However, the LA QPCR is not without limitations. The assay relies on the fluorophore DNA binding dye Picogreen to quantify PCR products which has comparable DNA quantification sensitivity with ^{32}P -radiolabeled nucleotides (Furda et al., 2014). However, it is not thermostable enough to be used in PCR reactions (Rengarajan et al., 2002) and is therefore added to the sample at the PCR reaction endpoint, risking contamination to PCR products. Furthermore, to obtain accurate measurements, the PCR products must be quantified during the exponential phase of the PCR reaction, necessitating laborious optimisations to determine the appropriate cycle number for each set of primers (Santos et al., 2006). PCR products are also required to be assessed by agarose gel electrophoresis to confirm product size and purity, considerably increasing assay time.

Therefore, there is scope to improve on the existing LA QPCR assay platform to address the drawbacks of the system. To achieve this, establishing a Real Time LA QPCR would significantly reduce assay time, increase accuracy and versatility of the assay.

4.2 Aims

Current techniques that measure DNA damage can be limited to detection of specific nuclear DNA lesions in cells only. The LA QPCR assay is an effective tool to measure DNA damage in nuclear and mitochondrial DNA in cells and tissues but has severe limitations affecting throughput. To address these issues, the LA QPCR can be adapted to a Real Time LA QPCR assay using the thermostable DNA binding dye SYBR Green I. Addition of a novel primer to the assay design can enable the quantification of mitochondrial copy number between samples. The hypothesis is that this adaption will improve throughput and accuracy in the detection of DNA damage.

The aims of the present study are:

- 1) To develop and optimise the LA QPCR DNA damage assay to a Real Time LA QPCR and design an additional primer to serve as a reference control to enable quantifying differences in mitochondrial copy number between samples.
- 2) Evaluate the Real Time LA QPCR assay using DNA extracted from FHL124 cells treated with the DNA strand break inducing agents NCS and bleomycin.

4.3 Results

4.31 Demonstration of DNA standards

Amplification of a range of DNA standards from DNA extracted from untreated FHL124 cells was performed in order to establish a standard curve and to determine amplification efficiency (Fig 4.1). Each 2-fold dilution of the standard amplified successive higher cycle threshold (ct) values, producing a standard curve above an R^2 value of 0.96 for small and large fragments from both nuclear and mitochondrial primers. 50 ng of sample DNA was chosen to be used all PCR reactions, producing ct values for β -Polymerase large and small fragments of 22 and 10 respectively. Mitochondrial ct values for large and small fragments were 17 and 11 respectively.

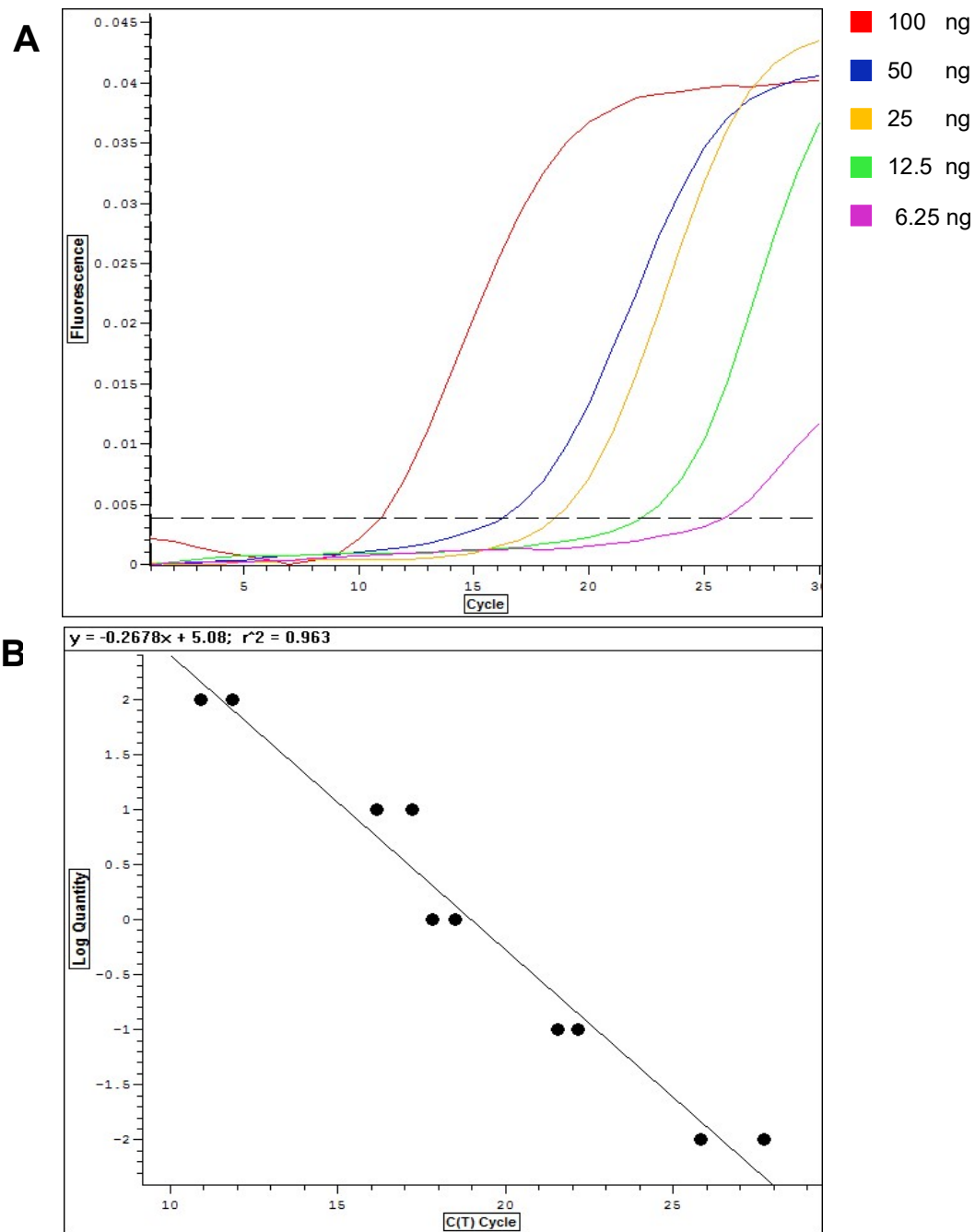


Figure 4.1 (A) An example of an amplification plot of DNA standards with 2-fold dilutions to generate a standard curve (B) with $R^2 = 0.963$ using primers to amplify the 8.9 kb mitochondrial fragment in FHL124 cells. Assessed by Opticon Monitor software.

4.32 Melting curve analysis

Each set of primers amplified their product successfully in the Real Time LA QPCR. All melting curves showed a single peak, demonstrating single product specificity. Melting curve analysis for the large nuclear and mitochondrial fragments (Fig 4.2) and small fragments displayed single peaks between 82 and 90 °C.

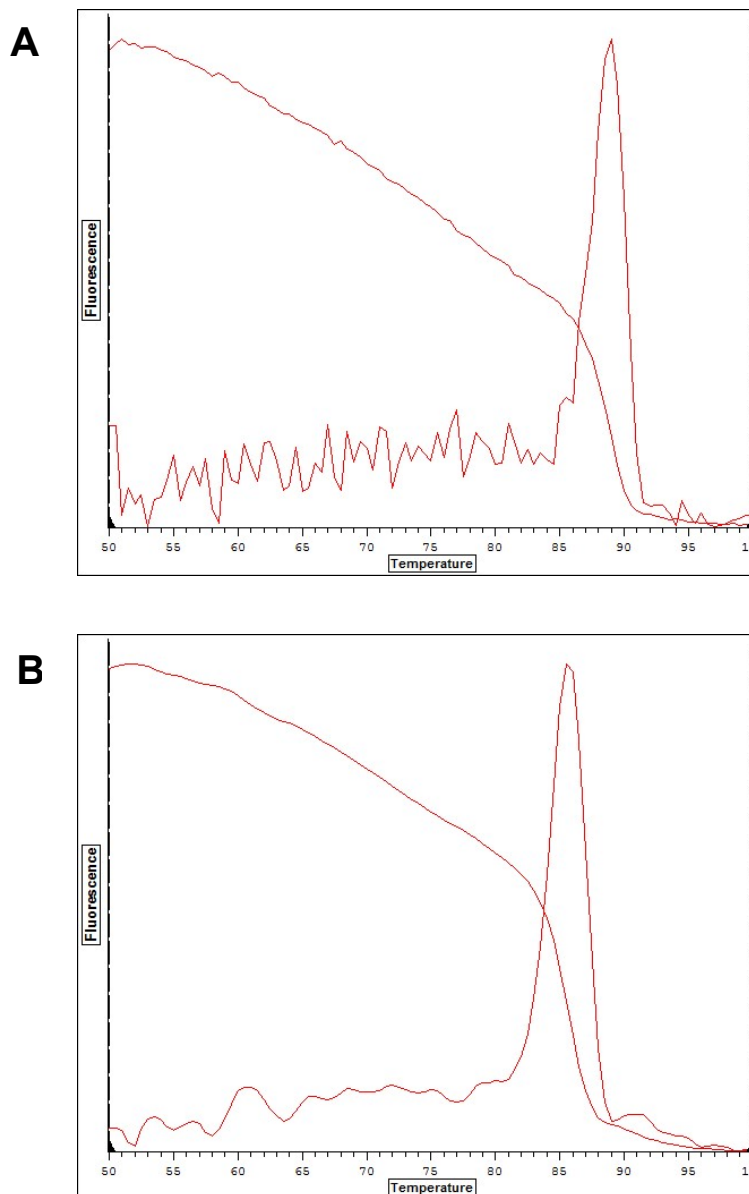


Figure 4.2 Melting curves for (A) nuclear 12.2 kb and (B) mitochondrial 8.9 kb fragments in DNA extracted from untreated FHL124 cells. As assessed by Opticon Monitor software.

4.33 Optimisation of SYBR Green I dye in master mix

SYBR Green I concentration was optimised for use in the bespoke mastermix to give maximum signal intensity and reduce polymerase inhibition. A SYBR Green I stock of 10,000 times concentrated was diluted to a range of concentrations of 0.05, 0.1, 0.3 and 0.5x. Concentrations of 0.05 and 0.1x amplified at a ct value of 15 but produced a weaker fluorescence signal than 0.3 and 0.5x. Both 0.3 and 0.5x dilutions produced a strong fluorescence signal with 0.5x presenting greater PCR amplification inhibition with a ct value of 24 compared to 0.3x ct value of 22. Hence, a 0.3x dilution of SYBR Green I was used in the master mix.

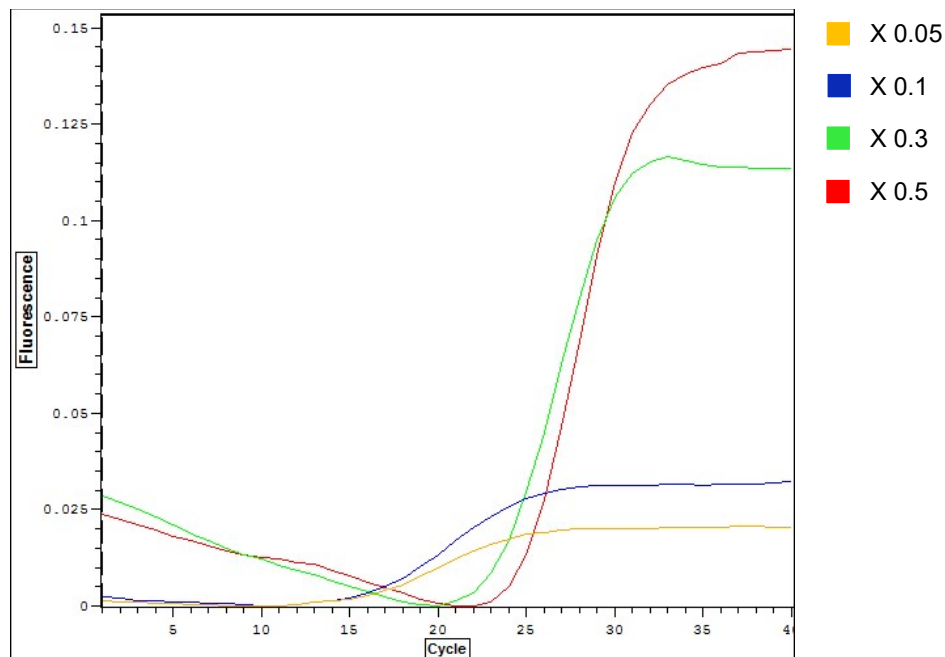


Figure 4.3 Amplification plot of 12.2 kb β-Polymerase fragment using a range of SYBR Green I concentrations diluted from x10000 stock. As assessed by Opticon Monitor software.

4.34 Concentration response curves for DNA damaging agents NCS and bleomycin in FHL124 cells

Concentration response curves for NCS and bleomycin were performed to determine optimal doses that affect FHL124 cell viability using the MTS assay after 48h (Fig 4.4), which in turn will be used to induce DNA strand breaks to be measured by the Real Time LA QPCR.

Treatment of 30 ng/mL NCS to FHL124 cells showed no change in cell viability, whilst 100 and 300 ng/mL showed a reduction in cell viability vs untreated controls but was not significant. However, 1000 ng/mL of NCS did show a significant reduction to 53.9% \pm 4 of untreated control.

Treatment of bleomycin to FHL124 cells only showed a significant reduction in cell viability at 30 and 100 μ g/mL with a reduction of 63.8% \pm 10.4 and 37.3% \pm 6.9 to untreated controls respectively.

Concentrations of 500 ng/mL for NCS and 10 μ g/mL for bleomycin was determined to be suitable enough to cause DNA lesions in FHL124 cells and therefore used to test the Real Time LA QPCR.

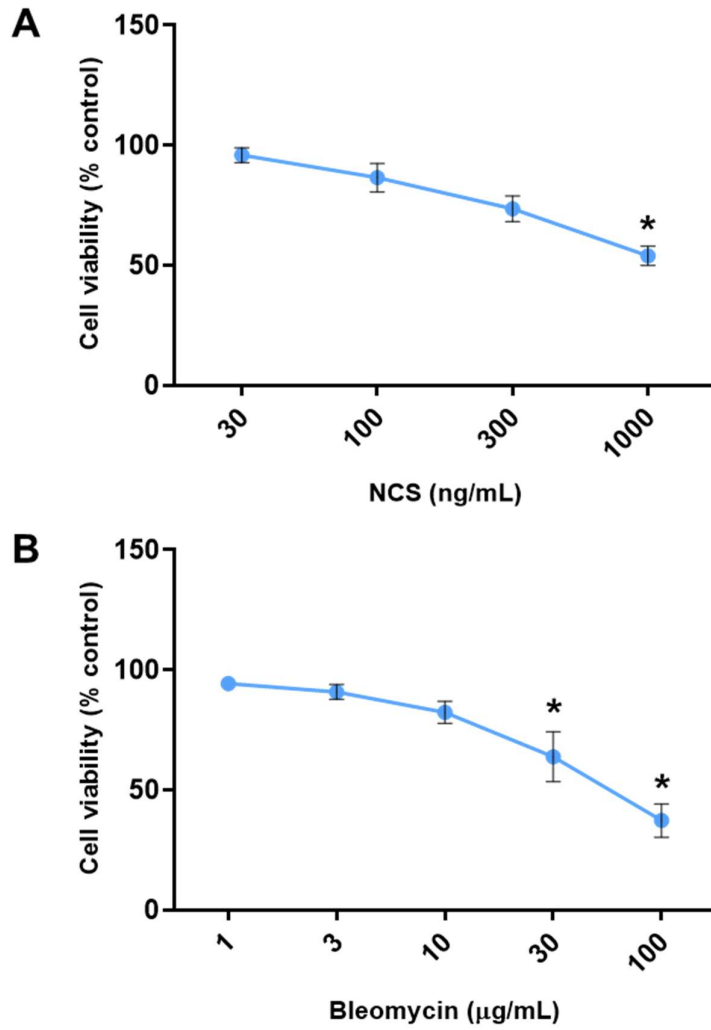


Figure 4.4 Dose response of (A) NCS and (B) bleomycin treatments on cell viability in FHL124 cells after 48 h, measured by the MTS assay. Data presented as mean \pm SEM (n=4). * indicates a significant difference between treated group and untreated control ($p \leq 0.05$; ANOVA with Dunnett's post hoc test).

4.35 NCS and bleomycin increase DNA strand breaks in FHL124 cells as measured by the comet assay

FHL124 cells were treated with 500 ng/mL NCS and 10 µg/mL bleomycin and DNA strand breaks assessed by the comet assay over 4 h. NCS and bleomycin both significantly increase DNA strand breaks in FHL124 (Fig 4.5) with both agents showing peak damage at 0.5 h compared to untreated controls after treatment.

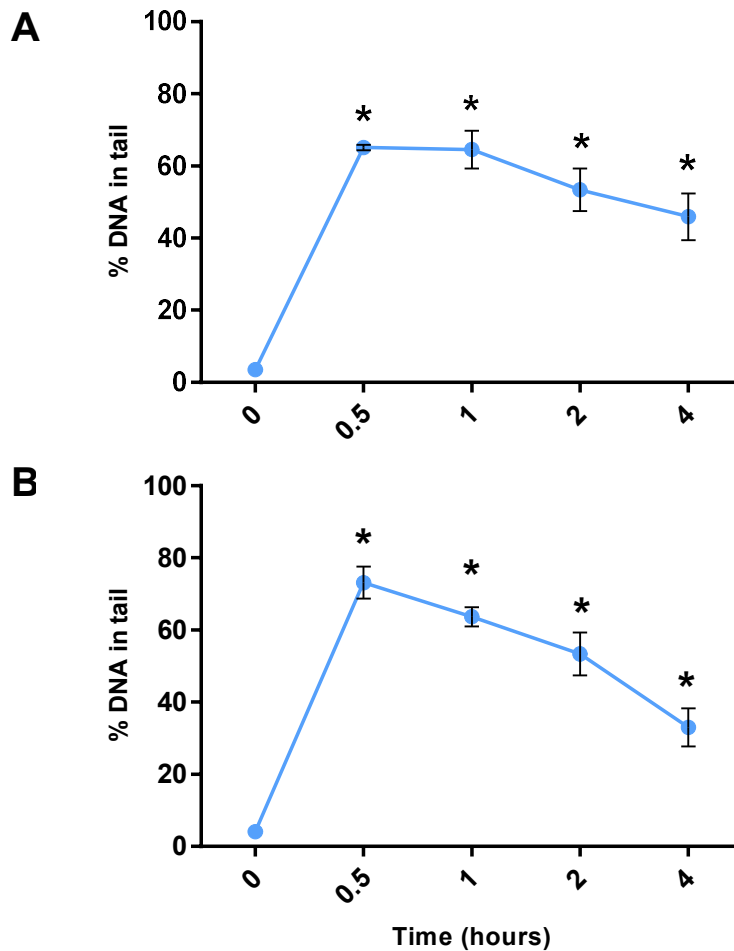


Figure 4.5 DNA strand breaks from treatment of 500 ng/mL (A) NCS and 10 µg/mL (B) bleomycin in FHL124 cells over 4 h, measured by the alkaline comet assay. Data presented as mean \pm SEM (n=3). * indicates a significant difference between treated groups and untreated control ($p \leq 0.05$; ANOVA with Dunnett's post hoc test).

4.36 NCS and bleomycin increase nuclear and mitochondrial DNA lesions in FHL124 cells

Using the Real Time LA QPCR assay, treatment of 500 ng/mL NCS significantly increases DNA lesions in nuclear and mitochondrial DNA in FHL124 cells over 4 h (Fig 4.6) after treatment when compared to untreated controls. Peak DNA lesions were measured to be at 1 hr in nuclear (1.2 lesions/10kb \pm 0.2) and mitochondrial DNA (2.16 lesions/10kb \pm 0.2).

Bleomycin also significantly increased DNA lesions in both nuclear and mitochondrial DNA in FHL124 cells over 4 h (Fig 4.7) after treatment when compared to untreated controls. Both peak DNA lesions were measured to be at 0.5 h in nuclear and mitochondrial DNA (1.3 lesions/10kb \pm 0.14 and 2.26 lesions/kb \pm 0.12).

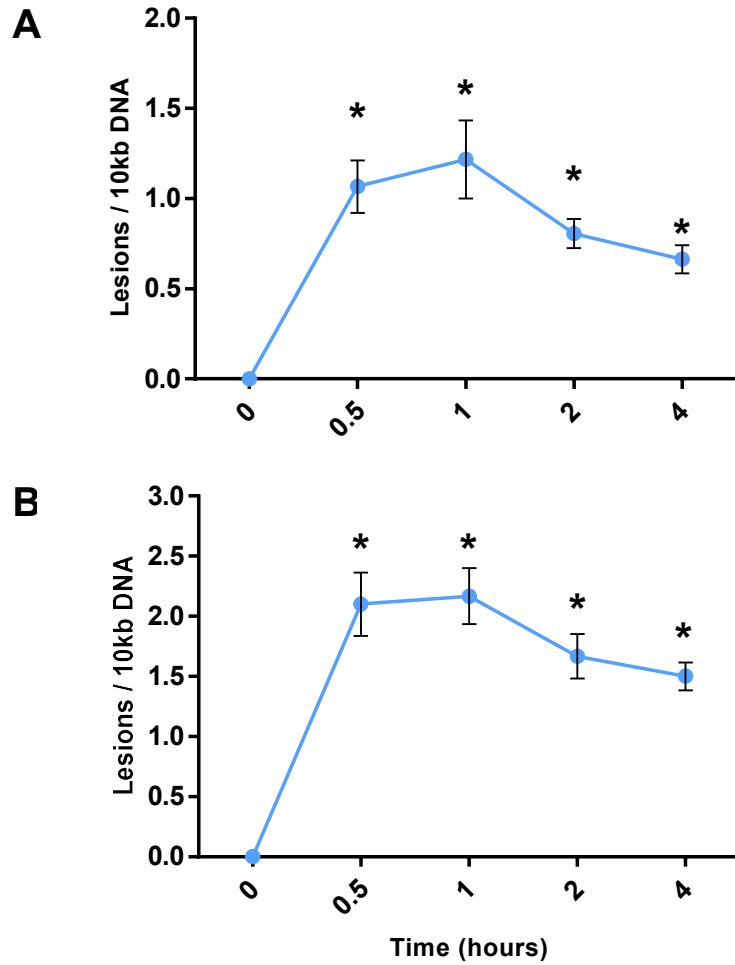


Figure 4.6 Lesions/10kb in (A) nuclear and (B) mitochondrial DNA in FHL124 cells treated with 500 ng/mL NCS over 4 h, measured by the Real Time LA QPCR assay. Data presented as mean \pm SEM (n=3). * indicates a significant difference between treated groups and untreated controls ($p \leq 0.05$; ANOVA with Dunnett's post hoc test).

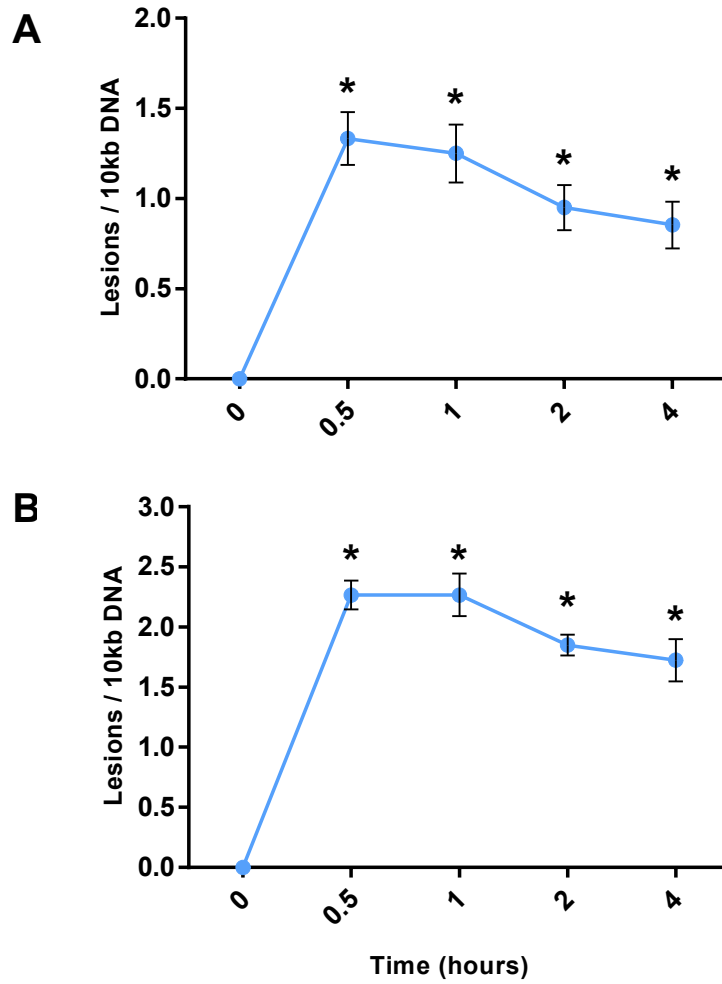


Figure 4.7 Lesions/10kb in (A) nuclear and (B) mitochondrial DNA in FHL124 cells treated with 10 $\mu\text{g}/\text{mL}$ bleomycin over 4 h, measured by the Real Time LA QPCR assay. Data presented as mean \pm SEM (n=3). * indicates a significant difference between treated groups and untreated controls ($p \leq 0.05$; ANOVA with Dunnett's post hoc test).

4.4 Discussion

DNA damage is thought to contribute to numerous disorders in the eye (Czarny et al., 2013; Zhang et al., 2010). Understanding their role in disease may help elucidate underlying mechanisms and help contribute to therapeutics. Designing effective assays to detect and quantify DNA damage is of vital importance to accomplish these goals.

The work presented in this chapter has shown a successful adaption of the long amplicon QPCR assay to a Real Time LA QPCR assay, which has many advantages over the LA QPCR. The original LA QPCR required laborious optimisations to determine the exponential phase of the PCR reaction for all sets of primers individually (Furda et al., 2014). The Real Time LA QPCR assay eliminates this as the complete PCR reaction is recorded in real time, allowing the user to pinpoint an exact cycle threshold. Product specificity can be analysed immediately after the PCR reaction has been completed using melting curve analysis as opposed to the requirement to use agarose gel electrophoresis. It also removes a complete step of the LA QPCR assay: The addition of Picogreen at the PCR reaction endpoint and reading on a fluorometer.

Since no commercially available PCR mastermix is available for this assay, a bespoke mastermix was developed using the polymerase AccuTaqTM DNA polymerase (Sigma, UK) which is designed to amplify PCR targets up to 40 kb in length. All primers used in the assay successfully amplified their respective fragments and produced a single product as determined by melting curve analysis. The primer designed to amplify the small 202 bp β -Polymerase fragment allowed the use of a reference to compare the large 12.2kb β -Polymerase fragment, replacing the need for a DNA standard curve and enabling the use of $2^{-\Delta\Delta CT}$ calculations to interpret data. Using the β -Polymerase small fragment can also help

determine differences in mitochondrial copy number between samples as shown in chapter 5.

The Real Time LA QPCR can effectively detect DNA lesions in nuclear and mitochondrial DNA. It has advantages over the alkaline comet assay which only detects DNA strand breaks. Additional DNA lesions that are detected include abasic sites, thymine dimers and 5-hydroxymethyl uracil (Cadet and Wagner, 2013).

The lens cell line FHL124 was used to test the Real Time LA QPCR. To induce DNA damage in FHL124 cells, agents that primarily induce DNA strand breaks were utilised. Neocarzinostatin (NCS) is an enediyne antibiotic consisting as a complex of a chromophore and a 10-kDa protein known to induce single and double stranded DNA breaks (Banuelos et al., 2003). Bleomycin, a glycopeptidic antibiotic bacterium derived from the bacterium *Streptomyces verticillus* cleaves DNA by binding to it simultaneously with Fe(II) and releasing hydroxyl radicals causing DNA strand breaks (Della Latta et al., 2013). Both agents have been used in cancer treatments and are well established research tools to induce DNA strand breaks (van Duijin-Goedhart et al., 2000; Della Latta et al., 2013).

DNA damage was detected from both NCS and bleomycin treatments, demonstrating that the Real Time LA QPCR can detect lesions from multiple DNA damaging agents. The Real Time LA QPCR data for NCS and bleomycin treated FHL124 cells both showed a marked increase in lesions per 10 kb in the amplified mitochondrial DNA fragment compared to the nuclear fragment in the same sample.

Comparing the data between the two assays for NCS treated FHL124 cells appears to display the Real Time LA QPCR's increased sensitivity when compared to the alkaline comet assay. Peak DNA damage in NCS treated FHL124 cells was observed at 0.5 h post

treatment in the alkaline comet assay with damage steadily decreasing over 4 h. However, the Real Time LA QPCR data measured the peak DNA damage at 1 h post treatment. The difference may be attributed to the additional DNA lesions present that are undetectable by the alkaline comet assay. Hence, the Real Time LA QPCR assay may give more accurate measurement of DNA damage and DNA repair kinetics.

Mitochondrial DNA is more susceptible to DNA damage when compared to nuclear DNA (Yakes and Van Houten, 1997). Detecting mitochondrial DNA damage is a useful owing to mitochondrial dysfunction prevalent in many disorders such as Fuchs dystrophy in the cornea. A novel addition to this assay was the ability to assess mitochondrial copy number relative to an untreated control. As well as determining DNA damage in the mitochondria, copy number can be assessed allowing the ability to determine if a change in the number of mitochondria occurred with treatment such as mitochondrial biogenesis. This was performed by designing a bespoke PCR primer designed to amplify a short nuclear fragment in the extracted DNA based on the fact that there is one nucleus to multiple mitochondria per cell, this ratio is used both as a reference gene to allow $2^{-\Delta\Delta CT}$ calculations and to enable mitochondrial copy number quantification. This is an important addition as mitochondrial copy number has been implicated in several diseases and can be used as a proxy to determine mitochondrial function (Longchamps et al., 2020). The Real Time LA QPCR data for NCS and bleomycin treated FHL124 cells both showed a marked increase in lesions per 10 kb in the amplified mitochondrial DNA fragment compared to the nuclear fragment in the same sample.

SYBR Green I was a successful substitute to the Picogreen dye used in the Real Time LA QPCR assay. It is a commonly used DNA binding dye and is substantially less expensive than Picogreen (Rengarajan et al., 2002). Although SYBR Green I was successfully utilised in this assay, the dye has been shown to inhibit PCR amplification (Johnson,

2001). This was demonstrated when optimising SYBR Green I in the master mix when increasing concentrations delayed the exponential phase of the PCR reaction. Other alternative DNA binding fluorophores such as EvagreenTM have similar emission spectra but are less inhibitory to PCR amplification (Edwards, 2009) could be used in lieu of SYBR Green I, potentially reducing assay runtime.

There have been similar PCR techniques that have been developed such as LORD-Q. This assay utilises smaller amplified fragment sizes ~3 kb compared to LA QPCR which uses 12 kb, therefore it significantly reduces run times (Lehle et al., 2014). However, this would also reduce sensitivity at a cost of time saved. Another unique feature is the DNA dye used is not commonly used and more expensive than the well known SYBR green I dye. The Real Time LA QPCR assay uses cheaper more readily available reagents and has increased sensitivity owing to large fragment sizes.

In summary, the work presented shows the development of a real-time tool to assess DNA damage that overcomes many of the shortcomings of its predecessor. The Real Time LA QPCR method described here offers more sensitivity than the commonly used comet assay and is applicable for assessment of both nuclear and mitochondrial DNA damage. This method therefore expands the toolkit available to study the impact of stress pathways on DNA damage, mitochondrial copy number and cell fate.

Chapter 5

Protective effects of SFN against an oxidative stress model in corneal endothelial cells: Implications for cornea tissue storage

5.1 Introduction

Corneal opacities account for 4-5% of blindness worldwide (Resnikoff et al., 2004), the major causes of which include corneal edema, keratoconus and corneal hereditary diseases such as Fuchs' dystrophy. In the majority of cases the only viable treatment is a cornea transplant; the replacement of the affected corneal tissue with that of a healthy donor.

The two most common types of corneal transplant are penetrating keratoplasty (PK), replacement of the full corneal thickness including Descemet's membrane and endothelial keratoplasty (DMEK), the replacement of the endothelial layer which accounts for one third of all corneal transplants (Gain et al., 2016).

Both procedures require donor tissue to have a functional endothelium to maintain stromal deturgescence and transparency. Endothelial cell density (ECD) has been shown to greatly affect graft survival and is therefore used as an indicator to determine transplant suitability. The minimum functional ECD is 500 cells/mm (Wakefield et al., 2015), however, due to the non-proliferative nature of corneal endothelial cells, ECD declines with age at a rate of 0.6% per year and this rate increases rapidly for up to five years after transplantation (Bourne et al., 1997). Based on this data most European eye banks set a donor age limit of 75 years and a required minimum ECD of 2000 cells/mm² for corneal tissue to be considered viable for transplant (Armitage, 2011). Therefore, cornea donor tissue needs to be preserved to limit tissue degradation before it is used for transplant.

Presently, there are two methods for corneal tissue storage: hypothermic storage, where tissue is stored at 2-6°C for 7-10 days and organ culture, where tissue is stored at 31-37°C for up to 4 weeks (Elisabeth et al., 2008). The most commonly used media for hypothermic storage is Optisol GS containing dextran and chondroitin sulphate to aid in stromal hydration maintenance (Layer et al., 2014) and organ culture which predominantly uses EMEM supplemented with FCS (Armitage, 2011). Although there is little difference in tissue quality outcomes between the two methods (Rijneveld et al., 1992), both have a considerable problem with endothelial cell survival during storage. Numerous studies have shown that 20-30% of stored tissue is rejected due to low endothelial cell density (ECD) (Armitage and Easty, 1997; Gavrilov et al., 2010). Hence, the primary aim for storage media is to develop a formulation that better preserves the corneal endothelium.

Research has been focused on the effects of storage media on cornea tissue. One study demonstrated that the endothelium of human corneas during organ culture showed a significant increase in TUNEL-positive cells, indicating apoptosis was a major factor in ECD loss (Albon et al., 2000). However, this view was refined by Crewe and Armitage, who showed that although the endothelium in organ culture demonstrated apoptosis via caspase 3 activation (a more direct indicator of apoptosis), it was not to the same extent as that obtained from TUNEL-positive data which detects fragmented DNA, which is also a feature of necrosis (Crewe and Armitage, 2001).

Histological examination of preserved corneas showed them to contain dead endothelial cells which could have potentially been caused by stresses such as oxidation whilst in storage medium (Kitazawa et al., 2017). Corneal tissue in storage media has been shown to continuously release nitric oxide increasingly exposing tissue to ROS over time (Jeng et al., 2002).

Malondialdehyde, a product of lipid peroxidation and a marker of oxidative stress, was significantly elevated in human corneal epithelial cells exposed to organ culture storage media, whilst anti-oxidative capacity was found to be reduced, over a period of 3 days (Johnsen-Soriano et al., 2012).

Studies have been made to use alternatives to conventional storage media to improve ECD survival. For example, human corneal endothelial cells (HCEC-12) stored in human endothelial serum free medium showed a reduced susceptibility to apoptosis when compared to using standard storage media (EMEM supplemented with FCS) (Jäckel et al., 2011). Modifications to storage media by the addition of additives could also provide protection to corneal ECD.

The isocyanate SFN has been largely studied for its cytotoxic properties (Liu et al., 2017) However, there have been several studies demonstrating SFN's cytoprotective effects, most notably in the eye (Liu et al., 2013; Ye et al., 2013; Ziaei et al., 2013).

A high concentration of SFN (100 μ M) has been shown to be detrimental to FHL124 cells, inducing ROS and DNA damage (Liu et al., 2017). These effects appear to be concentration dependant as lower SFN doses exhibited protection against oxidative stress in the same cell line. Pre-treatment with 1 μ M SFN 24 h before exposure to H₂O₂ significantly inhibited cell death, apoptosis and DNA strand breaks (Liu et al., 2013). SFN has also been shown to protect against oxidative stress-induced apoptosis in human RPE cells (Ye et al., 2013) and most notably, in a Fuchs' endothelial corneal dystrophy cell line (Ziaei et al., 2013).

These studies also demonstrate that SFN induces nuclear translocation of the transcription factor Nrf2 (Liu et al., 2013; Ye et al., 2013; Ziaei et al., 2013) which in turn, upregulates expression of phase II detoxification enzymes. Demonstrating a mechanism by which SFN

protects against oxidative stress. SFN is present in the diet via cruciferous vegetables and there has been no reported evidence of associated toxicity (Davidson et al., 2017) therefore indicating its suitability for use in human tissue.

Based on these studies in the eye, it is plausible that SFN could exhibit similar protective effects against H₂O₂ induced oxidative stress in corneal endothelial cells and therefore a potential candidate for use as a protective additive in corneal storage media.

In lieu of the limited availability of corneal tissue, the HCEC-12 cell line has been previously used as an experimental model for corneal graft survival in assessing different types of storage media (Jäckel et al., 2011; Schönfelder et al., 2014) and is therefore used in this study.

5.2 Aims

Whilst in storage media, corneal donor tissue is subjected to a range of stresses such as oxidative stress, contributing to the decline of ECD, a major determinant of tissue suitability for transplant. Lens epithelial cells treated with SFN has been shown to protect against H₂O₂ induced oxidative stress. Therefore, the present study will test the hypothesis that pre-treatment of SFN will protect HCEC-12 cells from H₂O₂ induced DNA damage and negative cell fate outcomes.

The aims of the study are:

- 1) To establish an oxidative stress model using H₂O₂ in HCEC-12 cells to measure the effects on cell fate outcomes and DNA damage.
- 2) To test HCEC-12 cells pre-treated with SFN against this model to assess its suitability as a protective additive for use in corneal storage media.

5.3 Results

5.31 H₂O₂ effect on viability in HCEC-12 cells

To determine an optimal concentration of H₂O₂ to use in the oxidative stress model a H₂O₂ concentration response was performed on HCEC-12 cells using the MTS assay to determine cell viability after 24 h (Fig 5.1). Within the experimental period, concentrations of 1-30 μ M H₂O₂ did not significantly affect cell viability. However, a significant reduction was observed with 100 μ M H₂O₂ such that the number of surviving cells was $49.3\% \pm 6.3$ relative to untreated controls. When exposed to concentrations of 300 or 1000 μ M H₂O₂, no surviving cells were observed. H₂O₂ concentrations of 30 and 100 μ M was selected to be used in future experiments.

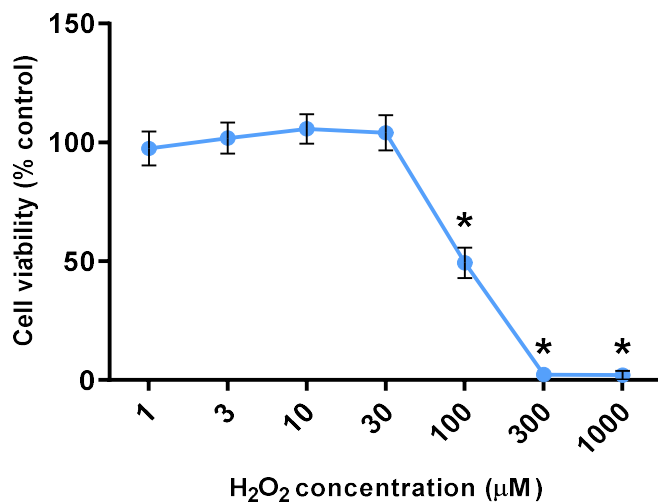


Figure 5.1 The effect of increasing concentrations of H₂O₂ treatment on cell viability in HCEC-12 cells over 24 h, measured by the MTS assay. Data presented as mean \pm SEM (n=4). * indicates a significant difference between treated group and untreated control ($p \leq 0.05$; ANOVA with Dunnett's post hoc test).

5.32 H₂O₂ effect on cell fate markers in HCEC-12 cells

The effects of H₂O₂ on cell death and apoptosis in HCEC-12 cells were determined using CytoTox-Fluor and Caspase-Glo assays respectively. Treatment with 30 μM H₂O₂ showed no effect on cell death or caspase 3/7 activity after 24 h. Caspase 3/7 is a marker for apoptosis and these caspases are known to initiate this process. A significant increase in both cell death and caspase 3/7 activity was shown with a concentration of a 100 μM H₂O₂ compared to untreated control with a 2.1- and 3.5-fold increase respectively (Fig 5.2).

The effects of H₂O₂ on cell senescence in HCEC-12 cells were measured by svβgal activity. Cells were only treated with one concentration of H₂O₂ at 100 μM and showed no effect on senescence after 24 h (Fig 5.3).

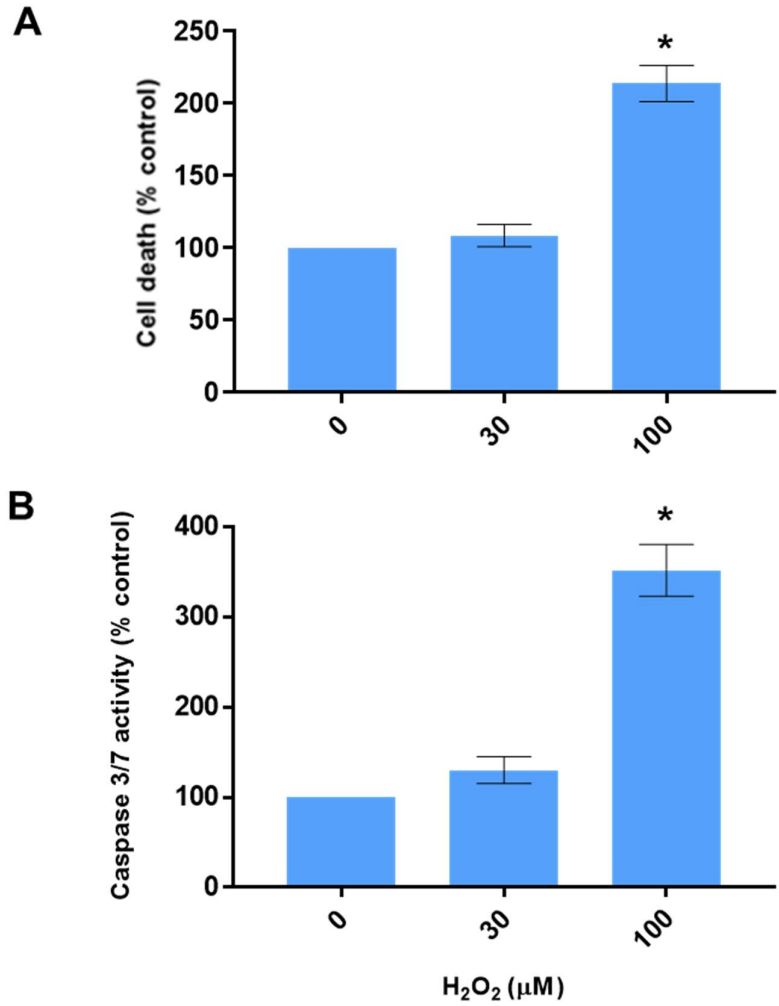


Figure 5.2 Measure of (A) cell death and (B) apoptosis of HCEC-12 cells in response to H₂O₂ treatment after 24 h using CytoTox-Fluor and Caspase-Glo assays respectively. Data presented as mean ± SEM (n=4). * indicates a significant difference between treated groups and untreated control ($p \leq 0.05$; ANOVA with Dunnett's post hoc test).

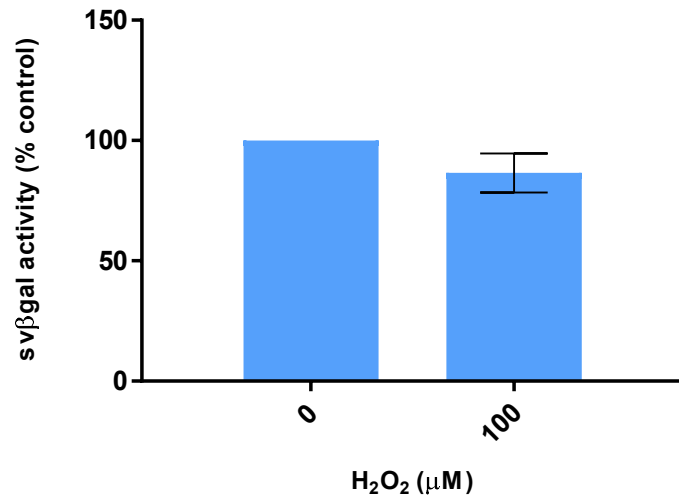


Figure 5.3 svβgal activity as a measure of cellular senescence in HCEC-12 cells in response to H₂O₂ treatment after 24 h using the cellular senescence activity assay. Data presented as mean ± SEM (n=4). No significant difference was determined between treated groups and untreated control ($p \leq 0.05$; Students t-test).

5.33 H₂O₂ effect on ROS and DNA strand breaks in HCEC-12 cells

Treatment of 30 and 100 μM H₂O₂ in HCEC-12 cells significantly increased the level of ROS after 2 h (Fig 5.4). While 100 μM H₂O₂ significantly increased DNA strand breaks with peak levels after 1 h exposure with levels decreasing after 4 h, as determined by the alkaline comet assay (Fig 5.5).

Overall, H₂O₂ has a dose dependant effect on HCEC-12 cell viability, cell fate and DNA damage.

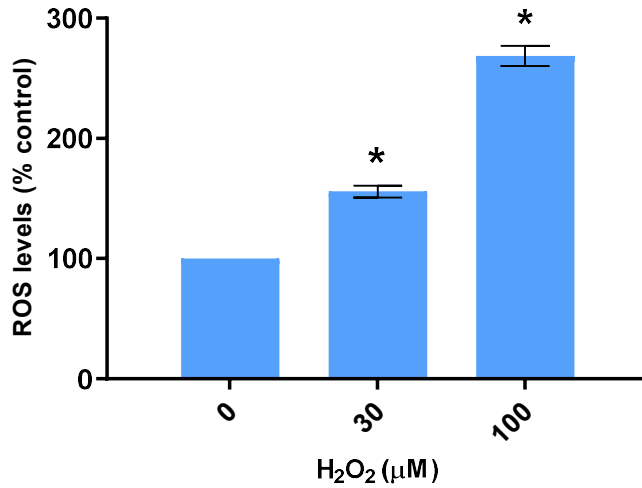


Figure 5.4 ROS levels in HCEC-12 cells resulting from treatment of H₂O₂ after 2 h, measured by the DCFDA assay. Data presented as mean ± SEM (n=4). * indicates a significant difference between treated groups and untreated control ($p \leq 0.05$; ANOVA with Dunnett's post hoc test).

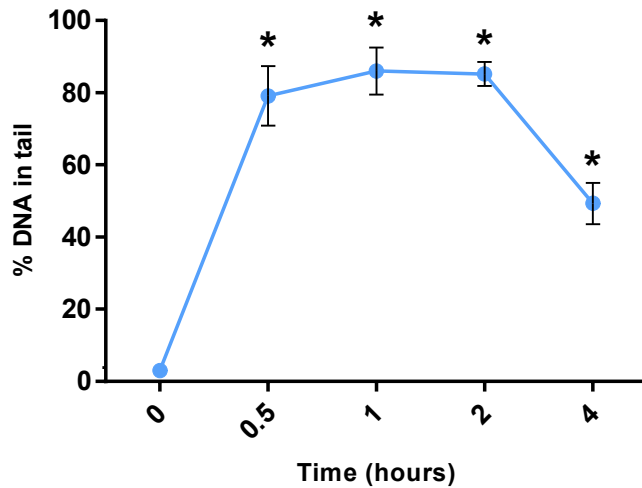


Figure 5.5 DNA strand breaks in HCEC-12 cells from treatment with 100 μM H₂O₂ over 4 h, measured by the alkaline comet assay. Data presented as mean ± SEM (n=4). * indicates a significant difference between treated groups and untreated control ($p \leq 0.05$; ANOVA with Dunnett's post hoc test).

5.34 Determining optimal SFN concentration in HCEC-12 cells

A concentration response of SFN in HCEC-12 cells was performed to find the optimal concentration to be used against the oxidative stress model. This was determined as the highest SFN concentration that had no effect on cell viability. A decrease in cell viability was observed at 10 μM SFN at 24 h and 48 h, while no effect was shown at 1 and 3 μM (Fig 5.6). 1 and 2 μM SFN was selected as the concentration for use in future experiments.

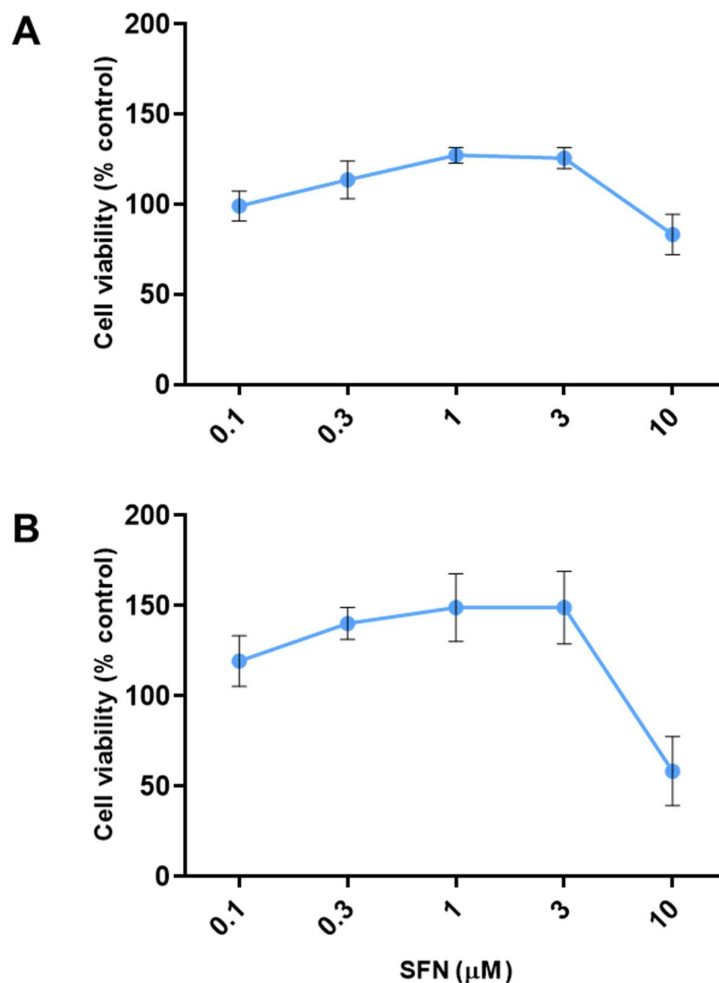


Figure 5.6 The effects of SFN concentration on HCEC-12 cell viability over (A) 24 h and (B) 72 h, measured by the MTS assay. Data presented as mean \pm SEM (n=4). * indicates a significant difference between treated groups and untreated control ($p \leq 0.05$; ANOVA with Dunnett's post hoc test).

5.35 SFN protects cell viability against H₂O₂ induced oxidative stress

Pre-treatment of 2 μ M SFN to HCEC-12 cells 24 h before experimental conditions confers protection against H₂O₂ induced loss of cell viability. However, 1 μ M SFN had no effect, whereas 2 μ M SFN pre-treatment significantly increased cell number compared to controls, including cells not treated with H₂O₂ (Fig 5.7). Therefore, 2 μ M SFN was selected as the optimal concentration in further experiments.

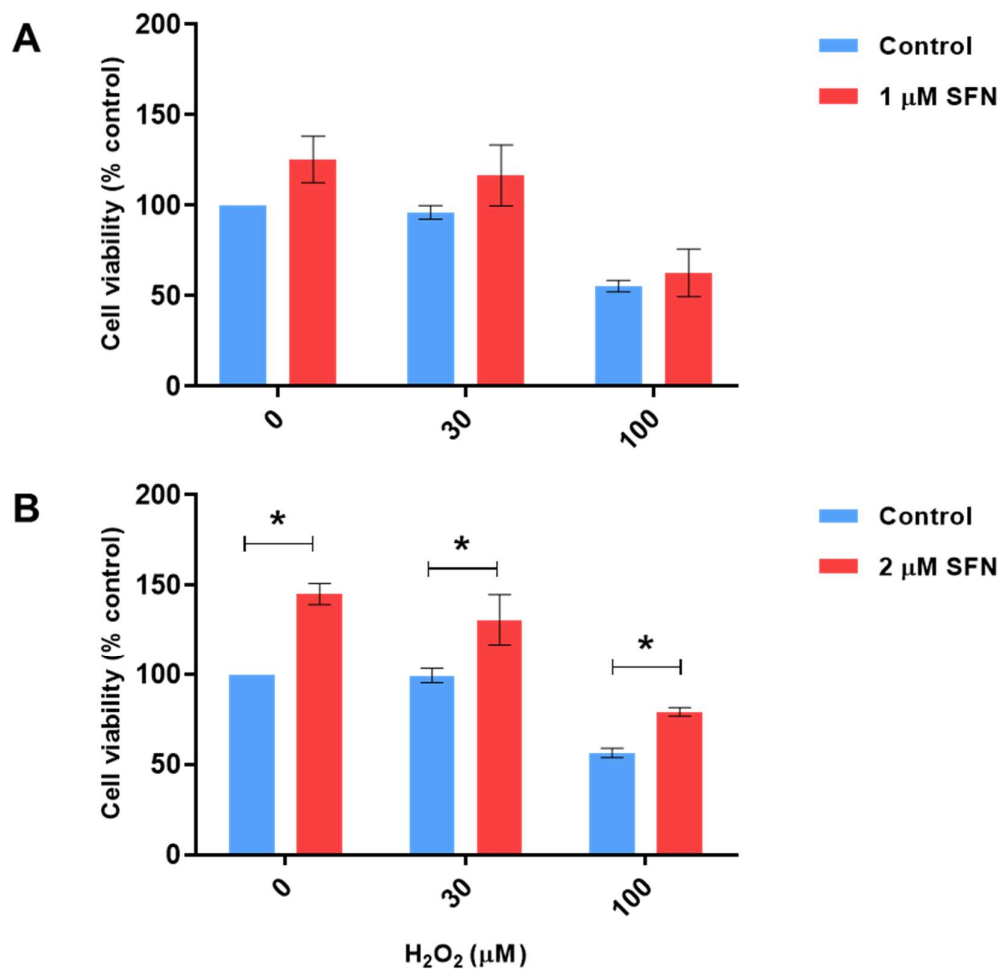


Figure 5.7 Cell viability of FHL124 cells, pre-treated with (A) 1 μ M and (B) 2 μ M SFN 24 h prior to H₂O₂ treatments, measured by the MTS assay after 24 h. Data presented as mean \pm SEM (n=4). * indicates a significant difference between treated groups and untreated controls ($p \leq 0.05$; ANOVA with Tukey's post hoc test).

5.36 SFN reduces H₂O₂ induced cell death and apoptosis

Pre-treatment of HCEC-12 cells with SFN decreases cell death and apoptosis markers caspase 3 and 7, against 100 μ M H₂O₂. However, there is no effect at the lower 30 μ M H₂O₂ concentration and non- H₂O₂ treated cells (Fig 5.8). SFN also had no effect on the levels of senescence marker sv β gal after 24 h (Fig 5.9).

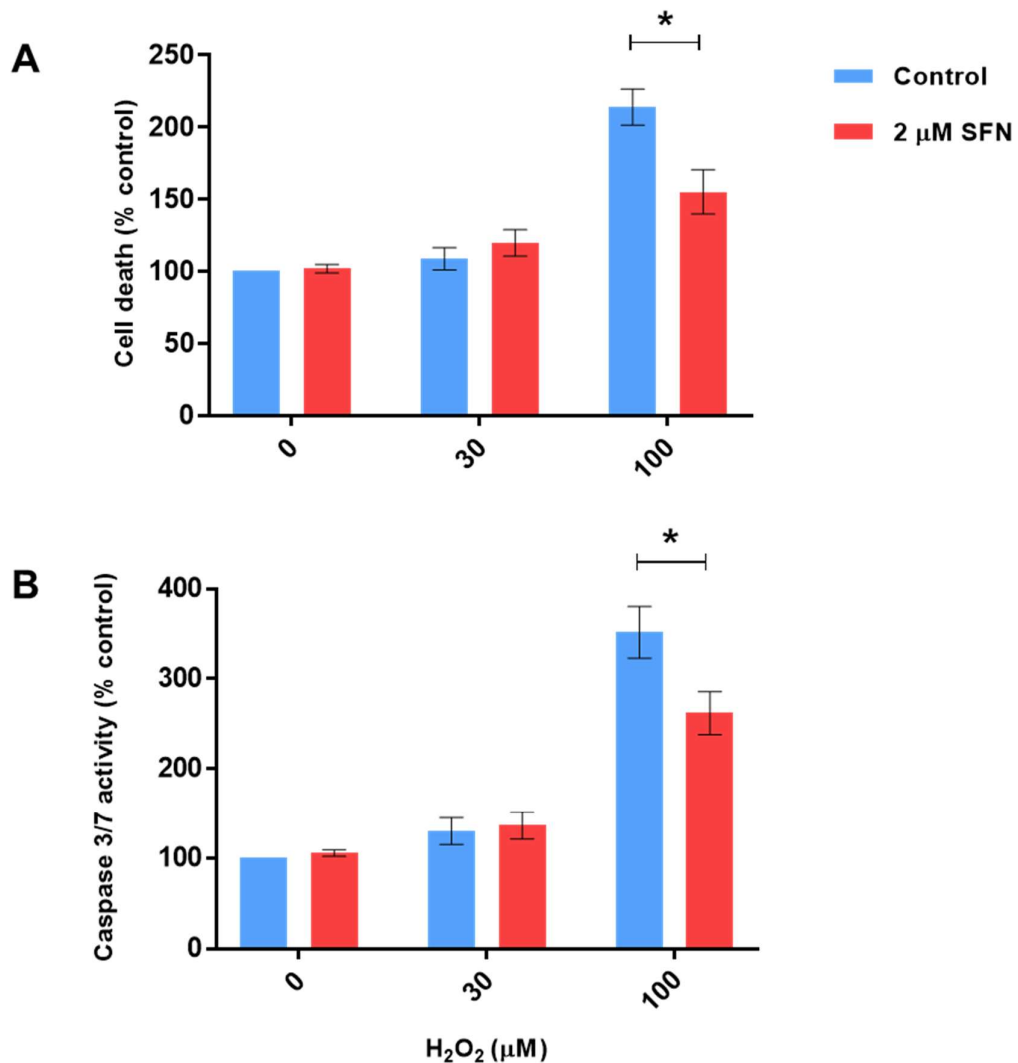


Figure 5.8 Measure of (A) cell death and (B) apoptosis in HCEC-12 cells pre-treated with 2 μ M SFN 24 h prior to H₂O₂ treatment after 24 h using CytoTox-Fluor and Caspase-Glo assays respectively. Data presented as mean \pm SEM (n=4). * indicates a significant difference between treated groups and untreated controls ($p \leq 0.05$; ANOVA with Tukey's post hoc test).

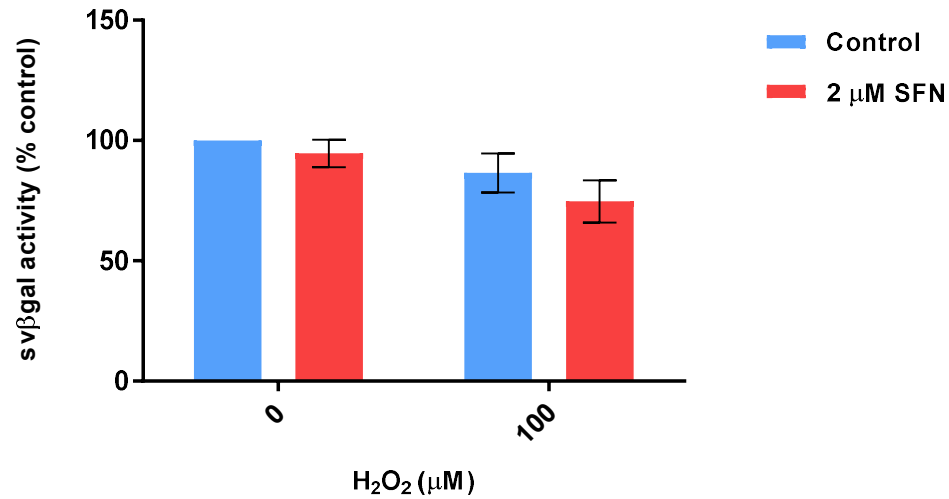


Figure 5.9 svβgal activity as a measure of cellular senescence in HCEC-12 cells pre-treated with 2 μM SFN 24 h prior to H₂O₂ treatments using the cellular senescence activity assay after 24 h. Data presented as mean ± SEM (n=4). * indicates a significant difference between treated groups and untreated controls ($p \leq 0.05$; ANOVA with Tukey's post hoc test).

5.37 SFN has no effect on cellular ROS induced by H₂O₂ but potentially decreases DNA strand breaks.

At all concentrations studied, pre-treatment with SFN appeared to have no effect on ROS levels compared to controls in HCEC-12 cells (Fig 5.10). SFN pre-treated cells did show a general trend in a reduction of DNA strand breaks compared to non-pre-treated cells, however, no significant differences were observed at any time point (Fig 5.11).

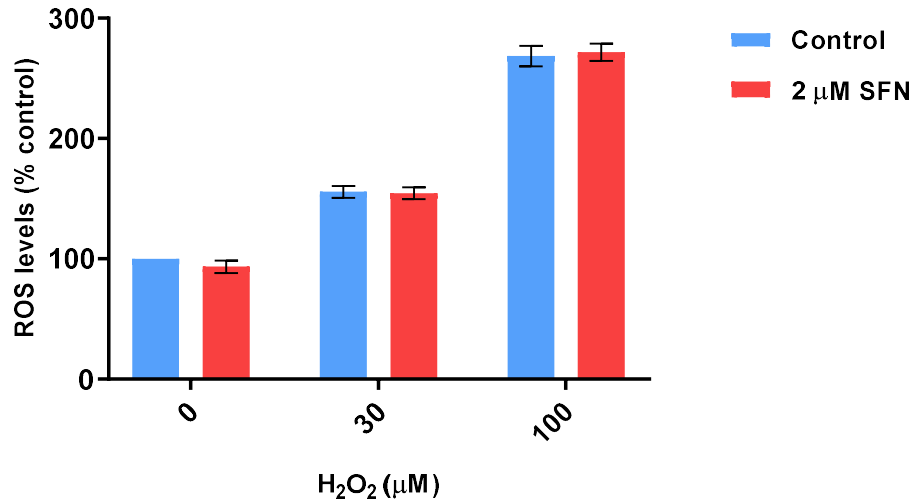


Figure 5.10 ROS levels in HCEC-12 cells pre-treated with 2 μM SFN 24 h prior to H₂O₂ treatments, measured by the DCFDA assay after 2 h. Data presented as mean ± SEM (n=4). * indicates a significant difference between treated groups and untreated controls ($p \leq 0.05$; ANOVA with Tukey's post hoc test).

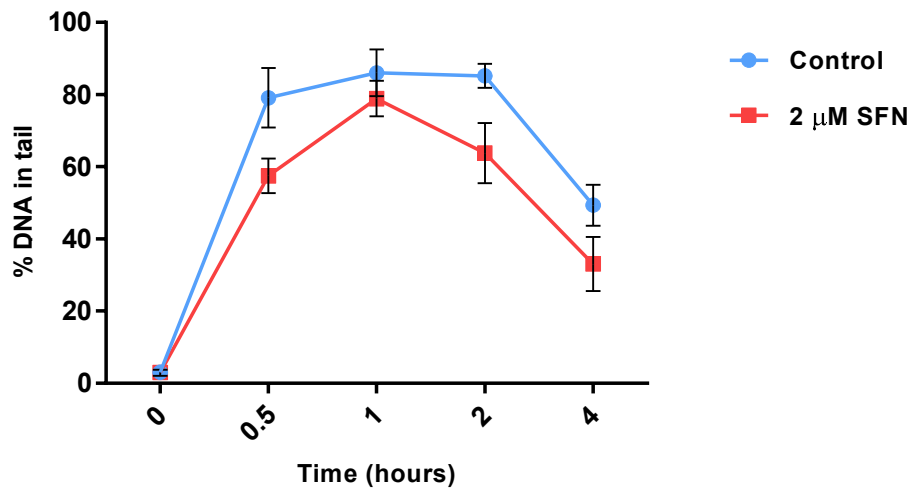


Figure 5.11 DNA strand breaks in HCEC-12 cells pre-treated with 2 μM SFN 24 h prior to treatment of 100 μM H₂O₂ over 4 h, measured by the alkaline comet assay. Data presented as mean ± SEM (n=4). No significant differences were determined between treated groups and untreated control ($p \leq 0.05$; ANOVA with Tukey's post hoc test).

5.38 SFN does protect against H₂O₂ induced nuclear and mitochondrial DNA lesions but does not affect mitochondrial copy number

Although SFN did not confer significant protection against H₂O₂ induced strand breaks, SFN does protect against H₂O₂ nuclear and mitochondrial DNA lesions as determined by the Real Time long amplicon QPCR assay (Fig 5.12). Pre-treatment with 2 μM SFN showed a significant decrease in nuclear DNA lesions at 0.5 h and 1 h and mitochondrial DNA lesions at 1 h after treatment with H₂O₂ when compared to non SFN treated controls. SFN had no effect on mitochondrial copy number in HCEC-12 cells (Fig 5.13).

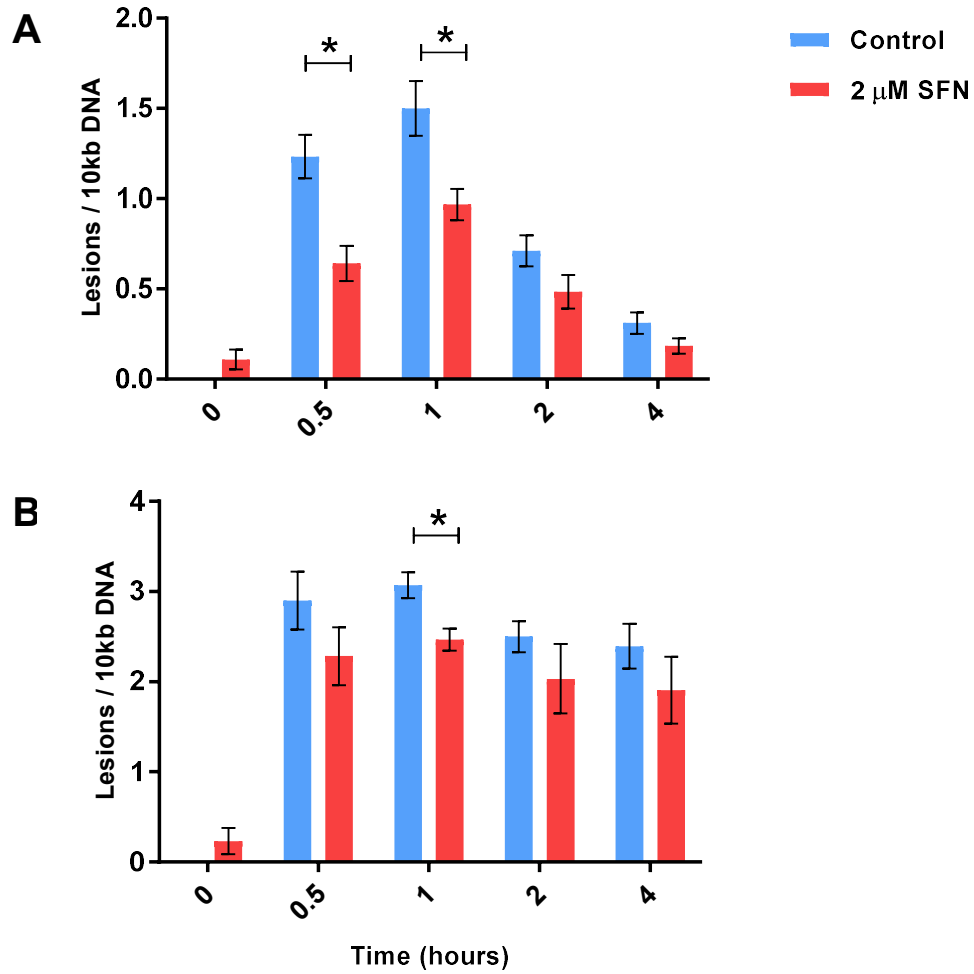


Figure 5.12 Lesions/10kb in nuclear (A) and mitochondrial (B) DNA in HCEC-12 cells pre-treated with 2 μ M SFN 24 h prior to treatment of 100 μ M H₂O₂ over 4 h, measured by the Real Time long amplicon QPCR assay. Data presented as mean \pm SEM (n=3). * indicates a significant difference between treated groups and untreated controls ($p \leq 0.05$; ANOVA with Tukey's post hoc test).

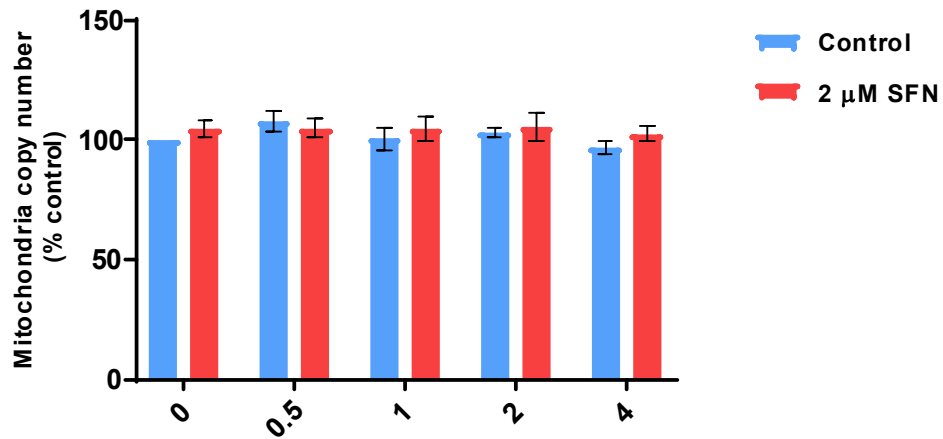


Figure 5.13 Mitochondrial DNA copy number in HCEC-12 cells pre-treated with 2 μ M SFN 24 h prior to treatment of 100 μ M H₂O₂ over 4 h, measured by the Real Time long amplicon QPCR assay. Data presented as mean \pm SEM (n=3). * indicates a significant difference between treated groups and untreated controls ($p \leq 0.05$; ANOVA with Tukey's post hoc test).

4.4 Discussion

Corneal transplant is the most common transplant procedure globally. Consequently, there is a considerable shortage of corneal donor tissue (Gain et al., 2016) and reduction in ECD during storage severely affects availability of viable donor tissue. Protecting against oxidative stress and thus minimising ECD loss in storage media could help alleviate this problem.

The oxidative stress model used in this study effectively demonstrated changes to cell fates in corneal endothelial cells associated with loss of ECD in storage media. Exposure to H₂O₂ significantly reduced HCEC-12 viability and increased cell death, apoptosis and DNA strand breaks. ROS levels were also significantly increased following H₂O₂ treatment, comparable with levels in a previous study (Jäckel et al., 2011). Thus, this model provides an important proof of principle step for the effectiveness of potential protective agents used as additives in tissue storage media against oxidative stress in HCECs before being assessed on scarcely available corneal tissue.

In this study, SFN has been shown to protect HCEC-12 cells from H₂O₂ induced oxidative stress. Pre-treatment of 2 µM SFN 24 hours prior to exposure to the oxidative stress model significantly protected against an H₂O₂ induced decrease in cell viability. However, SFN treated cells not exposed to H₂O₂ increased in cell number compared to control, untreated cells, indicating that SFN protected cell viability may be because of increased cell growth. This would have limited effect on corneal tissue as HCECs are non-proliferative in vivo. Importantly, SFN protected against H₂O₂ induced cell death, most likely by apoptosis that is associated with ECD loss in storage media (Albon et al., 2000; Crewe and Armitage, 2001). This coincides with previous studies in the eye where SFN has also been shown to

protect against H₂O₂ induced apoptosis in human RPE cells (Ye et al., 2013) and most notably, in a Fuchs' endothelial corneal dystrophy cell line (Ziaei et al., 2013).

Although there was no effect of SFN treated cells on the levels of the senescence marker β gal after 24 h, no difference was observed with H₂O₂ treated controls either. Therefore SFN's effect remains inconclusive due to the limitations of the oxidative stress model that was used. Inducing senescence experimentally with H₂O₂ is well established in cell culture (Chen et al., 2007), altering H₂O₂ concentration and assay time to induce an effect by which SFN pre-treatment can be compared to may be useful for future experiments. Current research is primarily focused on cell death outcomes and senescence testing was included in the present study to cover all aspects of cell fate.

Pre-treatment with SFN did not significantly reduce H₂O₂ induced DNA strand breaks as assessed by the alkaline comet assay but did significantly reduce H₂O₂ induced DNA lesions in nuclear DNA using the long amplicon method. This may be due the fact that the comet assay employed in the present study only detects one type of DNA lesion (DNA strand breaks) whereas the Real Time long amplicon QPCR assay detects multiple types of DNA lesions. This is a good example of the increased sensitivity of the Real Time long amplicon QPCR assay for detection of DNA damage.

DNA protection is particularly important as HCECs do not upregulate DNA damage repair proteins in response to DNA damage (Joyce et al., 2011) and older cornea donor tissue have been shown to have increased endogenous oxidative DNA damage compared to younger donors (Joyce et al., 2009). Therefore, SFN may reduce induction of apoptosis via DNA damage from oxidative stressors in storage media.

It has not yet been established whether the DNA damage protecting mechanism of SFN is due to free radical quenching or interaction with the DDR (Topè and Rogers, 2009) as SFN

has been shown to bind to DNA and RNA, the outcomes of which are unknown (Joozdani et al., 2015).

Although much focus has been on preventing ECD loss in storage media, disruption of mitochondrial function may also impact corneal endothelial cell ability to maintain stromal deturgescence, which is an ATP dependant process. Oxidative stress is a major cause of respiratory dysfunction in mitochondria as mtDNA which encodes proteins essential for ATP production is susceptible to damage from ROS (Ott et al., 2007). Utilising the Real Time long amplicon QPCR assay, SFN pre-treatment was shown to significantly reduce peak mtDNA damage from H₂O₂ induced oxidative stress compared to control. This protection may help prevent ATP levels from falling below the required threshold for fluid pump homeostasis, delaying the onset of corneal oedema whilst in storage media.

This mitochondrial protection may also contribute to the mechanism by which SFN prevents apoptosis in HCEC-12 cells, as oxidative stress causes opening of the membrane permeability transition pore, facilitating the release of pro-apoptotic proteins such as cytochrome c (Elmore, 2007).

SFN has been shown to induce mitochondrial biogenesis in porcine kidney cells and identified as a cytoprotective mechanism (Negrette-guzmán et al., 2017). Mitochondrial copy number, a hallmark of biogenesis, was assessed using the Real Time long amplicon QPCR assay and showed SFN had no effect in HCEC-12 cells.

The mechanism by which SFN typically protects against oxidative stress has been well established in the eye (Liu et al., 2013; Ye et al., 2013; Ziaei et al., 2013). SFN induces nuclear translocation of the transcription factor Nrf2 which in turn, binds to the ARE upregulating expression of phase II detoxification enzymes such as NQO1 (Liu et al.,

2013, Ziaei et al., 2013). Importantly, SFN has been shown to enhance Nrf2 signalling in response to oxidative stress in HCEC in ex vivo corneas (Ziaei et al., 2013).

HCEC-12 pre-treatment with SFN had no immediate effect on H₂O₂ induced ROS generation after 2 hours. This may be due to the limitations of the ROS assay as it was not possible to determine ROS levels over a longer time period. Nonetheless, this further demonstrates that SFN is not a direct antioxidant but rather as an indirect antioxidant, upregulating phase II antioxidant defence mechanisms (Liu et al., 2013).

Although SFN has been shown to be effective protecting HCEC from oxidative stress there are limitations in the study to consider. HCECs were pre-treated with SFN 24 hours prior to exposure to H₂O₂ induced oxidative stress, to allow significant time for SFN to accumulate into cells and induce changes. Although ITCs rapidly accumulate in cells within hours (Zhang, 2001), this potentially leaves a window in which donor tissue do not fully benefit from SFN's protective effects when first placed in media. Addition of an antioxidant such as NAC could be used to provide short term protection during SFN accumulation.

Cornea donor tissue can be stored in media for up to 30 days whilst continually being exposed to oxidative stress. Although this study assesses the protective effects of SFN 24 hours after exposure to oxidative stress, the most significant loss of ECD occurs in the first week of cultivation, most likely due to tissue adjusting to storage conditions (Hempel et al., 2001). This warrants further study of SFN in cornea donor tissue in media during typical storage times to fully assess its effectiveness as a candidate for use as an additive in corneal storage media.

This study provides a proof of principle step for the effectiveness of SFN as a protective agent against ECD loss from oxidative stress. This has important ramifications for corneal

tissue shortage, potentially increasing the number of viable donor corneas for transplant after storage thus reducing graft rejection and alleviating lost resources from rejected tissue. Effectively reducing ECD loss may allow for increasing the upper age limit for donor corneas, increasing supply and reducing the tissue shortage burden.

In summary, SFN is an effective candidate for use as a protective agent against oxidative stress in corneal storage media.

Chapter 6

ROS plays a critical role in SFN induced DNA damage and cell death

6.1 Introduction

Presently, the only treatment for cataract is the surgical removal of the affected lens and its replacement with an artificial intraocular lens (IOL). During this process, an incision is made in the anterior lens capsule and the lens fibres removed via emulsification, leaving behind a capsular bag that the IOL can be housed in, restoring visual clarity (Wormstone et al., 2009). However, residual lens epithelial cells remain, with the trauma from surgery initiating an inflammatory response where these cells grow and encroach onto the posterior lens capsule, eventually causing a secondary loss of vision (Nibourg et al., 2015). This condition is known posterior capsule opacification (PCO).

PCO can cause decreased visual acuity in 20-40 % of patients, 5 years post-surgery (Awasthi et al., 2009). Currently, the only treatment is a corrective procedure using a Nd:YAG laser to restore visual function (Wormstone et al., 2020). This is an expensive procedure and not without medical risk, imposing a significant economic impact (Aaronson et al., 2019). Thus, developing therapies for the prevention of PCO is an important area of research.

The isocyanate Sulforaphane (SFN) has been shown to exhibit both cytoprotective and cytotoxic properties. The difference in effect is concentration dependant (Juge et al., 2007; Liu et al., 2013). The cytotoxic properties of SFN have been shown to reduce proliferation of cells by inducing cell cycle arrest and apoptosis. SFN has been shown to induce ROS, which may mediate cell anti-proliferation (Lee and Lee, 2011).

In the lens SFN has been shown to protect cells at lower concentrations ($\leq 2 \mu\text{M}$) through activation of antioxidant defences. However, at higher concentrations ($\geq 10 \mu\text{M}$) SFN was found to reduce LEC growth and viability of FHL124 cells and in human lens capsular bags (Liu et al., 2013; Liu et al., 2017). Such actions could provide a therapeutic benefit in the prevention of PCO. It is however important to reveal the mechanisms that underpin this outcome. Previously, SFN has been reported to induce ER stress activating stress pathways such as pEIF2 α , IRE1 and ATF6, and increase levels of microtubule-associated protein 1A/1B-light chain 3 (LC3)-II, a marker for autophagy (Liu et al., 2017). Activation of these stress pathways is believed to enhance cell death. It is however important to understand the mechanisms governing SFN mediated lens cell death. In the present study it was hypothesised that generation of reactive oxygen species is a key mediator of SFN-induced lens cell death. This principle has not been tested in lens cells but work in other fields have demonstrated that a ROS scavenger N-acetylcysteine (NAC), a derivative of the amino acid L-cysteine and an antioxidant commonly used to scavenge ROS (Aruoma et al., 1999) could prevent SFN induced ROS accumulation in human bronchial cells and this resulted in greater cell viability (Lee and Lee, 2011).

6.2 Aims

SFN has been shown to exhibit cytotoxic effects against human lens epithelial cells and may provide a role as a therapeutic strategy in the prevention of PCO. If cells treated with NAC counters these effects, it may indicate ROS is a vital mediator of SFN-induced anti-PCO actions. The hypothesis for the present study is that ROS play a critical role in promoting SFN-induced DNA damage and reduced lens cell viability.

The aim of the study is to assess the effects of SFN treatment on viability, DNA damage and ROS generation in FHL124 cells and determine if the ROS scavenger NAC counters these effects.

6.3 Results

6.31 SFN reduces FHL124 cell viability

A concentration response for SFN was performed to assess the effect on cell viability in FHL124 cells, using the MTS assay after 24 h (Fig 6.1). There was no significant effect on cell viability from 1, 3 and 10 μM SFN treatments, whilst 30 μM significantly reduced cell viability to $42.7\% \pm 16.9$ compared to untreated control. At 100 and 300 μM treatments, few surviving cells were observed. 100 μM SFN was selected to be used in future experiments to assess its cytotoxic effects.

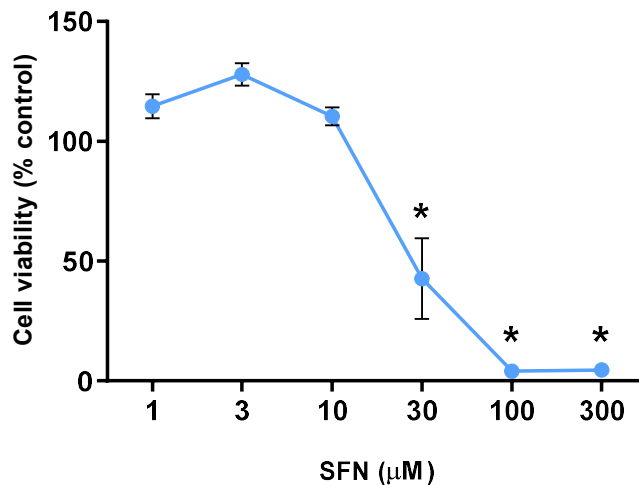


Figure 6.1 Concentration response of SFN treatment on cell viability in FHL124 cells over 24 h, measured by the MTS assay. Data presented as mean \pm SEM (n=4). * indicates a significant difference between treated group and untreated control ($p \leq 0.05$; ANOVA with Dunnett's post hoc test).

6.32 SFN increases ROS in FHL124 cells

The DCFDA assay was used to assess levels of ROS in FHL124 cells after treatment with SFN (Fig 6.2). ROS levels were significantly increased after 2 h following addition of 100 μ M SFN, increasing by 32.6% \pm 10.6 compared to untreated control.

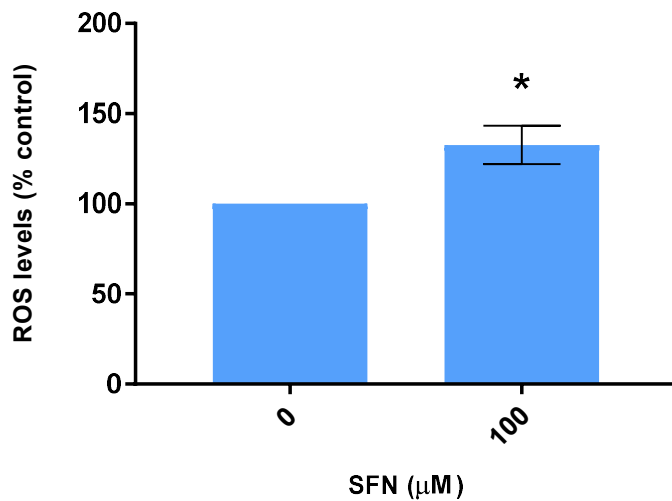


Figure 6.2 ROS levels from treatment of 100 μ M SFN in FHL124 cells after 2 h, measured by the DCFDA assay. Data presented as mean \pm SEM (n=4). * indicates a significant difference between treated group and untreated control ($p \leq 0.05$; Student's t-test).

6.33 SFN increases DNA strand breaks in FHL124 cells

The alkaline comet assay was performed to assess DNA strand breaks in FHL124 cells treated with 100 μ M SFN over a 4 h period (Fig 6.3). All time points showed an increase in DNA strand breaks but only peak damage at 2 h showed a significant difference compared to untreated control. At this timepoint, % DNA in tail was 11.7% \pm 1.8 compared to 3.4% \pm 0.9 of control, a three-fold increase.

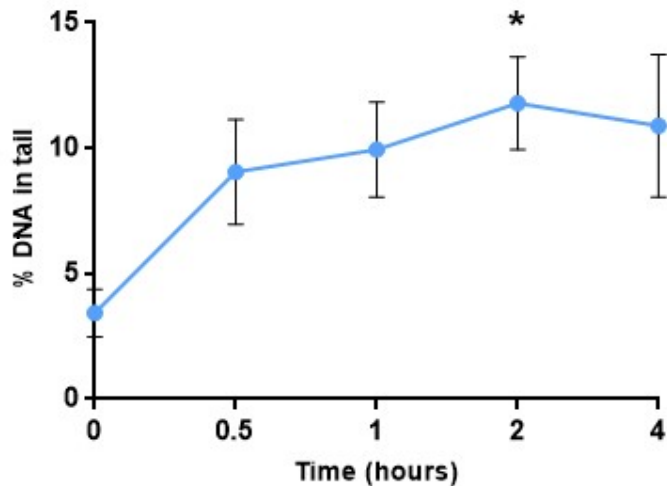


Figure 6.3 DNA strand breaks from treatment of 100 μ M SFN in FHL124 cells over 4 h, measured by the alkaline comet assay. Data presented as mean \pm SEM (n=3). * indicates a significant difference between treated group and untreated control ($p \leq 0.05$; ANOVA with Dunnett's post hoc test).

6.34 Optimisation of NAC concentration in FHL124 cells

A concentration response for NAC was performed to assess the effect on cell viability on FHL124 cells, using the MTS assay after 24 h (Fig. 6.4). Concentrations up to 1 mM had no effect on cell viability with 3 and 10 mM NAC significantly increasing viability compared to untreated control. 1mM was determined as the highest NAC concentration that had no effect on cell viability.

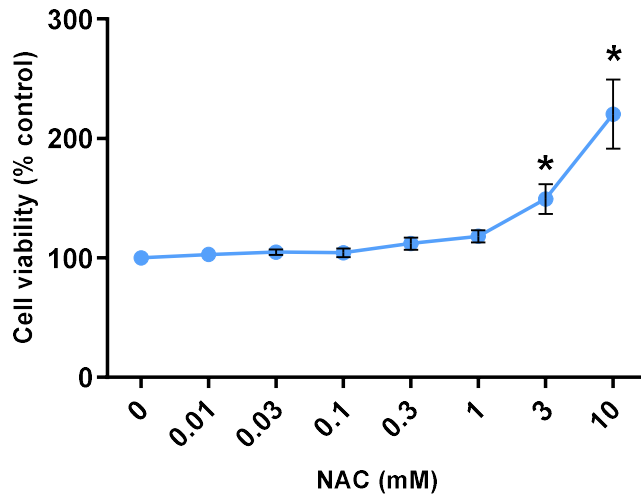


Figure 6.4 The effect of increasing concentrations of NAC treatment on cell viability in FHL124 cells over 24 h, measured by the MTS assay. Data presented as mean \pm SEM (n=4). * indicates a significant difference between treated group and untreated control ($p \leq 0.05$; ANOVA with Dunnett's post hoc test).

6.35 NAC protects FHL124 cell viability from SFN

FHL124 cells were pre-treated with increasing NAC concentrations 1 h prior to SFN treatment and assessed for viability using the MTS assay after 24 h (Fig. 6.5). FHL124 cells without NAC pre-treatment were observed to have few surviving cells following exposure to 100 μ M SFN, whereas 0.1 mM NAC only preserved cell viability to that of 29.3% \pm 9.7 of untreated control. Pre-treatment with either 0.3 or 1 mM NAC, fully protected the cells from SFN induced loss of cell viability.

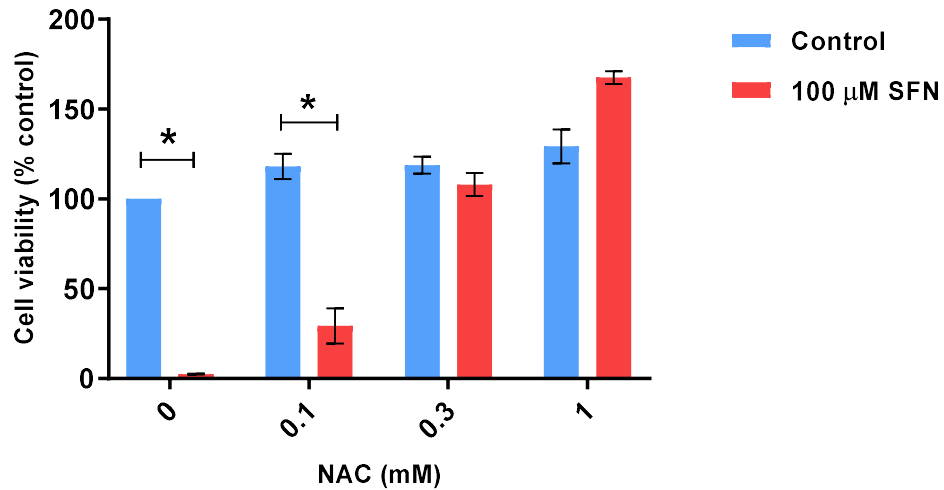


Figure 6.5 Cell viability of FHL124 cells after pre-treatment of different NAC concentrations 1 h prior to SFN treatment after 24 h, measured by the MTS assay. Data presented as mean \pm SEM (n=4). * indicates a significant difference between treated group and untreated controls ($p \leq 0.05$; ANOVA with Tukey's post hoc test).

6.36 NAC quenches SFN induced ROS

The DCFDA assay was used to assess levels of ROS in FHL124 cells pre-treated with NAC 1 h before exposure to SFN after 2 h (Fig 6.6). Treatment of 100 μ M SFN to untreated cells caused a significant increase of $30.2 \pm 9.8\%$ of ROS compared to control. Pre-treatment of 1 mM NAC completely quenched all ROS induced by SFN as well as endogenous ROS produced by untreated control.

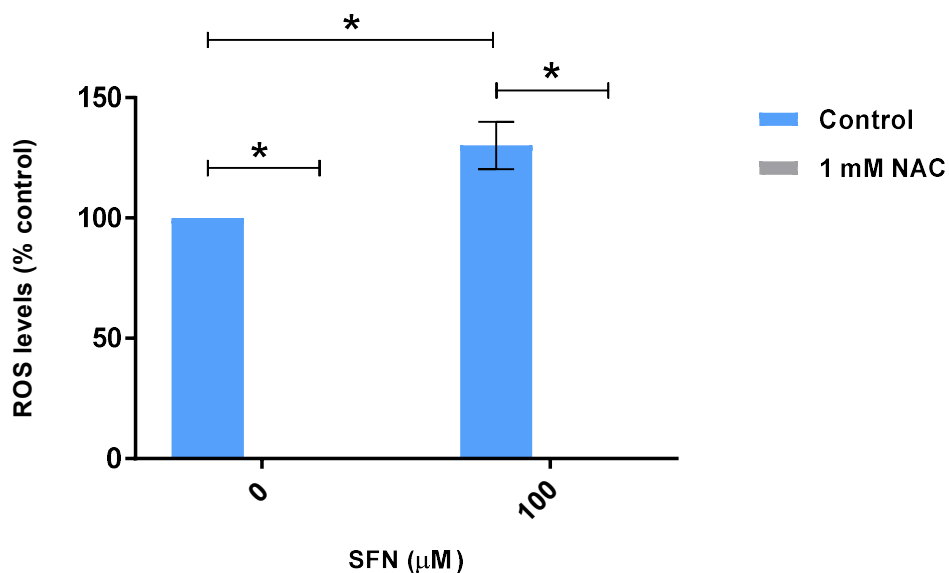


Figure 6.6 ROS levels in FHL124 cells pre-treated with NAC 1 h prior to treatment of SFN after 2 h, measured by the DCFDA assay. Data presented as mean \pm SEM (n=4). * indicates a significant difference between treated group and untreated controls ($p \leq 0.05$; ANOVA with Tukey's post hoc test).

6.37 NAC prevents SFN induced DNA damage

Pre-treatment with NAC significantly reduces SFN induced DNA strand breaks as assessed by the alkaline comet assay (Fig 6.7). NAC pre-treatment also reduces DNA lesions in nuclear and mitochondrial DNA against 100 μ M SFN treatment (Fig 6.8)

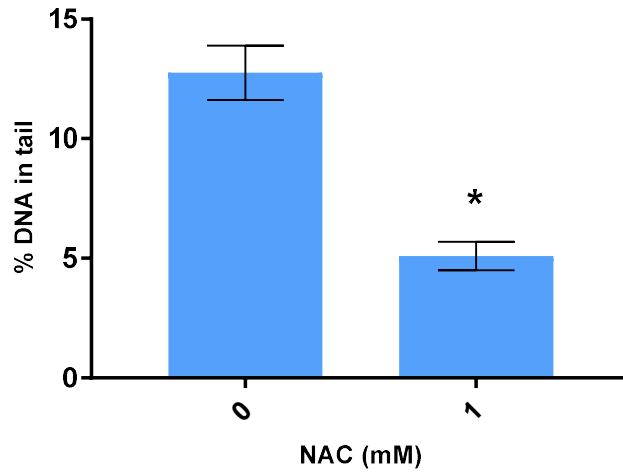


Figure 6.7 DNA strand breaks in FHL124 cells pre-treated with NAC 1 h prior to treatment of 100 μ M SFN after 2 h, measured by the alkaline comet assay. Data presented as mean \pm SEM (n=3). * indicates a significant difference between treated group and untreated control ($p \leq 0.05$; Student's t-test)

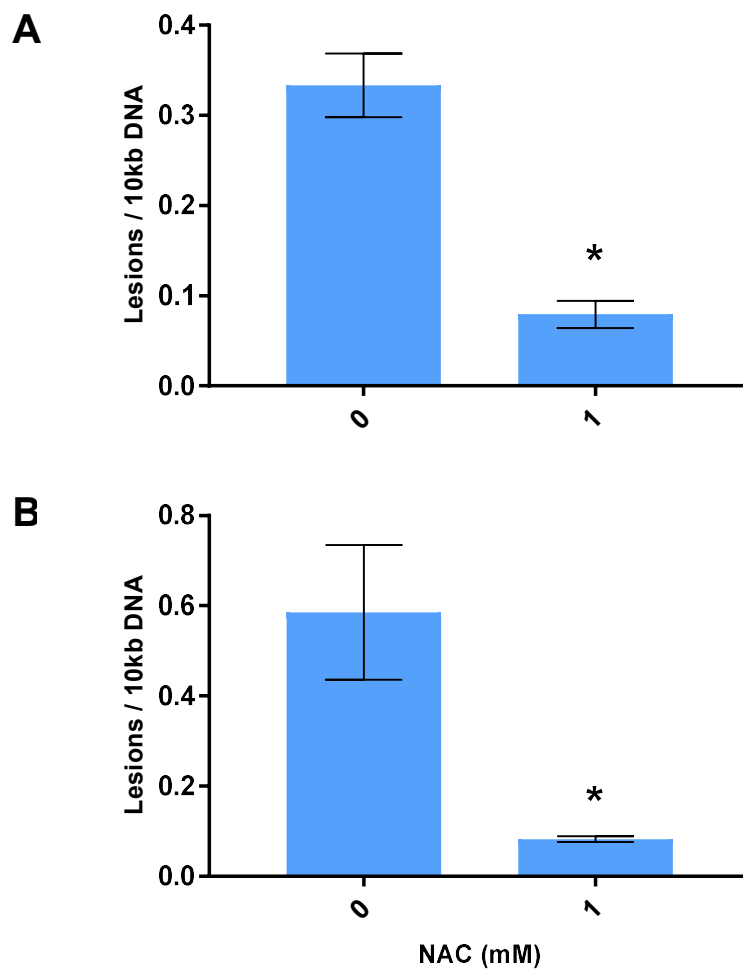


Figure 6.8 Lesions/10kb in (A) nuclear and (B) mitochondrial DNA in FHL124 cells pre-treated with NAC 1 h prior to treatment of 100 μ M SFN after 2 h, measured by the Real Time long amplicon QPCR assay. Data presented as mean \pm SEM (n=3). * indicates a significant difference between treated group and untreated control ($p \leq 0.05$; Student's t-test).

6.4 Discussion

PCO is the most common complication of cataract surgery (Wormstone et al., 2021) with the only means of treatment being surgical intervention. This presents numerous medical and economic complications and the need for other interventions that can help alleviate this problem. Preventing or severely delaying formation of PCO rather than treating the condition post-operatively can address these concerns.

SFN has been identified as a potential pharmacological agent to treat PCO owing to its cytotoxic effects on FHL124 cells (Liu et al., 2017). SFN was shown to induce ER stress by activating Bip which in turn activates stress pathways decreasing cell viability and increasing cell death (Liu et al., 2017). A key question however is what changes to the lens cell environment initiate stress pathways ultimately resulting in death. SFN induced ROS has been shown to be a potential mechanism for SFN cytotoxicity in other human cell types (Lee and Lee, 2011), therefore investigating this in LECs seemed logical. Expanding the effects of SFN on DNA damage could also be an important factor that affects LEC cell death was also explored.

SFN was shown to significantly reduce FHL124 cell viability with 30 and 100 μM SFN after 24 hours, with the 100 μM treatment leading to total annihilation of the cell population within 24 hours. This effectively demonstrates that SFN is cytotoxic to LECs beyond a concentration threshold. This range of concentration dependent effects also tallies well with other published works (Liu et al., 2013; Liu et al., 2017). Interestingly, pre-treatment with the ROS scavenger molecule NAC prevented SFN induced reduction in cell viability compared to non-treated controls in FHL124 cells. Therefore, it is reasonable to suggest ROS induction is a major mechanism by which SFN causes cytotoxicity.

To test this theory, utilising the DCFDA assay for detection of ROS, addition of 100 μ M SFN significantly increased ROS compared with untreated control. This seems to reinforce the notion that the cytotoxic actions of SFN are ROS mediated. The increased levels of ROS is what may induce the previously reported ER stress, in turn activating downstream stress pathways leading to apoptosis. Future studies should expand the current outputs tested and confirm that NAC treatment can prevent SFN induce ER stress and autophagy. Genotoxic stress, causing DNA strand breaks can lead to cell dysfunction and eventually cell death. Oxidative stress induced by excess ROS production can contribute significantly to DNA damage (Smith et al 2015; Smith et al., 2016). Therefore, the effect of SFN on DNA strands breaks was assessed to further expand the physiological events associated with SFN in the lens and was found to have a mild, but significant effect on DNA integrity. This is a less dramatic outcome that other agents, such as hydrogen peroxide, but this more controlled elevation of DNA damage could serve as a useful experimental platform for general studies of genotoxic damage in the future. Pre-treatment of NAC reduced SFN induced DNA strand break to levels similar to that of untreated controls. The more sensitive Real Time LA QPCR demonstrated similar results. This demonstrated that DNA damage caused by treatment of SFN is ROS mediated.

Another area that has not been fully investigated in the lens, is the effect of SFN on mitochondrial function, as this could also be a source of ROS. In the present study it was demonstrated that NAC could reduce the number of mitochondrial DNA lesions relative to SFN treatment alone. These data suggest that the mitochondria are susceptible to the actions of SFN and should be investigated further in the future. For example, mitochondrial membrane potential could be used as a marker of mitochondrial health and visualisation systems, such as mitotracker could be used to assess the mitochondrial network within cells.

Further to the current study it also worth considering additional ways in which ROS could be elevated in response to SFN. One possibility that could be studied in the future is the regulation of glutathione (GSH), which is the major antioxidant in the eye (Giblin, 2000; Fan et al., 2017). SFN is known to form conjugates with GSH and in addition is known to interfere with GSH regulatory enzymes, including glutathione reductase (Zhang et al., 1995; Hu et al., 2007)). Together these interactions could reduce availability of GSH, which would render lens cells vulnerable to oxidative stress and the actions of ROS. Therefore, studying the interactions of SFN on GSH will be a fascinating area of future study.

SFN is a promising compound for the prevention of PCO and potentially other conditions, such as cancers. The work described has provided further insight into the mechanisms mediating SFN-induced lens cell death. As with any agent general cytotoxicity is a concern and thus controlled drug delivery would be required for any putative clinical application. To this end, approaches such as the perfect capsule (Duncan et al., 2007; Rabsilber et al., 2007) and drug loaded IOLs (Duncan et al., 1997; Ongkasin et al., 2020) could be adapted to deliver SFN to the target cells i.e. lens cells. Moreover, any SFN that enters the surrounding humours would be diluted relative to the therapeutic level and thus based on many findings will shift from being cytotoxic to cytoprotective. However, full toxicity evaluation would be required before application on human patients.

Chapter 7

General Discussion

The eye is subject to a constant array of stressors that over time have deleterious effects on cell and overall tissue function. Exogenous stressors such as UV and endogenous stressors such as oxidative stress from metabolism have serious deleterious effects on all components of the cell such as DNA and proteins (Wormstone and Wride, 2011). In response, the cell may act on different cell fate outcomes, such as apoptosis or cellular senescence. Understanding the extent of DNA damage to a cell may give us insights into whether what effect certain drugs or cellular processes have on the integrity of a cell's DNA (Lombard et al., 2005). Furthermore, the cells own unique processes such as the breakdown of DNA during lens cellular denucleation and understanding the mechanisms involved, may provide greater insight into cell development and changes throughout its lifecycle.

DNA damage can be the result of stress to the cell whether from exogenous or endogenous sources. Detection of DNA damage is vital in research, as genomic lesions are thought to contribute to the aetiology of numerous diseases (Nelson and Dizdaroglu, 2020) including the eye (Czarny et al., 2013; Zhang et al., 2010; Ates et al, 2010). Commonly used DNA damage assays usually only detect specific DNA lesions and can be limited in throughput. Examples of these include the alkaline comet assay that detect DNA strand breaks in cell lines only and γ H2AX immunostaining that is an indirect marker of DSBs.

The present study successfully developed and enhanced a QPCR based DNA damage assay for the study of nuclear and mitochondrial DNA in cells and tissue. The Real Time LA QPCR assay allows for the detection of DNA damage from multiple types of DNA lesions

providing a broader scale of DNA damage in a sample. This allows for a more sensitive detection than other commonly used DNA damage assays. A unique feature of the assay is detection of mitochondrial DNA lesions which allows the expansion of research into mitochondrial DNA damage. This is an important feature as mitochondrial DNA damage has been linked with several disorders such as neurodegenerative diseases and cancer (Singh et al., 2015). More uniquely, mitochondrial copy number can be assessed, allowing the experimental evaluation of mitochondrial copy number in disease states, response to treatments or quantification of mitochondrial biogenesis. Although mitochondrial DNA damage is thought to play a role in numerous diseases, evidence is growing that mitochondrial copy number is also a determinant in their pathogenesis (Filograna et al., 2020). Overall, the Real Time LA QPCR was instrumental for the detection of DNA lesions throughout this thesis, becoming a valuable tool in research.

The human lens is bombarded with exogenous and endogenous stressors that can affect cell function and potentially cell death. However, lens epithelial cells possess DNA repair systems to counter stress induced DNA lesions, thereby maintaining cell function.

Epithelial cell viability is critical for the whole of the lens as the fibre cells lacking nuclei and organelles are fully reliant on LECs for nutrition and maintaining a reduced state, thereby preserving lens clarity (Wormstone and Wride, 2011). Therefore, DNA repair systems such as NHEJ and PARP-1 are important in maintaining this homeostasis.

The current study demonstrated the expression of these systems in human lens tissue. As expected, these systems were present in the nuclei of LECs in the central epithelium.

Further investigation was warranted for the role of NHEJ and PARP-1 in epithelial to fibre cell transition in the bow region of the lens. Lens fibre cells undergo an 'attenuated apoptosis' whereby nuclei and organelles degrade as the cell moves toward the OFZ (Dahm, 1999). Nuclear degradation involves DNAses thereby the hypothesis was that

NHEJ and PARP-1 expression would be attenuated before this event in order to not impede the process by DNA repair. Both NHEJ and PARP-1 expression receded after nuclear condensation and fragmentation, thereby allowing nuclear breakdown to occur.

Parthanatos, a caspase independent form of cell death, seems not to be involved in the lens fibre differentiation process as AIF shared the same staining pattern as mitochondria suggesting it remained localised to the mitochondria before being degraded. The lens fibre differentiation is still a relatively unknown process but some light has been shed on the role of DNA repair system in this process.

In the current study, SFN has been shown to protect against oxidative damage in HCEC-12 endothelial cells. Protecting human cornea donor tissue from oxidative stress whilst in storage is urgent problem to address. Cornea transplant is the most common transplant surgery and donor tissue is scarce (Gain et al., 2016). However once in storage, Corneal endothelial cells are subjected to oxidative stress and ECD is quickly compromised leading to rejection of the donor tissue as viable for transplant (Johnsen-Soriano et al., 2012).

Corneal donor tissue is greatly affected by stress and this has a serious impact of the availability of donor tissue for patients (Jäckel et al., 2011).

SFN treatment in H₂O₂ induced oxidative stress HCEC-12 cells, protected from cell death and DNA damage to both nuclear and mitochondria DNA compared to untreated controls.

This study provides a proof of principle step for the effectiveness of SFN as a protective agent against ECD loss from oxidative stress. This has important ramifications for corneal tissue shortage, potentially increasing the number of viable donor corneas for transplant after storage thus reducing graft rejection and alleviating lost resources from rejected tissue. Effectively reducing ECD loss may allow for increasing the upper age limit for donor corneas, increasing supply and reducing the tissue shortage burden (Gavrilov et al.,

2010). This study provides a proof of principle step for the effectiveness of SFN as a protective agent against ECD loss from oxidative stress.

High doses of SFN ($\geq 10 \mu\text{M}$) have previously been shown to reduce LEC growth and viability of FHL124 cells and in human lens capsular bags (Liu et al 2013; Liu et al., 2017). This in turn suggests a use of SFN as a therapeutic in the prevention of PCO. This study set out to determine if ROS mediated SFN cytotoxic effects as SFN has been shown to induce ROS (Lee and Lee, 2011). SFN significantly increased ROS levels in FHL124 cells, reduced cell viability and increased nuclear and mitochondrial DNA damage. However, when cells were pre-treated with the ROS scavenger NAC, all these effects were perturbed, demonstrating that ROS may be an important mediator of SFN's cytotoxic properties.

In conclusion the present body of work has developed our understanding on lens and cornea cell reaction to stress and the prescribed fate of the cell that occurs. The role of DNA repair items in the much-misunderstood mechanisms of lens epithelial to lens fibre transition has been much more elucidated. Specifically, the role of DSB repair enzymes in the repair systems NHEJ and PARP-1 in the denucleation of lens epithelial cells and the subsequent loss of organelles which leads to lens clarity and continuing function of the eye lens.

Sulforaphane (SFN) has long been studied for its protective effects. In the important issue of corneal transplant organ storage, whereby the constant process of keeping tissue viable, SFN has shown in vitro that it protects against oxidative stress for corneal endothelial cells, therefore potentially making it a suitable candidate as an additive for corneal storage in order to prolong donor tissue life, easing the burden of limited organ available for transplant.

Lastly, DNA damage, a significant consequence of cellular stress is an important area of study, hence the need for laboratory assay to detect it. This work has developed an assay that is more sensitive than conventional DNA assays commonly in use today. It is designed to be higher throughput, at higher volume, therefore increasing the rate of experimental investigation. Specifically, the detection of mitochondrial DNA damage, opens up possibilities of study that were limited before the redesign of the assay, which was limited in throughput, time and scope.

References

AARONSON, A., GRZYBOWSKI, A. & TUUMINEN, R. 2019. The health economic impact of posterior capsule opacification in Finland comparing the two single-piece intraocular lenses: a cost-consequence analysis. *Acta Ophthalmol*, 97, e1152-e1153.

ALBON, J., TULLO, A. B., AKTAR, S. & BOULTON, M. E. 2000 'Apoptosis in the endothelium of human corneas for transplantation', *Invest Ophthalmol Vis Sci*, 41(10), pp. 2887-93.

ALLEN D, VASAVADA A. 2006. Cataract and surgery for cataract. *BMJ* 333: 128-132.

ANDLEY, U. P. 2007 'Crystallins in the eye: Function and pathology', *Prog Retin Eye Res*, 26, 78-98.

ARMITAGE, W. J. 2011 'Preservation of Human Cornea', *Transfusion Medicine and Hemotherapy*, 38(2), pp. 143-147.

ARMITAGE, W. J. AND EASTY, D. L. 1997 'Factors influencing the suitability of organ-cultured corneas for transplantation', *Investigative Ophthalmology & Visual Science*, 38(1), pp. 16-24.

ARUOMA, O. I., SPENCER, J. P. & MAHMOOD, N. 1999. Protection against oxidative damage and cell death by the natural antioxidant ergothioneine. *Food Chem Toxicol*, 37, 1043-53.

ASBELL, P. A., DUALAN, I., MINDEL, J., BROCKS, D., AHMAD, M. & EPSTEIN, S. 2005. Age-related cataract. *Lancet*, 365, 599-609.

ATES, O., ALP, H. H., KOCER, I., BAYKAL, O. & SALMAN, I. A. 2010. Oxidative DNA damage in patients with cataract. *Acta Ophthalmol*, 88, 891-5.

AWASTHI, N., GUO, S. & WAGNER, B. J. 2009. Posterior capsular opacification: a problem reduced but not yet eradicated. *Arch Ophthalmol*, 127, 555-62.

BANUELOS, A., REYES, E., OCADIZ, R., ALVAREZ, E., MORENO, M., MONROY, A. & GARIGLIO, P. 2003. Neocarzinostatin induces an effective p53-dependent response in human papillomavirus-positive cervical cancer cells. *J Pharmacol Exp Ther*, 306, 671-80.

BASTEN, G. P., BAO, Y. & WILLIAMSON, G. 2002. Sulforaphane and its glutathione conjugate but not sulforaphane nitrile induce UDP-glucuronosyl transferase (UGT1A1) and glutathione transferase (GSTA1) in cultured cells. *Carcinogenesis*, 23, 1399-404.

BOLLINGER KE, LANGSTON RH. 2008. What can patients expect from cataract surgery? *Cleveland Clinic journal of medicine* 75: 193-196, 199-200.

BONANNO, J. A. 2012 "Molecular Mechanisms Underlying the Corneal Endothelial Pump", *Experimental Eye Research*, 95(1), pp. 2-7.

BOURNE, W. M. 2003 'Biology of the corneal endothelium in health and disease', *Eye*, 17, pp. 912.

BOURNE, W. M., NELSON, L. R. & HODGE, D. O. 1997 'Central corneal endothelial cell changes over a ten-year period', *Invest Ophthalmol Vis Sci*, 38(3), pp. 779-82.

BRENNAN, L. A., MCGREAL, R. S. & KANTOROW, M. 2012 'Oxidative stress defense and repair systems of the ocular lens', *Front Biosci (Elite Ed)*, 4, pp. 141-55.

BRICKER, G. V., RIEDL, K. M., RALSTON, R. A., TOBER, K. L., OBERYSZYN, T. M. & SCHWARTZ, S. J. 2014. Isothiocyanate metabolism, distribution, and interconversion in mice following consumption of thermally processed broccoli sprouts or purified sulforaphane. *Molecular nutrition & food research*, 58, 1991-2000.

- BROOKS, J. D., PATON, V. G. & VIDANES, G. 2001. Potent Induction of Phase 2 Enzymes in Human Prostate Cells by Sulforaphane. *Cancer Epidemiology, Biomarkers & Prevention*, 10, 949-954.
- BURKLE, A., BRABECK, C., DIEFENBACH, J. & BENEKE, S. 2005 'The emerging role of poly(ADP-ribose) polymerase-1 in longevity', *Int J Biochem Cell Biol*, 37(5), pp. 1043-53.
- CADET, J. & WAGNER, J. R. 2013. DNA base damage by reactive oxygen species, oxidizing agents, and UV radiation. *Cold Spring Harb Perspect Biol*, 5.
- CEJKA, C. & CEJKOVA, J. 2015 'Oxidative Stress to the Cornea, Changes in Corneal Optical Properties, and Advances in Treatment of Corneal Oxidative Injuries', *Oxidative Medicine and Cellular Longevity*, 2015, pp. 10.
- CHAFFEE, B. R., SHANG, F., CHANG, M. L., CLEMENT, T. M., EDDY, E. M., WAGNER, B. D., NAKAHARA, M., NAGATA, S., ROBINSON, M. L. & TAYLOR, A. 2014. Nuclear removal during terminal lens fiber cell differentiation requires CDK1 activity: appropriating mitosis-related nuclear disassembly. *Development*, 141, 3388-98.
- CHAITANYA, G. V., STEVEN, A. J. & BABU, P. P. 2010. PARP-1 cleavage fragments: signatures of cell-death proteases in neurodegeneration. *Cell communication and signaling : CCS*, 8, 31-31.
- CHEN, J.-H., OZANNE, S. E. & HALES, C. N. 2007 'Methods of Cellular Senescence Induction Using Oxidative Stress', in Tollefsbol, T.O. (ed.) *Biological Aging: Methods and Protocols*. Totowa, NJ: Humana Press, pp. 179-189.
- CHO, K. S., LEE, E. H., CHOI, J. S. & JOO, C. K. 1999 'Reactive oxygen species-induced apoptosis and necrosis in bovine corneal endothelial cells', *Investigative Ophthalmology & Visual Science*, 40(5), pp. 911-919.

- CHUI, J., DI GIROLAMO, N., WAKEFIELD, D. & CORONEO, M. T. 2008 'The pathogenesis of pterygium: current concepts and their therapeutic implications', *Ocul Surf*, 6(1), pp. 24-43.
- CIMPEAN, A. M., SAVA, M. P. & RAICA, M. 2013 'DNA damage in human pterygium: one-shot multiple targets', *Mol Vis*, 19, pp. 348-56.
- COLLINS, A. R. 2004. The comet assay for DNA damage and repair. *Molecular Biotechnology*, 26, 249.
- COOKE, M. S., EVANS, M. D., DIZDAROGLU, M. & LUNEC, J. 2003. Oxidative DNA damage: mechanisms, mutation, and disease. *The FASEB Journal*, 17, 1195-1214.
- COSTANTINI, S., WOODBINE, L., ANDREOLI, L., JEGGO, P. A. & VINDIGNI, A. 2007. Interaction of the Ku heterodimer with the DNA ligase IV/Xrcc4 complex and its regulation by DNA-PK. *DNA Repair (Amst)*, 6, 712-22.
- CREWE, J. M. & ARMITAGE, W. J. 2001 'Integrity of Epithelium and Endothelium in Organ-Cultured Human Corneas', *Investigative Ophthalmology & Visual Science*, 42(8), pp. 1757-1761.
- CZARNY, P., KASPRZAK, E., WIELGORSKI, M., UDZIELA, M., MARKIEWICZ, B., BLASIAK, J., SZAFLIK, J. & SZAFLIK, J. P. 2013. DNA damage and repair in Fuchs endothelial corneal dystrophy. *Molecular biology reports*, 40, 2977-2983.
- DAHM, R. 1999. Lens fibre cell differentiation - A link with apoptosis? *Ophthalmic Res*, 31, 163-83.
- DAVIDSON, R., GARDNER, S., JUPP, O., BULLOUGH, A., BUTTERS, S., WATTS, L., DONELL, S., TRAKA, M., SAHA, S., MITHEN, R., PEFFERS, M., CLEGG, P., BAO, Y., CASSIDY, A. & CLARK, I. 2017 'Isothiocyanates are detected in human

synovial fluid following broccoli consumption and can affect the tissues of the knee joint', *Scientific Reports*, 7, pp. 3398.

DE MARIA, A. & BASSNETT, S. 2007. DNase II β Distribution and Activity in the Mouse Lens. *Investigative Ophthalmology & Visual Science*, 48, 5638-5646.

DELLA LATTA, V., CECCHETTINI, A., DEL RY, S. & MORALES, M. A. 2015. Bleomycin in the setting of lung fibrosis induction: From biological mechanisms to counteractions. *Pharmacological Research*, 97, 122-130.

DÍAZ, J. 2009. *Optical Design Techniques in Current Eye models Development*, Nova Science.

DINKOVA-KOSTOVA, A. T., FAHEY, J. W., KOSTOV, R. V. & KENSLER, T. W. 2017. KEAP1 and Nrf2: Targeting the NRF2 Pathway with Sulforaphane. *Trends in food science & technology*, 69, 257-269.

DOLLFUS, H., PORTO, F., CAUSSADE, P., SPEEG-SCHATZ, C., SAHEL, J., GROSSHANS, E., FLAMENT, J. & SARASIN, A. 2003 'Ocular manifestations in the inherited DNA repair disorders', *Surv Ophthalmol*, 48(1), pp. 107-22.

DUEVA, R. & ILIAKIS, G. J. T. C. R. 2013. Alternative pathways of non-homologous end joining (NHEJ) in genomic instability and cancer. *2013*, 2, 163-177.

DUNCAN G, WANG L, NEILSON GJ, WORMSTONE IM. 2007 Lens cell survival after exposure to stress in the closed capsular bag. *Invest Ophthalmol Vis Sci*. Jun;48(6):2701-7. doi: 10.1167/iops.06-1345. PMID: 17525202.

DUNCAN, G., WORMSTONE, I. M. & DAVIES, P. D. 1997. The aging human lens: structure, growth, and physiological behaviour. *British Journal of Ophthalmology*, 81, 818.

- EDWARDS, J. G. (2009) 'Quantification of mitochondrial DNA (mtDNA) damage and error rates by real-time QPCR', *Mitochondrion*, 9(1), pp. 31-5.
- ELISABETH, P., HILDE, B. & ILSE, C. 2008 'Eye bank issues: II. Preservation techniques: warm versus cold storage', *International Ophthalmology*, 28(3), pp. 155-163.
- ELMORE, S. 2007 'Apoptosis: A Review of Programmed Cell Death', *Toxicologic pathology*, 35(4), pp. 495-516.
- FAHEY, J. W., HARISTOY, X., DOLAN, P. M., KENSLER, T. W., SCHOLTUS, I., STEPHENSON, K. K., TALALAY, P. & LOZNIIEWSKI, A. 2002. Sulforaphane inhibits extracellular, intracellular, and antibiotic-resistant strains of *Helicobacter pylori* and prevents benzo[a]pyrene-induced stomach tumors. *Proceedings of the National Academy of Sciences of the United States of America*, 99, 7610-7615.
- FAN, X., MONNIER, V. M. & WHITSON, J. 2017. Lens glutathione homeostasis: Discrepancies and gaps in knowledge standing in the way of novel therapeutic approaches. *Exp Eye Res*, 156, 103-111.
- FARAGHER, R., MULHOLLAND, B., TUFT, S., SANDEMAN, S. & KHAW, P. 1997 'Aging and the cornea', *The British Journal of Ophthalmology*, 81(10), pp. 814-817.
- FILOGRANA, R., MENNUNI, M., ALSINA, D. & LARSSON, N.-G. 2021. Mitochondrial DNA copy number in human disease: the more the better? *FEBS Letters*, 595, 976-1002.
- FORRESTER, J. V., DICK, A. D., MCMENAMIN, P. G., ROBERTS, F. & PEARLMAN, E. 2016. *The eye: basic sciences in practice*, Elsevier.
- FURDA, A., SANTOS, J. H., MEYER, J. N. & VAN HOUTEN, B. 2014. Quantitative PCR-based measurement of nuclear and mitochondrial DNA damage and repair in mammalian cells. *Methods Mol Biol*, 1105, 419-37

GAIN, P., JULLIENNE, R., HE, Z., ALDOSSARY, M., ACQUART, S., COGNASSE, F. & THURET, G. 2016 'Global Survey of Corneal Transplantation and Eye Banking', *JAMA Ophthalmol*, 134(2), pp. 167-73.

GAVRILOV, J. C., BORDERIE, V. M., LAROCHE, L. & DELBOSC, B. 2010 'Influencing factors on the suitability of organ-cultured corneas', *Eye*, 24, pp. 1227.

GEORGE, A. J. T. & LARKIN, D. F. P. 2004 'Corneal Transplantation: The Forgotten Graft', *American Journal of Transplantation*, 4(5), pp. 678-685.

GIBLIN, F. J. 2000. Glutathione: a vital lens antioxidant. *J Ocul Pharmacol Ther*, 16, 121-35.

GOLDBERG, I. H. 1987 'Free radical mechanisms in neocarzinostatin-induced DNA damage', *Free Radic Biol Med*, 3(1), pp. 41-54.

GREEN, K. 1995 'Free radicals and aging of anterior segment tissues of the eye: a hypothesis', *Ophthalmic Res*, 27 Suppl 1, pp. 143-9.

GRUBE, K. & BÜRKLE, A. 1992 'Poly(ADP-ribose) polymerase activity in mononuclear leukocytes of 13 mammalian species correlates with species-specific life span', *Proceedings of the National Academy of Sciences of the United States of America*, 89(24), pp. 11759-11763.

GUDNASON, H., DUFVA, M., BANG, D. D. & WOLFF, A. 2007 'Comparison of multiple DNA dyes for real-time PCR: effects of dye concentration and sequence composition on DNA amplification and melting temperature', *Nucleic Acids Res*, 35(19), pp. e127.

GUO, Z., KOZLOV, S., LAVIN, M. F., PERSON, M. D. & PAULL, T. T. 2010 'ATM activation by oxidative stress', *Science*, 330(6003), pp. 517-21.

- HEERES, J. T. & HERGENROTHER, P. J. 2007. Poly(ADP-ribose) makes a date with death. *Curr Opin Chem Biol*, 11, 644-53.
- HEJTMANCIK, J. F. & SHIELS, A. 2015. Overview of the Lens. *Progress in molecular biology and translational science*, 134, 119-127.
- HEMPEL, B., BEDNARZ, J. & ENGELMANN, K. 2001 'Use of a serum-free medium for long-term storage of human corneas. Influence on endothelial cell density and corneal metabolism', *Graefes Arch Clin Exp Ophthalmol*, 239(10), pp. 801-5.
- HU Y, URIG S, KONCAREVIC S, WU X, FISCHER M, RAHLFS S, 2007 Glutathione- and thioredoxin-related enzymes are modulated by sulfur-containing chemopreventive agents. *Biol Chem.*;388:1069–81.
- HURLEY, P. J. & BUNZ, F. 2007 'ATM and ATR: components of an integrated circuit', *Cell Cycle*, 6(4), pp. 414-7.
- ISHIZAKI, Y., JACOBSON, M. D. & RAFF, M. C. 1998. A role for caspases in lens fiber differentiation. *J Cell Biol*, 140, 153-8.
- JÄCKEL, T., KNELS, L., VALTINK, M., FUNK, R. H. W. & ENGELMANN, K. 2011 'Serum-free corneal organ culture medium (SFM) but not conventional minimal essential organ culture medium (MEM) protects human corneal endothelial cells from apoptotic and necrotic cell death', *British Journal of Ophthalmology*, 95(1), pp. 123.
- JACKSON, S. P. & BARTEK, J. 2009. The DNA-damage response in human biology and disease. *Nature*, 461, 1071-1078.
- JARRETT, S. G., LEWIN, A. S. & BOULTON, M. E. 2010. The importance of mitochondria in age-related and inherited eye disorders. *Ophthalmic Res*, 44, 179-90.

JENG, B. H., MEISLER, D. M., HOLLYFIELD, J. G., CONNOR, J. T., AULAK, K. S. & STUEHR, D. J. 2002 'Nitric oxide generated by corneas in corneal storage media', *Cornea*, 21(4), pp. 410-4.

JOHNSEN-SORIANO, S., HAUG, K., ARNAL, E., PERIS-MARTINEZ, C., MOE, M. C., ROMERO, F. J. & NICOLAISSEN, B. 2012 'Oxidative stress gradient in a medium during human corneal organ culture', *Molecular Vision*, 18, pp. 1604-1608.

JOHNSON, D. R. 2001. PCR with the fluorogenic DNA stain SYBR® Green I. *Technical Tips Online*, 6, 8-9.

JOOZDANI, F. A., YARI, F., JOOZDANI, P. A. & NAFISI, S. 2015. Interaction of sulforaphane with DNA and RNA. *PloS one*, 10, e0127541-e0127541.

JOYCE, N. C., HARRIS, D. L. & ZHU, C. C. 2011 'Age-related gene response of human corneal endothelium to oxidative stress and DNA damage', *Invest Ophthalmol Vis Sci*, 52(3), pp. 1641-9.

JOYCE, N. C., ZHU, C. C. & HARRIS, D. L. 2009 'Relationship among oxidative stress, DNA damage, and proliferative capacity in human corneal endothelium', *Invest Ophthalmol Vis Sci*, 50(5), pp. 2116-22.

JUGE, N., MITHEN, R. F. & TRAKA, M. 2007. Molecular basis for chemoprevention by sulforaphane: a comprehensive review. *Cell Mol Life Sci*, 64, 1105-27.

KEEFFE JE, TAYLOR HR. 1996. Cataract surgery in Australia 1985-94. *Aust N Z J Ophthalmol* 24: 313-317.

KISE, K., KOSAKA, H., NAKABAYASHI, M., KISHIDA, K., SHIGA, T. & TANO, Y. 1994. Reactive oxygen species involved in phenazine-methosulfate-induced rat lens opacification. An experimental model of cataract. *Ophthalmic Res*, 26, 41-50.

KITAZAWA, K., INATOMI, T., TANIOKA, H., KAWASAKI, S., NAKAGAWA, H., HIEDA, O., FUKUOKA, H., OKUMURA, N., KOIZUMI, N., ILIAKIS, B., SOTOZONO, C. & KINOSHITA, S. 2017 'The existence of dead cells in donor corneal endothelium preserved with storage media', *British Journal of Ophthalmology*, 101(12), pp. 1725-1730.

KLEIMAN, N. J. & SPECTOR, A. 1993. DNA single strand breaks in human lens epithelial cells from patients with cataract. *Curr Eye Res*, 12, 423-31.

KLEIN BE. 1993. Lens opacities in women in Beaver Dam, Wisconsin: is there evidence of an effect of sex hormones? *Trans Am Ophthalmol Soc* 91: 517-544.

KROKAN, H. E. & BJØRÅS, M. 2013. Base excision repair. *Cold Spring Harbor perspectives in biology*, 5, a012583-a012583.

LAM, D., RAO, S. K., RATRA, V., LIU, Y., MITCHELL, P., KING, J., TASSIGNON, M.-J., JONAS, J., PANG, C. P. & CHANG, D. F. 2015. Cataract. *Nature Reviews Disease Primers*, 1, 15014.

LAYER, N., CEVALLOS, V., MAXWELL, A. J., HOOVER, C., KEENAN, J. D. & JENG, B. H. 2014 'Efficacy and safety of antifungal additives in optisol-gs corneal storage medium', *JAMA Ophthalmology*, 132(7), pp. 832-837.

LEE, Y. J. & LEE, S. H. 2011. Sulforaphane induces antioxidative and antiproliferative responses by generating reactive oxygen species in human bronchial epithelial BEAS-2B cells. *J Korean Med Sci*, 26, 1474-82.

LEHLE, S., HILDEBRAND, D. G., MERZ, B., MALAK, P. N., BECKER, M. S., SCHMEZER, P., ESSMANN, F., SCHULZE-OSTHOFF, K. & ROTHFUSS, O. 2014. LORD-Q: a long-run real-time PCR-based DNA-damage quantification method for nuclear and mitochondrial genome analysis. *Nucleic Acids Res*, 42, e41.

- LEKAWA- A. ILCZUK, A., ANTOSZ, H., RYMGAYLLO-JANKOWSKA, B. & ZARNOWSKI, T. 2011 'Expression of double strand DNA breaks repair genes in pterygium', *Ophthalmic Genet*, 32(1), pp. 39-47.
- LI, W.-C., KUSZAK, J. R., WANG, G.-M., WU, Z.-Q. & ABRAHAM, S. 1995 'Calcimycin-induced lens epithelial cell apoptosis contributes to cataract formation', *Experimental Eye Research*, 61(1), pp. 91-98.
- LI, F., WANG, Y., ZHANG, G., ZHOU, J., YANG, L. & GUAN, H. 2014 'Expression and methylation of DNA repair genes in lens epithelium cells of age-related cataract', *Mutation Research/Fundamental and Molecular Mechanisms of Mutagenesis*, 766–767(0), pp. 31-36.
- LINETSKY, M. & ORTWERTH, B. J. 1995. The generation of hydrogen peroxide by the UVA irradiation of human lens proteins. *Photochem Photobiol*, 62, 87-93.
- LIU, H., SMITH, A. J., BALL, S. S., BAO, Y., BOWATER, R. P., WANG, N. & WORMSTONE, I. M. 2017. Sulforaphane promotes ER stress, autophagy, and cell death: implications for cataract surgery. *J Mol Med (Berl)*, 95, 553-564.
- LIU, H., SMITH, A. J., LOTT, M. C., BAO, Y., BOWATER, R. P., REDDAN, J. R. & WORMSTONE, I. M. 2013 'Sulforaphane can protect lens cells against oxidative stress: implications for cataract prevention', *Invest Ophthalmol Vis Sci*, 54(8), pp. 5236-48.
- LODOVICI, M., RAIMONDI, L., GUGLIELMI, F., GEMIGNANI, S. & DOLARA, P. 2003 'Protection against ultraviolet B-induced oxidative DNA damage in rabbit corneal-derived cells (SIRC) by 4-coumaric acid', *Toxicology*, 184(2-3), pp. 141-7.
- LOMBARD, D. B., CHUA, K. F., MOSTOSLAVSKY, R., FRANCO, S., GOSTISSA, M. & ALT, F. W. 2005. DNA repair, genome stability, and aging. *Cell*, 120, 497-512.

LONGCHAMPS, R. J., CASTELLANI, C. A., YANG, S. Y., NEWCOMB, C. E.,
SUMPTER, J. A., LANE, J., GROVE, M. L., GUALLAR, E., PANKRATZ, N.,
TAYLOR, K. D., ROTTER, J. I., BOERWINKLE, E. & ARKING, D. E. 2020. Evaluation
of mitochondrial DNA copy number estimation techniques. *PloS one*, 15, e0228166-
e0228166.

LUO, X. & KRAUS, W. L. 2012. On PAR with PARP: cellular stress signaling through
poly(ADP-ribose) and PARP-1. *Genes & development*, 26, 417-432.

MAIDMENT, J. M., DUNCAN, G., TAMIYA, S., COLLISON, D. J., WANG, L. &
WORMSTONE, I. M. 2004. Regional Differences in Tyrosine Kinase Receptor Signaling
Components Determine Differential Growth Patterns in the Human Lens. *Investigative
Ophthalmology & Visual Science*, 45, 1427-1435.

MANSOUR, R., ABDELRAHIM, E. & AL-JOHANI, A. 2013. Identification of Diabetic
Retinal Exudates in Digital Color Images Using Support Vector Machine. *Journal of
Intelligent Learning Systems and Applications*, 05, 135-142.

MEACOCK, W. R., SPALTON, D. J., BOYCE, J. & MARSHALL, J. 2003. The effect of
posterior capsule opacification on visual function. *Invest Ophthalmol Vis Sci*, 44, 4665-9.

MICHAEL, R. & BRON, A. J. 2011 'The ageing lens and cataract: a model of normal and
pathological ageing', *Philosophical transactions of the Royal Society of London. Series B,
Biological sciences*, 366(1568), pp. 1278-1292.

MYZAK, M. C. & DASHWOOD, R. H. 2006. Chemoprotection by sulforaphane: keep
one eye beyond Keap1. *Cancer letters*, 233, 208-218.

NEGRETTE-GUZMÁN, M., HUERTA-YEPEZ, S., VEGA, M. I., LEÓN-CONTRERAS,
J. C., HERNÁNDEZ-PANDO, R., MEDINA-CAMPOS, O. N., RODRÍGUEZ, E., TAPIA,
E. & PEDRAZA-CHAVERRI, J. 2017 'Sulforaphane induces differential modulation of

mitochondrial biogenesis and dynamics in normal cells and tumor cells', *Food and Chemical Toxicology*, 100, pp. 90-102.

NELSON, B. C. & DIZDAROGLU, M. 2020. Implications of DNA damage and DNA repair on human diseases. *Mutagenesis*, 35, 1-3.

NERI, M., MILAZZO, D., UGOLINI, D., MILIC, M., CAMPOLONGO, A., PASQUALETTI, P. & BONASSI, S. 2015. Worldwide interest in the comet assay: a bibliometric study. *Mutagenesis*, 30, 155-63.

NIBOURG, L. M., GELENS, E., KUIJER, R., HOOYMANS, J. M., VAN KOOTEN, T. G. & KOOPMANS, S. A. 2015. Prevention of posterior capsular opacification. *Exp Eye Res*, 136, 100-15.

ONGKASIN K, MASMOUDI Y, WERTHEIMER CM, HILLENMAYER A, EIBL-LINDNER KH, BADENS E. 2020 Supercritical fluid technology for the development of innovative ophthalmic medical devices: Drug loaded intraocular lenses to mitigate posterior capsule opacification. *Eur J Pharm Biopharm*. Apr;149:248-256. doi: 10.1016/j.ejpb.2020.02.011. Epub 2020 Feb 26. PMID: 32112896.

OTT, M., GOGVADZE, V., ORRENIUS, S. & ZHIVOTOVSKY, B. 2007 'Mitochondria, oxidative stress and cell death', *Apoptosis*, 12(5), pp. 913-922.

PATHAI, S., SHIELS, P. G., LAWN, S. D., COOK, C. & GILBERT, C. 2013 'The eye as a model of ageing in translational research--molecular, epigenetic and clinical aspects', *Ageing Res Rev*, 12(2), pp. 490-508.

RABSILBER TM, LIMBERGER IJ, REULAND AJ, HOLZER MP, AUFFARTH GU. 2007 Long-term results of sealed capsule irrigation using distilled water to prevent posterior capsule opacification: a prospective clinical randomised trial. *Br J Ophthalmol*.

Jul;91(7):912-5. doi: 10.1136/bjo.2006.106468. Epub 2007 Jan 3. PMID: 17202203; PMCID: PMC1955631.

REDDAN, J. R., LINDEMANN, C. B., HITT, A. L. & AL., E. 1999. Generation of two non-transfected human lens cell lines [ARVO Abstract]. Invest Ophthalmol Vis Sci, 40, S970. Abstract nr 5110.

RENGARAJAN, K., CRISTOL, S. M., MEHTA, M. & NICKERSON, J. M. 2002. Quantifying DNA concentrations using fluorometry: a comparison of fluorophores. Mol Vis, 8, 416-21.

RESNIKOFF, S., PASCOLINI, D., ETYA'ALE, D., KOCUR, I., PARARAJASEGARAM, R., POKHAREL, G. P. & MARIOTTI, S. P. 2004 'Global data on visual impairment in the year 2002', Bulletin of the World Health Organization, 82(11), pp. 844-851.

RESNIKOFF, S., PASCOLINI, D., MARIOTTI, S. P. & POKHAREL, G. P. 2008. Global magnitude of visual impairment caused by uncorrected refractive errors in 2004. Bulletin of the World Health Organization, 86, 63-70.

RIJNEVELD, W. J., BEEKHUIS, W., VAN RIJ, G., RINKEL-VAN DRIEL, B. & PELS, E. 1992 'Clinical comparison of grafts stored in mccarey-kaufman medium at 4°C and in corneal organ culture at 31°C', Archives of Ophthalmology, 110(2), pp. 203-205.

ROH, D. S., DU, Y., GABRIELE, M. L., ROBINSON, A. R., NIEDERNHOFER, L. J. & FUNDERBURGH, J. L. 2013 'Age-related dystrophic changes in corneal endothelium from DNA repair-deficient mice', Aging Cell, 12(6), pp. 1122-1131.

RUHEE, R. T. & SUZUKI, K. 2020. The Integrative Role of Sulforaphane in Preventing Inflammation, Oxidative Stress and Fatigue: A Review of a Potential Protective Phytochemical. Antioxidants, 9.

- SANCAR, A., LINDSEY-BOLTZ, L. A., UNSAL-KACMAZ, K. & LINN, S. 2004 'Molecular mechanisms of mammalian DNA repair and the DNA damage checkpoints', *Annu Rev Biochem*, 73, pp. 39-85.
- SANTOS, J. H., MEYER, J. N., MANDAVILLI, B. S. & VAN HOUTEN, B. 2006. Quantitative PCR-Based Measurement of Nuclear and Mitochondrial DNA Damage and Repair in Mammalian Cells. In: HENDERSON, D. S. (ed.) *DNA Repair Protocols: Mammalian Systems*. Totowa, NJ: Humana Press.
- SCHÖNFELDER, J., VALTINK, M., KNELS, L., FUNK, R. H. W., ENGELMANN, K. & WETZEL, C. 2014 'Quality assessment of corneal storage media and their components', *Graefe's Archive for Clinical and Experimental Ophthalmology*, 252(1), pp. 77-82.
- SELUANOV, A., MITTELMAN, D., PEREIRA-SMITH, O. M., WILSON, J. H. & GORBUNOVA, V. 2004 'DNA end joining becomes less efficient and more error-prone during cellular senescence', *Proc Natl Acad Sci U S A*, 101(20), pp. 7624-9.
- SHARMA, K. K. & SANTHOSHKUMAR, P. 2009 'Lens aging: effects of crystallins', *Biochim Biophys Acta*, 1790(10), pp. 1095-108.
- SHOHAM, A., HADZIAHMETOVIC, M., DUNAIEF, J. L., MYDLARSKI, M. B. & SCHIPPER, H. M. 2008 'Oxidative stress in diseases of the human cornea', *Free Radic Biol Med*, 45(8), pp. 1047-55.
- SINGH, G., PACHOURI, U. C., KHAIDEM, D. C., KUNDU, A., CHOPRA, C. & SINGH, P. 2015. Mitochondrial DNA Damage and Diseases. *F1000Research*, 4, 176-176.
- SINGH, S. V., SRIVASTAVA, S. K., CHOI, S., LEW, K. L., ANTOSIEWICZ, J., XIAO, D., ZENG, Y., WATKINS, S. C., JOHNSON, C. S., TRUMP, D. L., LEE, Y. J., XIAO, H. & HERMAN-ANTOSIEWICZ, A. 2005 'Sulforaphane-induced cell death in human

prostate cancer cells is initiated by reactive oxygen species', *J Biol Chem*, 280(20), pp. 19911-24.

SMITH, A. J., BALL, S. S., BOWATER, R. P. & WORMSTONE, I. M. 2016. PARP-1 inhibition influences the oxidative stress response of the human lens. *Redox Biol*, 8, 354-62.

SMITH, A. J., BALL, S. S., MANZAR, K., BOWATER, R. P. & WORMSTONE, I. M. 2015. Ku80 Counters Oxidative Stress-Induced DNA Damage and Cataract Formation in the Human Lens. *Invest Ophthalmol Vis Sci*, 56, 7868-74.

SONG, S., LANDSBURY, A., DAHM, R., LIU, Y., ZHANG, Q. & QUINLAN, R. A. 2009. Functions of the intermediate filament cytoskeleton in the eye lens. *The Journal of Clinical Investigation*, 119, 1837-1848.

SONG, Z., WANG, Y., XIE, L., ZANG, X. & YIN, H. 2008 'Expression of senescence-related genes in human corneal endothelial cells', *Molecular Vision*, 14, pp. 161-170.

SORTE, K., SUNE, P., BHAKE, A., SHIVKUMAR, V. B., GANGANE, N. & BASAK, A. 2011 'Quantitative assessment of DNA damage directly in lens epithelial cells from senile cataract patients', *Mol Vis*, 17, pp. 1-6.

SOUSA, F. G., MATUO, R., SOARES, D. G., ESCARGUEIL, A. E., HENRIQUES, J. A., LARSEN, A. K. & SAFFI, J. 2012 'PARPs and the DNA damage response', *Carcinogenesis*, 33(8), pp. 1433-40.

SPECTOR, A. 1995 'Oxidative stress-induced cataract: mechanism of action', *Faseb j*, 9(12), pp. 1173-82.

SRIDHAR, M. S. 2018. Anatomy of cornea and ocular surface. *Indian journal of ophthalmology*, 66, 190-194.

SRINIVAS, S. P. 2012 'Cell signaling in regulation of the barrier integrity of the corneal endothelium', *Exp Eye Res*, 95(1), pp. 8-15.

TALALAY, P. 2000. Chemoprotection against cancer by induction of phase 2 enzymes. *Biofactors*, 12, 5-11.

TAN, D. T., LIM, A. S., GOH, H. S. & SMITH, D. R. 1997 'Abnormal expression of the p53 tumor suppressor gene in the conjunctiva of patients with pterygium', *Am J Ophthalmol*, 123(3), pp. 404-5.

TAYLOR, V. L., AL-GHOUL, K. J., LANE, C. W., DAVIS, V. A., KUSZAK, J. R. & COSTELLO, M. J. 1996. Morphology of the normal human lens. *Invest Ophthalmol Vis Sci*, 37, 1396-410.

TENG, P. N., BATEMAN, N. W., DARCY, K. M., HAMILTON, C. A., MAXWELL, G. L., BAKKENIST, C. J. & CONRADS, T. P. 2015 'Pharmacologic inhibition of ATR and ATM offers clinically important distinctions to enhancing platinum or radiation response in ovarian, endometrial, and cervical cancer cells', *Gynecol Oncol*.

THOLOZAN, F. M. & QUINLAN, R. A. 2007. Lens cells: more than meets the eye. *Int J Biochem Cell Biol*, 39, 1754-9

TOPE, A. M. & ROGERS, P. F. 2009 'Evaluation of protective effects of sulforaphane on DNA damage caused by exposure to low levels of pesticide mixture using comet assay', *Journal of Environmental Science and Health, Part B*, 44(7), pp. 657-662.

VALTINK, M., GRUSCHWITZ, R., FUNK, R. H. & ENGELMANN, K. 2008 'Two clonal cell lines of immortalized human corneal endothelial cells show either differentiated or precursor cell characteristics', *Cells Tissues Organs*, 187(4), pp. 286-94.

VAN DUIJN-GOEDHART, A., ZDZIENICKA, M. Z., SANKARANARAYANAN, K. & VAN BUUL, P. P. W. 2000. Differential responses of Chinese hamster mutagen sensitive

cell lines to low and high concentrations of calicheamicin and neocarzinostatin. *Mutation Research/Genetic Toxicology and Environmental Mutagenesis*, 471, 95-105.

VANDUCHOVA, A., ANZENBACHER, P. & ANZENBACHEROVA, E. 2018.

Isothiocyanate from Broccoli, Sulforaphane, and Its Properties. *Journal of Medicinal Food*, 22, 121-126.

WAKEFIELD, M. J., ARMITAGE, W. J., JONES, M. N. A., KAYE, S. B., LARKIN, D.

F. P., TOLE, D. & PRYDAL, J. 2015 'The impact of donor age and endothelial cell density on graft survival following penetrating keratoplasty', *British Journal of Ophthalmology*.

WANG, Y., KO, B. C., YANG, J. Y., LAM, T. T., JIANG, Z., ZHANG, J., CHUNG, S. K.

& CHUNG, S. S. 2005. Transgenic mice expressing dominant-negative osmotic-response element-binding protein (OREBP) in lens exhibit fiber cell elongation defect associated with increased DNA breaks. *J Biol Chem*, 280, 19986-91.

WORMSTONE, I. M., COLLISON, D. J., HANSOM, S. P. & DUNCAN, G. 2006 'A

focus on the human lens in vitro', *Environ Toxicol Pharmacol*, 21(2), pp. 215-21.

WORMSTONE, I. M., TAMIYA, S., ELDRED, J. A., LAZARIDIS, K., CHANTRY, A.,

REDDAN, J. R., ANDERSON, I. & DUNCAN, G. 2004 'Characterisation of TGF-beta2 signalling and function in a human lens cell line', *Exp Eye Res*, 78(3), pp. 705-14.

WORMSTONE, I. M., WANG, L. & LIU, C. S. 2009. Posterior capsule opacification. *Exp*

Eye Res, 88, 257-69.

WORMSTONE, I. M., WORMSTONE, Y. M., SMITH, A. J. O. & ELDRED, J. A. 2021.

Posterior capsule opacification: What's in the bag? *Prog Retin Eye Res*, 82, 100905.

WORMSTONE, I. M. & WRIDE, M. A. 2011. The ocular lens: a classic model for

development, physiology and disease. *Philosophical transactions of the Royal Society of London. Series B, Biological sciences*, 366, 1190-1192.

WRIDE, M. A., PARKER, E. & SANDERS, E. J. 1999. Members of the bcl-2 and caspase families regulate nuclear degeneration during chick lens fibre differentiation. *Dev Biol*, 213, 142-56.

YAKES, F. M. & VAN HOUTEN, B. 1997. Mitochondrial DNA damage is more extensive and persists longer than nuclear DNA damage in human cells following oxidative stress. *Proceedings of the National Academy of Sciences of the United States of America*, 94, 514-519.

YE, L., YU, T., LI, Y., CHEN, B., ZHANG, J., WEN, Z., ZHANG, B., ZHOU, X., LI, X., LI, F., CAO, W. & HUANG, Z. 2013 'Sulforaphane Enhances the Ability of Human Retinal Pigment Epithelial Cell against Oxidative Stress, and Its Effect on Gene Expression Profile Evaluated by Microarray Analysis', *Oxidative Medicine and Cellular Longevity*, 2013, pp. 413024.

ZANDY, A. J., LAKHANI, S., ZHENG, T., FLAVELL, R. A. & BASSNETT, S. 2005. Role of the executioner caspases during lens development. *J Biol Chem*, 280, 30263-72.

ZAVALA, J., LÓPEZ JAIME, G. R., RODRÍGUEZ BARRIENTOS, C. A. & VALDEZ-GARCIA, J. 2013 'Corneal endothelium: developmental strategies for regeneration', *Eye*, 27(5), pp. 579-588.

ZHANG, Y. 2001 'Molecular mechanism of rapid cellular accumulation of anticarcinogenic isothiocyanates', *Carcinogenesis*, 22(3), pp. 425-31.

ZHANG Y, KOLM R, MANNERVIK B, TALALAY P. 1995 Reversible conjugation of isothiocyanates with glutathione catalyzed by human glutathione transferases. *Biochem Biophys Res Commun*. 206:748–55.

ZHANG, Y., ZHANG, L., ZHANG, L., BAI, J., GE, H. AND LIU, P. (2010) 'Expression changes in DNA repair enzymes and mitochondrial DNA damage in aging rat lens', *Mol Vis*, 16, pp. 1754-63.

ZIAEI, A., SCHMEDT, T., CHEN, Y. AND JURKUNAS, U. V. (2013) 'Sulforaphane decreases endothelial cell apoptosis in fuchs endothelial corneal dystrophy: a novel treatment', *Invest Ophthalmol Vis Sci*, 54(10), pp. 6724-34.

Publications

SMITH, A. J. O., **BALL, S. S. R.**, MANZAR, K., BOWATER, R. P. & WORMSTONE, I. M. 2015. Ku80 Counters Oxidative Stress–Induced DNA Damage and Cataract Formation in the Human Lens. *Investigative Ophthalmology & Visual Science*, 56, 7868-7874.

SMITH, A. J., **BALL, S. S.**, BOWATER, R. P. & WORMSTONE, I. M. 2016. PARP-1 inhibition influences the oxidative stress response of the human lens. *Redox Biol*, 8, 354-62.

LIU, H., SMITH, A. J., **BALL, S. S.**, BAO, Y., BOWATER, R. P., WANG, N. & WORMSTONE, I. M. 2017. Sulforaphane promotes ER stress, autophagy, and cell death: implications for cataract surgery. *J Mol Med (Berl)*, 95, 553-564.

DNA repair proteins in the anatomical organisation and protection of the human lens (2025)

Simon S.R. Ball, Andrew J.O. Smith, Richard P. Bowater, I. Michael Wormstone
School of Biological Sciences, University of East Anglia, Norwich, UK.



Purpose
DNA repair systems maintain genome stability in all cells, but these are a neglected area of research in the human lens. This study identifies in human lens cells, the expression of Ku80, DNA-PK and PARP-1 which are all involved in the repair of DNA strand breaks. The purpose of the current study was to evaluate the distribution of these proteins in the human lens in relation to lens anatomy and mechanisms that defend against genotoxic stress (Figure 1).

Methods
Non-cultured whole human lenses (av. donor age 76 ± 3.3 years) were fixed in 4% v/v formaldehyde, paraffin embedded and sectioned at 6 μ m. Samples were subjected to antigen retrieval before fluorescent immunohistochemistry using Alexa-488 secondary antibody and nuclear counterstaining with DAPI. Sections were visualised using a Zeiss AxioPlan fluorescence microscope and digital camera.

The lens epithelial cell line, FHL124 was also used as an experimental system with immunofluorescence techniques employed to study the effects of specific pharmacological agents. The effects of specific pharmacological agents AG14361 and NU7026 respectively while Ku80 was knocked down using targeted siRNA methods. Genotoxic stress was invoked in the cell line by treatments with hydrogen peroxide or the radiomimetic neocarzinostatin (NCS). DNA damage was assessed using the alkaline comet assay.

Results
Ku80, DNA-PK and PARP-1 were present in the cell nucleus in the lens epithelium and the FHL124 cell line (Figure 2 and 3). Within lens fibres, newly laid cells also presented a predominantly nuclear expression before levels rapidly declined for all three proteins (Figure 2). This reduced expression appeared to precede changes in chromatin appearance that could be attributed to lens fibre cell denucleation.

The role of PARP-1 was investigated through expression of PARP associated molecules. Poly ADP-ribose (PAR) was used as a measure of PARP-1 activity and showed a predominant nuclear expression. This remained present in fibre cells until a later stage of denucleation than PARP-1 itself. Apoptosis inducing factor (AIF), a mitochondrial bound protein, which is proposed to play a role in PARP-1 specific cell death, known as parthanatos (Figure 1), showed cytoplasmic staining in the epithelium and fibre cells, which abruptly declines prior to denucleation. A similar pattern was observed with mitochondrial staining.

With respect to DNA damage, FHL124 cells were sensitive to both hydrogen peroxide and NCS, with significant changes being observed following treatment. The scale of this damage was increased in cases where PARP-1, DNA-PK and Ku80 were inhibited/suppressed.

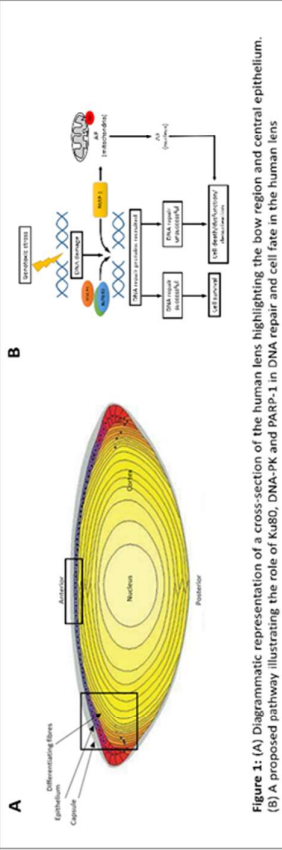


Figure 1: (A) Diagrammatic representation of a cross-section of the human lens highlighting the bow region and central epithelium.

(B) A proposed pathway illustrating the role of Ku80, DNA-PK and PARP-1 in DNA repair and cell fate in the human lens

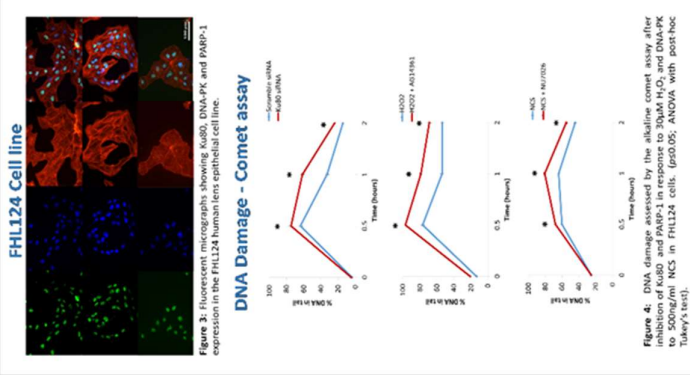


Figure 3: Fluorescent micrographs showing Ku80, DNA-PK and PARP-1 expression in the FHL124 human lens epithelial cell line.

Conclusions

DNA repair proteins Ku80, DNA-PK and PARP-1 are present in human lens epithelial and cortical fibre cells.

The DNA repair proteins studied appeared to exhibit reduced expression prior to fibre cell denucleation and could play a role in this process.

Ku80, DNA-PK and PARP-1 appear to play a role in the defence against genotoxic stress to lens epithelial cells.

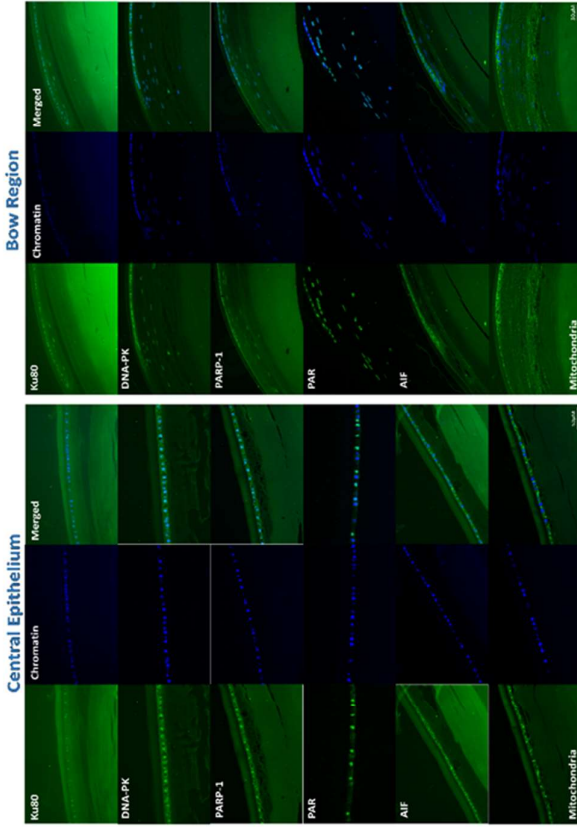


Figure 2: Expression of DNA repair and PARP-1 associated molecules in the central epithelium and bow region of the human lens.

Acknowledgments: The authors would like to thank The Humane Research Trust their generous financial support and The East Anglian Eye Bank for providing donor material.
Contact: s.ball@uea.ac.uk
Commercial interests: none